ERCB/AGS Open File Report 2012-05

Geochemistry of Groundwater and Springwater in the Paskapoo Formation and Overlying Glacial Drift, South-Central Alberta

Energy Resources Conservation Board

Alberta Geological Survey

ERCB/AGS Open File Report 2012-05

Geochemistry of Groundwater and Springwater in the Paskapoo Formation and Overlying Glacial Drift, South-Central Alberta

G.F. Huff[1], L. Woods[2], H. Moktan[1] and G. Jean[1]

[1]Energy Resources Conservation Board
Alberta Geological Survey
[2]formerly of Alberta Geological Survey

December 2012

ISBN 978-1-4601-0079-0

Huff, G.F., Woods, L., Moktan, H. and Jean, G. (2012): Geochemistry of groundwater and springwater in the Paskapoo Formation and overlying glacial drift, south-central Alberta; Energy Resources Conservation Board, ERCB/AGS Open File Report 2012-05, 58 p.

Author address
L. Woods
Infrastructure and Environment
Worley Parsons
4500 – 16th Avenue NW
Calgary, AB T3B 0M6
Canada
Tel: 403.247.0200
E-mail: landon.woods@worleyparsons.com

Published December 2012 by
Energy Resources Conservation Board
Alberta Geological Survey
4th Floor, Twin Atria Building
4999 – 98th Avenue
Edmonton, AB T6B 2X3
Canada

Tel: 780.422.1927
Fax: 780.422.1918
E-mail: AGS-Info@ercb.ca
Website: www.ags.gov.ab.ca

Contents

Tables

Figures

Acknowledgements

We thank all of the private well owners who graciously allowed us to collect samples for this study. A.A. Barker, T. Graf and A. Mukherjee (Alberta Geological Survey) provided field and data-management assistance. We thank M. Grobe, D. Palombi and T.G. Lemay (Alberta Geological Survey) for helpful discussion and review of drafts of this report and D. Magee (Energy Resources Conservation Board) for assistance with figure preparation.

Abstract

The Paskapoo Formation contains approximately one-third of all water wells present in the Canadian Prairies, illustrating its importance as a source of groundwater in central and southern Alberta. Our report describes and interprets the results of chemical analyses of groundwater and springwater samples collected from the Paskapoo Formation and overlying glacial drift between June and September 2009. Our samples represent an east-west transect across the outcrop/subcrop area of the Paskapoo Formation, bounded by Ponoka in the north and Crossfield in the south.

Groundwater in the Paskapoo Formation and overlying glacial drift shows lateral and vertical changes in geochemistry within our study area. Lateral changes from west to east include increasing concentrations of dissolved solids, dissolved Na, dissolved SO_4 and alkalinity and decreasing concentrations of dissolved Ca and $^{14}C_{(DIC)}$. Dissolved O_2 concentrations, with the exception of one groundwater sample, are all <3.0 mg/L and most are <0.01 mg/L. Most ^{3}H concentrations in the eastern part of our study area are <0.8 tritium units; however, ^{3}H concentrations are generally greater in the western samples. Vertical changes in groundwater geochemistry within the Paskapoo Formation are, in some instances, more subtle than lateral changes. Field pH values generally increase and concentrations of dissolved Ca and dissolved Mg generally decrease with depth. Values of $\delta^{2}H$, $\delta^{18}O$ and $\delta^{13}C_{(DIC)}$ and concentrations of dissolved CH_4 show anomalous values in a number of deeper samples. Values of $\delta^{18}O$ and $\delta^{2}H$ in most water samples fall parallel to the global meteoric water, the approximate Edmonton meteoric waterline and the Calgary meteoric waterline.

Mass-balance modelling of chemical weathering of Laurentide-derived glacial drift identified alteration of albite to kaolinite as the source of dissolved Na and alkalinity and the primary source of dissolved SiO_2 in springwater, glacial-drift groundwater and relatively shallow Paskapoo Formation groundwater. Mass-balance budgets of Na and SiO_2 are balanced principally by alteration of kaolinite to Na-smectite. Processes including carbonate-mineral dissolution/precipitation and cation exchange play relatively minor roles in the geochemical evolution of springwater, glacial-drift groundwater and relatively shallow Paskapoo Formation groundwater. Dissolved SO_4 in groundwater and springwater originates primarily from oxidation of pyrite with apparent local contributions from oxidation of organic S. Changes in the geochemistry of Paskapoo Formation groundwater with increasing depth appear to be largely controlled by alteration of albite to kaolinite, equilibrium between kaolinite and Na-smectite, precipitation of carbonate minerals and possible dissolution of SiO_2.

Differing ^{3}H-based apparent residence times imply that water flows through glacial drift in the western part of our study area more rapidly than through glacial drift in the eastern part of our study area. Shorter western residence times, coupled with a general east-to-west increase in annual precipitation in central Alberta, suggests increasing groundwater recharge rates from east to west across our study area.

1 Introduction

The Edmonton–Calgary Corridor (ECC; Figure 1) is undergoing rapid urban expansion and is a focus area for resource-management planning. An improved understanding of water quality and availability within the ECC is needed to ensure adequate future resources for public, industrial, and agricultural use. The Energy Resources Conservation Board/Alberta Geological Survey began a partnership with Alberta Environment and Water (now Environment and Sustainable Resource Development [ESRD]) in 2007 to characterize nonsaline groundwater resources within the ECC. Characterization of nonsaline groundwater resources is a step towards a better understanding of water availability within the ECC.

1.1 Scope

This report describes and interprets the results of chemical analyses of groundwater and springwater samples collected from the Paskapoo Formation and overlying glacial drift between June and September 2009. Specific topics addressed in our report include the sources of dissolved constituents in groundwater and springwater, the isotopic composition of selected constituents in groundwater and springwater, the apparent relative residence times of groundwater and corresponding implications on groundwater flow rates and directions.

1.2 Study Area

Our samples represent an east–west transect across the outcrop/subcrop area of the Paskapoo Formation, bounded by Ponoka in the north and Crossfield in the south (Figure 2). Sampling depths ranged from land surface to 201 m below land surface, representing water collected from springs and groundwater pumped from wells screened in the Paskapoo Formation or overlying glacial drift.

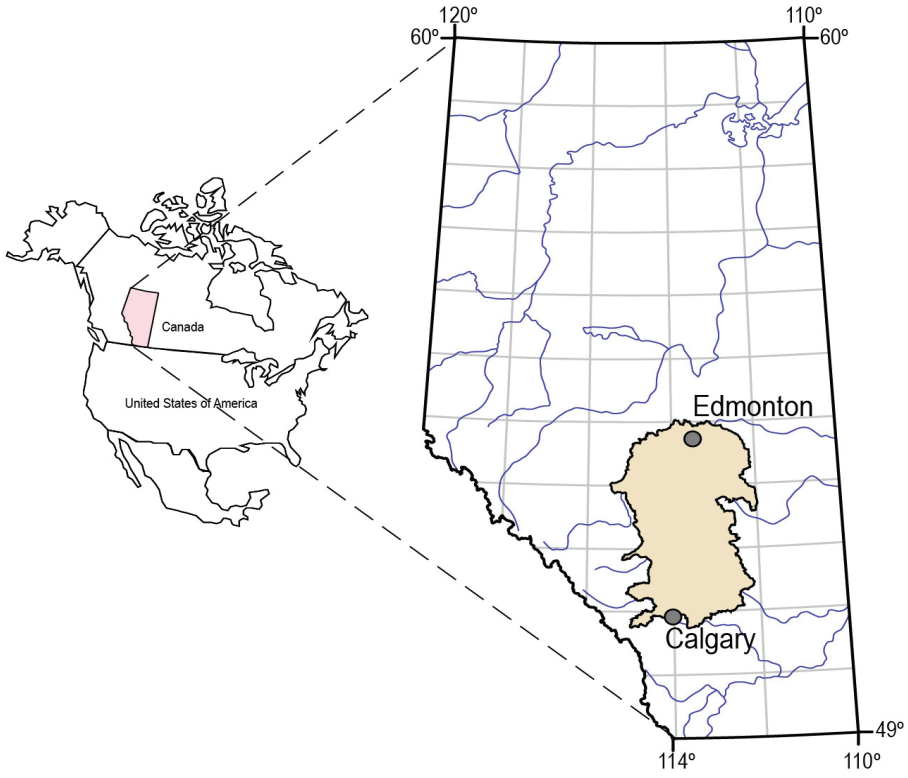

Figure 1. Location of the Edmonton–Calgary Corridor (ECC), south-central Alberta.

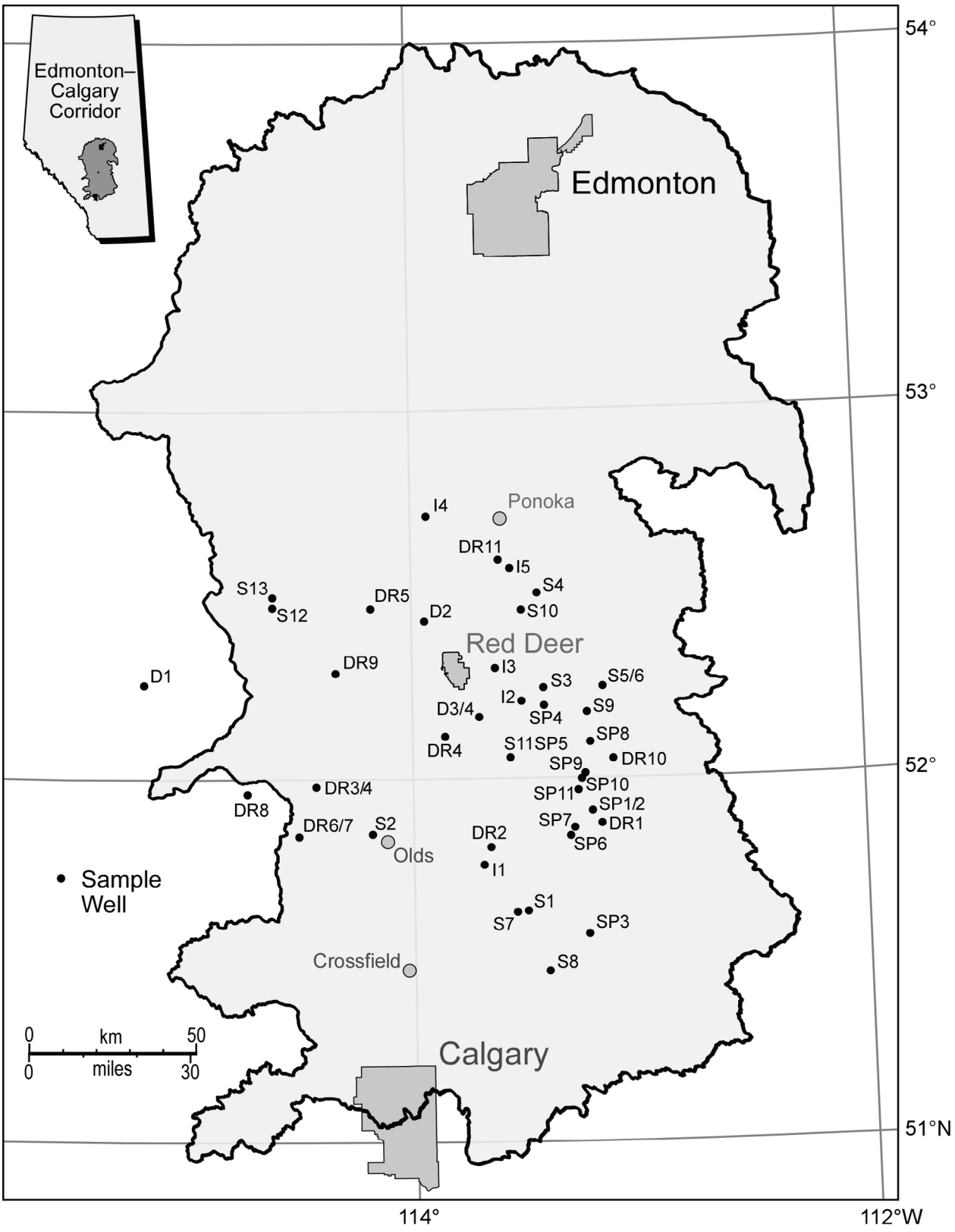

Figure 2. Locations of water samples collected in our study, south-central Alberta.

1.3 Geological Setting

The Paskapoo Formation forms an eastward-thinning wedge of nonmarine sedimentary rocks composed mostly of siltstone, mudstone and sandstone with minor amounts of coal and bentonite. The Paleogene Paskapoo Formation unconformably overlies the Upper Cretaceous–Paleogene Scollard Formation and underlies the Quaternary glacial drift (Figure 3). The Paskapoo Formation is up to 800 m thick at its western margin (Grasby et al., 2008, 2010) and forms the uppermost-consolidated rocks within the Western Canada Sedimentary Basin. The internal architecture of the Paskapoo Formation is that of a mudstone/siltstone containing channel sand features with local maximum thicknesses of 15 to 30 m (Le Breton, 1971; Hamblin, 2007). Farvolden (1961) described the Paskapoo Formation as a heterogeneous mixture of silt and clay with coarse- to fine-grained sandstone units cemented by calcium carbonate. Le Breton (1971) described the Paskapoo Formation sandstones in our study area as local to extensive, medium to coarse grained, friable, calcareous, and bentonitic. The reader is referred to Demchuk and Hills (1991), Jerzykiewicz (1997) and Lyster and Andriashek (2012) for detailed descriptions of the stratigraphy of the Paskapoo Formation.

Sandstone intervals of the Paskapoo Formation contain detrital quartz, feldspar, assorted rock fragments and accessory grains, mica, and glauconite, along with coal and plant fragments. Authigenic minerals include calcite, kaolinite, chlorite and pyrite. Both feldspar and volcanic rock fragments are highly altered, with authigenic chlorite being primarily associated with altered volcanic rock fragments (Grasby et al., 2007, 2008). Relatively thin (<1 to 6 m) coal intervals are present throughout the Paskapoo Formation (Demchuk and Hills, 1991). Tóth (1966) noted the presence of bentonite beds and disseminated montmorillonite (smectite) in sandstone intervals of the Paskapoo Formation within our study area.

The Quaternary glacial drift overlying the Paskapoo Formation was deposited in association with Cordilleran and Laurentide ice sheets. Laurentide and Cordilleran ice met along a roughly north–south line near the middle of present-day Alberta (Fulton, 1995). As such, Cordilleran-derived glacial deposits dominate in the western part of our study area, whereas Laurentide-derived deposits dominate in the eastern part. The reader is referred to Jackson (1980) and Moran (1986) for more detailed descriptions of the extent and timing of Quaternary glaciation in southern Alberta. Cordilleran-derived glacial sediments include quartzite rock fragments and carbonate minerals. Laurentide-derived glacial sediments include granitic and gneissic pebbles to cobbles, quartzite rock fragments and sulphide minerals, and have a greater clay content than is present in Cordilleran-derived glacial sediments (Grasby et al., 2008, 2010). Glacial sediments near Red Deer were described by Le Breton (1971) as till containing lacustrine clay, sand and gravel, and eolian deposits and by Tóth (1966) as unconsolidated clays, fine to coarse sands, boulders and till. Tóth (1966) identified quartz, feldspar (commonly altered), mafic minerals, carbonate minerals, gypsum, chert and coal as the primary components of glacial sediments near Olds, Alberta (Figure 2). Tharin (1960) noted that the Laurentide-derived glacial sediments contained illite and smectite in approximately equal amounts, whereas Cordilleran-derived glacial sediments contained an illite to smectite ratio of approximately 3:1.

1.4 Hydrogeochemical Setting

The Paskapoo Formation contains approximately one-third of all water wells present in the Canadian Prairies (Grasby et al., 2010) illustrating its importance as a source of groundwater in central and southern Alberta. The Paskapoo Formation contains a complex three-dimensional groundwater flow system. Although recharge to the Paskapoo Formation is likely areal in extent, the generally thinner and less-smectitic glacial drift covering the western part of the Paskapoo Formation likely allows for more efficient infiltration than the thicker and more-smectitic glacial drift found to the east (Meyboom, 1961).

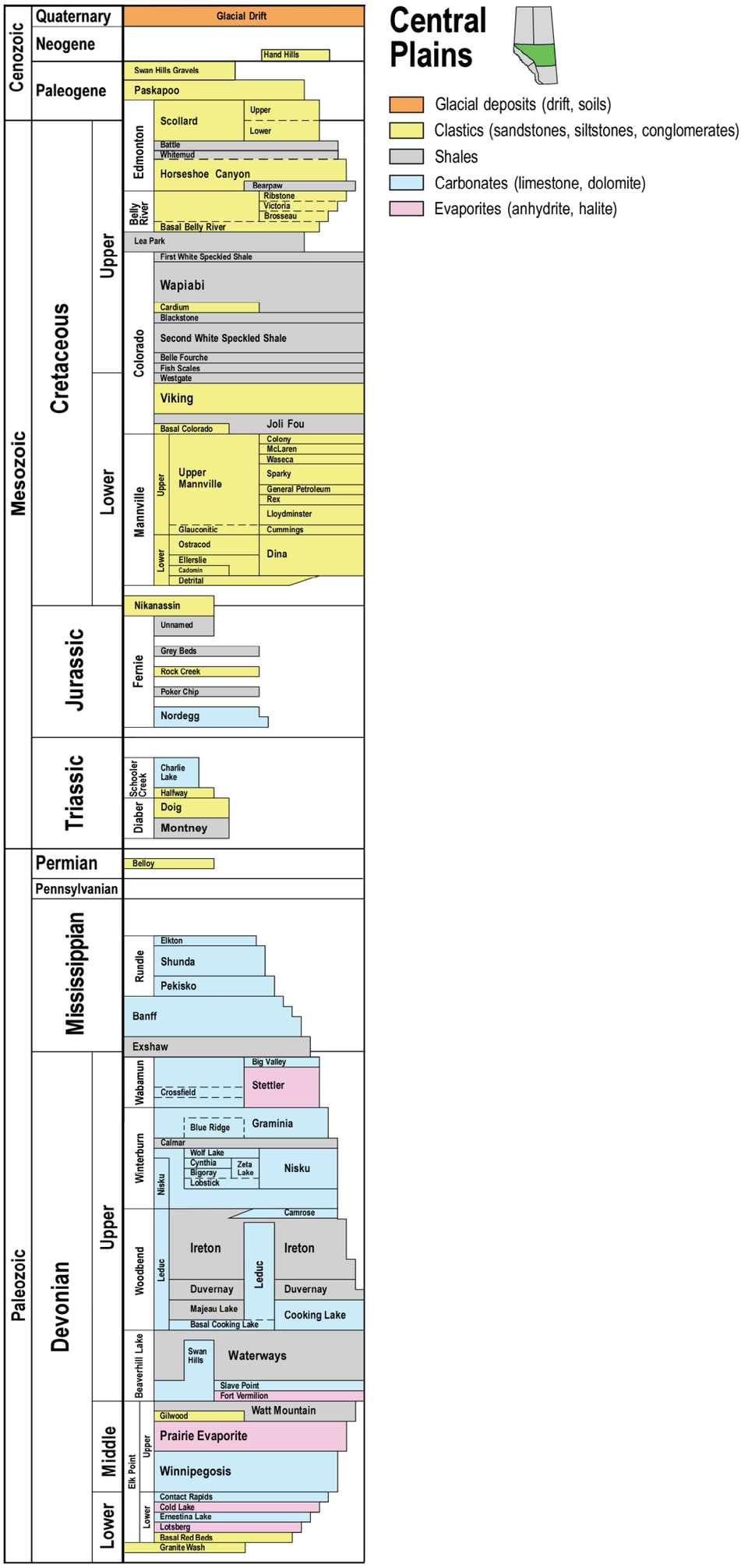

Figure 3. Generalized geological column (Devonian to Quaternary) of the Central Plains area of Alberta. Modified from Energy Resources Conservation Board (2009) per Hamilton et al. (1999), Johnston et al. (2010), Macqueen and Sandberg (1970), Richards and Higgins (1988), Storer (1976) and Vonhof (1969).

Numerous hydrological studies have cited evidence for the presence of local, intermediate and regional groundwater flow systems within the Paskapoo Formation (Meyboom, 1961; Tóth, 1966; Clissold, 1967; Le Breton, 1971; Gabert, 1975; Michael and Bachu, 2002; Bachu and Michael, 2003). Flow systems of local to intermediate extent are thought to contain the majority of groundwater flux through the Paskapoo Formation (Clissold, 1967; Gabert, 1975). Questions exist concerning the nature of basin-scale lateral groundwater flow in the Paskapoo Formation. Bachu and Michael (2003) proposed the presence of a topographically driven, large-scale, regional flow system moving groundwater laterally from recharge areas in the western uplands to discharge areas to the east and northeast, whereas Grasby et al. (2008) argue that no regional lateral flow systems exist within the Paskapoo Formation.

Numerous hydrological studies cite evidence for downward flow of groundwater within the Paskapoo Formation (Meyboom, 1961; Le Breton, 1971; Michael and Bachu, 2002; Bachu and Michael, 2003; Grasby el al., 2008, 2010). The hydraulic gradient driving downward flow of groundwater has been linked to areas of subhydrostatic fluid pressure both below and within the Paskapoo Formation (Parks and Tóth, 1995; Michael and Bachu, 2002; Bachu and Michael, 2003). Subhydrostatic fluid pressures reach minimum values at 500 to 1000 m below present-day land surface and may persist upwards to depths of <100 m (Parks and Tóth, 1995). Subhydrostatic fluid pressures in southern Alberta are attributed to rebound of low hydraulic-conductivity sediments in response to erosional unloading (Neuzil and Pollock, 1983; Tóth and Corbet, 1986; Corbet and Bethke, 1992; Bachu and Underschultz, 1995; Parks and Tóth, 1995; Bekele et al., 2003). Quantifying the effects of post-Paleogene sediment rebound is complicated by the relatively rapid addition and removal of 1 to 2 km of ice during Pleistocene time (Matthews, 1974) in southern Alberta (Michael and Bachu, 2002; Bekele et al., 2003).

The chemical composition of groundwater in the Paskapoo Formation systematically evolves from lesser dissolved-solids, Ca(±Mg)-HCO_3–type water in the west to greater dissolved-solids, Na-SO_4(±HCO_3)–type water in the east (Gabert, 1975; Grasby et al., 2008, 2010). Grasby et al. (2008, 2010) argue that the chemical composition of Paskapoo Formation groundwater is directly attributable to the results of chemical weathering of overlying carbonate-rich, Cordilleran-derived glacial drift in the west and of smectitic, sulphide-mineral–bearing, Laurentide-derived, glacial drift in the east coupled with dominantly downward groundwater flow. Previous studies have suggested production of Na-SO_4(±HCO_3)–type waters by chemical weathering of smectitic, sulphide-mineral–bearing, glacial drift through a number of mechanisms, including oxidation of sulphide minerals and organic S, cation exchange, alteration of aluminosilicate minerals and dissolution of carbonate minerals (Wallick, 1981; Hendry et al., 1986; Mermut and Arshad, 1987; Keller et al., 1991; Van Stempvoort et al., 1994; Grasby et al., 2010). Decreasing SO_4 concentrations along groundwater flow paths (Meyboom, 1961) and decreasing values of SO_4/Cl with increasing depth (Gabert, 1975) have been observed within the Paskapoo Formation.

2 Methodology and Analytical Results

Sample-collection protocols were based on those of the U.S. Geological Survey (2006) and Wilde (variously dated). A peristaltic pump was used to collect all water samples, either from the outflow of a submersible pump or from a temporarily installed ‘push’ device used to sample springs. Care was taken not to entrain atmospheric gases into the sample stream during sample collection.

Outflow from the peristaltic pump was monitored for field parameters, including temperature, pH, dissolved O_2 and specific conductance. Samples were collected after monitored field parameters reached stable values. All collected samples, except those for determining dissolved CH_4, were passed through a 0.45 μm cartridge filter. Alkalinity was determined by potentiometric titration to pH values <3.5 using 0.16 Normal H_2SO_4 within 12 hours of sample collection. Samples collected for determining dissolved cations were preserved by lowering pH values to <2 using HNO_3. Samples collected for determination of dissolved sulphide were preserved by adding sodium hydroxide and zinc acetate. Samples collected for

determination of dissolved CH_4 were analyzed within three days of collection. All samples, except those collected to determine O, H and Sr isotopes, were kept in the dark and chilled to 4°C until analysis.

Quality control was implemented through use of equipment blanks and collection and analysis of replicate samples. Equipment blanks collected prior to and during the sample-collection period showed no apparent equipment-derived contamination. Replicate sample pairs include DR6-DR7, S5-S6, D3-D4 and SP1-SP2 (Table 1). Charge balance on all analyses used in our study fall within ±3.5%.

All analytical results are shown in Tables 1 and 2. Table 1 shows the values of field parameters and concentrations of dissolved constituents determined in our study. Analytical results shown in Table 1, with the exception of those for field parameters, were determined by Exova Laboratories (Edmonton, AB). Table 2 shows the results of isotopic determinations of O, H, C and S (Environmental Isotope Laboratory, University of Waterloo, ON) and of isotopic determinations of Sr (Dr. R. Creaser, University of Alberta, AB). Reference materials used in reporting the results of isotopic determinations include Vienna Standard Mean Ocean Water (VSMOW) for O and H, Vienna Pee Dee Belemnite (VPDB) for ^{13}C, 1950 Oxalic Acid Standard (1950 OAS) for ^{14}C and Vienna Canyon Diablo Meteorite (VCDT) for S.

Sample names beginning with DR (drift) denote a sample collected from glacial drift overlying the Paskapoo Formation. Sample names beginning with S (shallow) denote a sample collected from the Paskapoo Formation at depths of 4 to 75 m below land surface (BLS). Sample names beginning with I (intermediate) or D (deep) denote samples collected from the Paskapoo Formation at depths of 91 to 162 m BLS or 163 to 201 m BLS, respectively. Sample names beginning with SP denote samples collected from springs. The depth ranges specified for Paskapoo Formation samples in our study carry no implication of any particular stratigraphic or hydrogeological interval. Rather, specified depth ranges serve as a convenient way to organize the vertical distribution of collected data.

3 Geochemical Evolution of Groundwater

Groundwater in the Paskapoo Formation and overlying glacial drift shows lateral and vertical changes in geochemistry within the study area. Lateral changes shown in all figures are described in terms of the 10-Degree Transverse Mercator (10TM) projection with a false easting of 500 000 m corresponding to 115°W longitude.

3.1 Systematic Changes in Water Geochemistry

Laterally continuous changes in groundwater geochemistry are evident in the 'shallow' Paskapoo Formation and overlying glacial drift from west to east across the study area. These changes include increasing concentrations of dissolved solids (Figure 4), dissolved Na (Figure 5), dissolved SO_4 (Figure 6) and alkalinity (Figure 7) and generally decreasing concentrations of dissolved Ca (Figure 8) and ^{14}C in dissolved inorganic carbon ($^{14}C_{(DIC)}$; Figure 9). Little to no systematic laterally continuous variations are evident in concentrations of dissolved Mg (Figure 10), dissolved Cl (Figure 11), dissolved O_2 (Figure 12), dissolved CH_4 (Figure 13) and dissolved SiO_2 (Figure 14). Likewise, little to no systematic laterally continuous variations are evident in isotopic abundances of ^{18}O in structural O of the H_2O molecule ($\delta^{18}O$; Figure 15), ^{13}C in dissolved organic carbon ($\delta^{13}C_{(DIC)}$; Figure 16) and ^{34}S in dissolved SO_4 ($\delta^{34}S_{(SO4)}$; Figure 17). Additionally, little to no systematic laterally continuous variations are evident in field pH (Figure 18). Dissolved O_2 concentrations, with the exception of one shallow groundwater sample, are all <3.0 mg/L and most are <0.01 mg/L (Figure 12). Most ^{3}H concentrations in the eastern part of the study area are <0.8 tritium units (TU). However, ^{3}H concentrations are generally greater in the western shallow and drift samples (Figure 19). Values of $^{87}Sr/^{86}Sr$ are slightly greater in western drift samples, likely due to differing glacial drift mineralogies (Figure 20).

Table 1. Values of field parameters and concentrations of dissolved constituents in groundwater and springwater samples, south-central Alberta. Abbreviations: 10TM, 10-Degree Transverse Mercator; ESRD, Alberta Environment and Sustainable Resource Development; BLS, below land surface; Eh, standard oxidation-reduction potential; n/a, information not available; ND, not determined.

Sample Number	Easting 10TM (m)	Northing 10TM (m)	ESRD ID	Sampled Interval (m BLS)	Sample Date	Dissolved Sulphide (mg/L)	Dissolved Br (mg/L)	Dissolved Inorganic C (mg/L)	Si (mg/L)	Calculated SiO_2 (mg/L)	Sr (mg/L)	Gravimetric Dissolved Solids @ 180°C (mg/L)	Field pH	Temperature (°C)	Specific conductance (µS/cm @ 25°C)	Dissolved O_2 (mg/L)
DR1	625940	5743626	1470074	7–9	25/06/2009	<0.005	<0.5	197	3.46	7.40	0.160	1490	8.43	8.9	1835	<0.01
DR2	592406	5735713	n/a	8	26/06/2009	<0.005	<0.1	46.6	4.24	9.07	0.107	146	7.62	10.3	341	<0.01
DR3	539417	5753641	n/a	9	29/06/2009	<0.005	<0.1	95.2	3.18	6.80	0.426	454	7.37	11.4	643	<0.01
DR4	578839	5768919	n/a	9	30/06/2009	<0.005	<0.1	159	2.96	6.33	0.722	1150	7.77	6.1	1412	<0.01
DR5	555831	5808104	469678	4–10	30/06/2009	<0.005	<0.1	108	4.38	9.37	0.818	454	7.46	6.2	690	1.61
DR6	533885	5738735	341072	3–5	03/07/2009	<0.005	<0.1	84.1	5.10	10.91	0.286	354	7.36	7.0	621	<0.01
DR7	533885	5738735	341072	3–5	03/07/2009	<0.005	<0.1	83.8	5.38	11.51	0.295	360	7.36	7.0	621	<0.01
DR8	518460	5751262	n/a	6	03/07/2009	<0.005	<0.1	84.4	5.12	10.95	0.417	362	7.46	5.7	586	<0.01
DR9	545316	5788437	477981	9	06/07/2009	<0.005	<0.1	132	5.24	11.21	1.280	678	7.33	4.8	873	<0.01
DR10	628970	5763092	n/a	9	06/07/2009	0.008	<0.5	124	3.59	7.68	0.468	1400	8.33	8.2	2069	2.13
DR11	594646	5823135	93325	9	17/07/2009	0.014	<0.1	152	4.62	9.88	0.302	694	8.06	9.8	1041	<0.01
S1	603771	5716317	41627	44–52	14/07/2009	0.183	<0.1	118	3.08	6.59	0.313	1190	8.82	7.5	1296	<0.01
S2	556462	5739583	1480030	46–58	14/07/2009	0.075	<0.1	144	3.02	6.46	0.602	694	7.83	4.8	1043	2.25
S3	607991	5784059	116872	61–73	15/07/2009	<0.005	<0.1	139	4.24	9.07	2.220	1260	7.64	7.6	1808	1.42
S4	605617	5812804	273393	42–50	15/07/2009	<0.005	<0.1	117	3.65	7.81	0.311	772	7.95	6.2	1224	0.7
S5	626295	5784882	1470399	26–27	16/07/2009	<0.005	<0.5	185	3.74	8.00	0.364	1440	7.98	8.5	1800	<0.01
S6	626295	5784882	1470399	26–27	16/07/2009	<0.005	<0.5	185	3.69	7.90	0.352	1420	7.98	8.5	1800	<0.01
S7	600676	5715976	1470037	47–61	16/07/2009	<0.005	0.1	145	4.40	9.41	0.980	1100	7.74	8.8	1130	<0.01
S8	610673	5698302	1470470	18–37	21/07/2009	<0.005	<0.1	89.6	3.03	6.48	0.054	532	9.26	7.7	708	<0.01
S9	621263	5776903	290675	18–20	23/07/2009	<0.005	<0.005	210	4.89	10.46	0.286	1790	7.83	6.9	2823	<0.01
S10	601489	5807846	273794	30–37	23/07/2009	<0.005	<0.1	123	4.00	8.56	0.654	558	7.85	9.1	998	<0.01
S11	597591	5762957	288564	4–9	26/06/2009	<0.005	<0.1	118	3.29	7.04	0.745	696	7.77	6.1	1126	<0.01
S12	525928	5807822	n/a	8	29/06/2009	<0.005	<0.1	107	4.45	9.52	0.830	450	7.35	9.8	706	6.59
S13	525999	5811158	474543	61–73	05/08/2009	0.111	<0.1	94.4	3.80	8.13	0.748	444	7.87	10.2	634	<0.01
I1	590047	5730343	229031	91–122	21/07/2009	0.76	0.2	138	3.23	6.91	0.280	746	8.71	9.5	1198	<0.01
I2	601604	5780365	162110	139–158	22/07/2009	0.086	<0.1	144	3.43	7.34	0.134	1150	9.02	9.3	1663	<0.01
I3	593868	5789988	n/a	140–152	29/07/2009	<0.005	<0.5	131	2.79	5.97	0.150	1230	8.88	8.6	1774	0.86
I4	572805	5835995	151716	95–135	06/08/2009	0.02	0.2	104	3.11	6.65	0.070	606	9.34	8.6	985	<0.01
I5	597871	5820452	235123	118–162	06/08/2009	<0.005	<0.1	94.9	2.86	6.12	0.088	856	9.10	7.6	1322	<0.01
D1	487112	5784877	469616	162–179	29/07/2009	0.45	<0.1	78	3.35	7.17	0.026	352	9.69	7.4	578	<0.01
D2	571887	5804065	1035227	165–183	05/08/2009	0.186	0.3	94.6	3.13	6.70	0.074	686	9.31	9.4	1057	<0.01
D3	588717	5775513	1470210	171–201	18/08/2009	<0.005	0.2	114	3.07	6.57	0.044	594	9.36	9.3	1041	<0.01
D4	588717	5775513	1470210	171–201	18/08/2009	<0.005	0.2	114	3.11	6.65	0.044	620	9.36	9.3	1041	<0.01
SP1	622966	5747179	n/a	n/a	14/09/2009	<0.005	<0.5	160	4.02	8.60	0.590	1700	7.93	8.6	3039	1.35
SP2	622966	5747179	n/a	n/a	14/09/2009	<0.005	<0.5	160	3.98	8.52	0.582	1720	7.93	8.6	3039	1.35
SP3	622011	5709450	n/a	n/a	15/09/2009	<0.005	<0.5	204	5.00	10.70	1.280	2460	7.32	8.6	4212	<0.01
SP4	608312	5779061	n/a	n/a	21/09/2009	<0.005	<0.1	132	3.77	8.07	0.404	888	7.70	7.8	1442	1.99
SP5	597655	5762847	n/a	n/a	21/09/2009	0.047	<0.5	157	4.26	9.11	0.590	1340	7.73	8.0	2049	<0.01
SP6	616644	5739920	n/a	n/a	22/09/2009	0.007	<0.1	117	3.35	7.17	0.174	1270	8.04	14.1	2069	2.76
SP7	617758	5741804	n/a	n/a	22/09/2009	0.01	<0.1	77.2	4.69	10.03	0.845	464	7.47	9.4	751	1.39
SP8	622057	5768279	n/a	n/a	29/09/2009	0.005	<0.1	105	4.72	10.10	0.642	590	7.37	11.3	590	ND
SP9	621285	5757716	n/a	n/a	30/09/2009	<0.005	<0.1	123	4.74	10.14	1.300	866	7.32	7.9	800	ND
SP10	619698	5756865	n/a	n/a	30/09/2009	0.011	<0.5	162	4.78	10.23	1.320	1650	7.35	8.2	1480	ND
SP11	619262	5753574	n/a	n/a	25/06/2009	<0.005	<0.5	170	4.82	10.31	1.530	1720	7.59	7.7	2272	<0.01

Table 1 (continued)

Sample Number	Calculated Eh (mV)	Dissolved Ca (mg/L)	Dissolved Mg (mg/L)	Dissolved Na (mg/L)	Dissolved K (mg/L)	Dissolved Fe (mg/L)	Dissolved Mn (mg/L)	Dissolved Cl (mg/L)	Dissolved NO_3 (mg/L as N)	Dissolved NO_2 (mg/L as N)	Dissolved SO_4 (mg/L)	Alkalinity CO_3 (mg/L)	Alkalinity HCO_3 (mg/L)	Total alkalinity (mg/L as $CaCO_3$)	Hardness (mg/L as $CaCO_3$)	Dissolved methane (mg/L)
DR1	100.9	7.0	1	530	1.0	0.03	0.010	3.3	<0.05	<0.02	457	3	941	777	22	0.019
DR2	42.4	57.5	7.9	2.9	1.9	0.14	0.596	5.3	0.05	<0.005	1.0	<6	216	177	176	4.03
DR3	228.7	98.7	27.7	10.2	1.7	0.03	0.029	10.3	0.88	<0.005	33.7	<6	401	329	361	0.192
DR4	80.7	37.4	13	345	2.7	0.52	0.030	1.7	<0.01	<0.005	336	<6	703	577	147	0.036
DR5	172.3	66.2	44.2	29.6	2.4	0.56	0.030	3.7	1.00	<0.005	26.0	<6	458	376	347	<0.003
DR6	146.7	93.6	24	4.8	1.6	1.46	0.781	0.9	0.09	<0.005	14.0	<6	423	347	333	0.188
DR7	146.7	96.6	25.5	4.9	1.7	1.47	0.799	1.0	0.02	<0.005	14.0	<6	423	347	346	0.191
DR8	300.5	78.7	31	13.4	2.4	0.02	<0.005	2.6	0.03	<0.005	9.5	<6	416	341	324	<0.003
DR9	225.2	104.0	61.6	61.8	3.3	0.13	0.425	28.1	0.55	<0.005	79.4	<6	670	550	513	0.018
DR10	-22.3	22.8	8.1	432	2.0	1.04	0.022	5.7	<0.05	<0.02	530	<6	632	518	90	0.018
DR11	11.2	17.7	6.2	259	1.2	<0.01	0.016	2.4	<0.01	<0.005	39.1	<6	736	604	70	0.006
S1	-35.5	13.6	13.6	384	1.5	0.04	0.013	8.2	0.24	<0.005	416	16	569	493	89.9	7.44
S2	97.3	30.9	18.7	212	2.2	<0.01	0.022	20.3	0.22	<0.005	27.0	<6	695	570	154	0.26
S3	165.2	78.7	24.3	321	3.8	0.06	0.109	3.5	<0.01	<0.005	445	<6	648	532	297	0.007
S4	76.9	16.7	6.5	275	1.6	0.01	0.039	1.6	<0.01	<0.005	189	<6	578	474	68	0.016
S5	82.5	20.2	2.6	521	2.4	<0.02	0.044	2.2	0.12	<0.02	435	<6	854	700	1420	0.012
S6	82.5	20.0	2.5	513	2.2	<0.02	0.044	2.4	<0.05	<0.02	429	<6	864	709	1410	0.012
S7	127.6	46.7	38.6	290	3.7	<0.01	0.065	10.1	<0.01	<0.005	327	<6	675	554	276	0.003
S8	79.6	2.9	0.6	208	0.6	<0.01	0.600	8.4	<0.01	<0.005	76.3	19	417	374	10	0.135
S9	38.9	21.5	4.2	633	2.4	0.29	0.045	0.8	<0.05	<0.02	628	<6	1045	857	71	<0.003
S10	90.4	36.6	10.1	178	2.9	0.34	0.060	0.8	<0.01	<0.005	44.5	<6	596	489	133	<0.003
S11	137.1	50.0	23.4	188	2.5	0.19	0.042	2.4	<0.01	<0.005	178	<6	601	493	221	<0.003
S12	232.8	101.0	29.5	20.1	1.8	<0.01	<0.005	6.1	4.45	<0.005	20.0	<6	447	367	375	<0.003
S13	40.2	36.3	12.6	127	1.5	0.23	0.040	3.9	<0.01	<0.005	24.0	<6	472	387	142	1.04
I1	-120.8	13.7	3.9	290	1.4	0.06	3.900	30.3	0.11	<0.005	92.4	6	657	549	50	41.1
I2	-38.6	4.1	0.6	411	1.2	0.03	0.009	1.9	<0.01	<0.005	348	11	677	574	13	0.165
I3	474.0	15.0	0.7	449	1.0	<0.02	0.020	11.8	0.15	<0.02	467	12	597	510	41	<0.003
I4	-65.9	1.8	<0.2	249	0.7	0.11	0.010	49.6	<0.01	<0.005	<0.9	32	499	463	4.4	90.2
I5	138.1	2.5	0.4	325	0.7	0.06	0.011	3.0	<0.01	<0.005	272	19	475	421	457	0.061
D1	-64.1	0.8	<0.2	158	<0.4	<0.01	<0.005	2.3	<0.01	<0.005	12.0	48	296	323	2	1.11
D2	-117.5	2.0	0.3	255	0.6	0.20	0.006	52.2	<0.01	<0.005	64.6	29	455	422	6	48.6
D3	240.6	1.1	<0.2	253	0.6	<0.01	<0.005	26.6	<0.01	<0.005	6.8	36	543	505	2.7	50.4
D4	240.6	1.0	<0.2	252	0.6	<0.01	<0.005	27.0	<0.01	<0.005	7.1	34	537	497	2.6	52.3
SP1	147.6	32.3	15	532	2.2	<0.02	0.150	5.4	<0.05	<0.02	652	<6	789	647	140	<0.003
SP2	147.6	31.8	15	530	2.1	<0.02	0.150	3.2	<0.05	<0.02	653	<6	796	653	140	<0.003
SP3	116.8	81.6	18	709	2.7	<0.02	0.293	7.8	<0.05	<0.02	971	<6	1062	871	277	0.016
SP4	322.6	29.3	12.8	301	2.0	<0.01	<0.005	12.4	1.48	<0.005	218	<6	642	527	126	<0.003
SP5	14.9	43.2	32.0	399	2.5	<0.02	0.211	1.4	<0.05	<0.02	459	<6	766	628	240	<0.003
SP6	304.3	8.7	2.2	422	2.0	0.06	0.037	1.7	0.20	<0.005	488	<6	566	464	31	<0.003
SP7	147.3	58.3	17.3	76.6	3.0	<0.01	0.208	1.5	<0.01	<0.005	91.2	<6	360	295	217	<0.003
SP8	ND	42.2	19.1	159	2.5	0.03	0.367	0.8	0.17	0.017	92.7	<6	534	438	184	0.004
SP9	ND	58.6	44.8	185	3.0	0.02	0.015	1.4	0.41	<0.005	223	<6	617	506	331	<0.003
SP10	ND	84.2	49.4	430	4.4	<0.02	0.250	3.2	<0.05	<0.02	596	<6	818	671	414	0.01
SP11	181.4	93.4	67.9	389	4.0	0.14	0.288	3.6	<0.05	<0.02	727	<6	805	660	513	<0.003

Table 2. Values of C, H, O and Sr isotopes in groundwater and springwater samples, south-central Alberta. Abbreviations: PMC, per cent modern carbon; TU, tritium units.

Sample number	^{3}H (TU)	δ D (‰)	$\delta\ ^{18}O$ (‰)	^{14}C (PMC)	$\delta\ ^{13}C$ (‰)	$^{87}Sr/^{86}Sr$	$\delta\ ^{34}S$ (‰)
DR1	<0.8	-143.53	-17.40	11.35	-12.73	0.70550	4.83
DR2	8.1	-148.01	-18.36	94.67	-11.05	0.70831	
DR3	7.5	-142.45	-18.38	94.12	-13.79	0.70824	5.94
DR4	<0.8	-148.62	-18.40	26.09	-11.28	0.70677	-12.10
DR5	3.5	-147.17	-18.98	67.81	-13.52	0.70693	-5.31
DR6	14.3	-143.40	-17.80	80.09	-13.43	0.70809	-7.72
DR7	13.3	-143.60	-17.75	79.37	-13.30	0.70808	-8.17
DR8	6.3	-145.68	-18.22	69.67	-12.19	0.70795	-4.99
DR9	3.3	-141.51	-17.45	85.35	-14.62	0.70706	-0.69
DR10	<0.8	-150.15	-18.33	17.17	-14.85	0.70605	-5.69
DR11	<0.8	-144.27	-17.55	72.62	-11.03	0.70596	-5.45
S1	<0.8	-146.96	-17.62	6.52	-8.58	0.70710	-7.18
S2	3.5	-150.15	-18.14	49.71	-12.42	0.70720	0.69
S3	<0.8	-149.10	-18.07	22.80	-16.45	0.70617	-8.56
S4	<0.8	-150.30	-18.83	36.27	-12.16	0.70614	-1.83
S5	<0.8	-144.70	-17.22	34.74	-14.97	0.70615	-9.41
S6	<0.8	-145.68	-16.83	34.61	-14.73	0.70612	
S7	<0.8	-169.25	-20.99	1.35	-17.21	0.70669	-1.37
S8	<0.8	-138.60		1.04	-9.65	0.70657	2.33
S9	<0.8	-142.89	-17.35	27.09	-13.95	0.70645	-5.31
S10	1.6	-144.93	-17.78	58.67	-11.74	0.70646	-10.76
S11	4.1	-151.02	-19.16	54.41	-12.39	0.70676	-7.92
S12	13.4	-142.97	-18.42	82.75	-14.75	0.70707	-3.36
S13	9.6	-148.27	-18.51	61.04	-13.76	0.70638	-0.88
I1	1.4	-128.28	-15.59	6.72	-7.72	0.70656	-13.54
I2	<0.8	-146.24	-17.72	21.86	-12.56	0.70603	-10.11
I3	<0.8	-150.59	-18.05	29.64	-10.71	0.70622	-11.74
I4	<0.8	-117.98	-13.52	0.33	-0.63	0.70581	
I5	<0.8	-151.73	-18.79	5.19	-12.62	0.70580	-7.23
D1	<0.8	-144.48	-18.36	30.33	-8.81	0.70641	11.40
D2	<0.8	-122.10	-13.98	0.22	-3.80	0.70623	-9.06
D3	<0.8	-123.18	-14.74	3.83	-4.53	0.70609	-14.31
D4	<0.8	-123.48	-14.85	4.19	-3.31	0.70610	
SP1	<0.8	-154.97	-19.15	18.96	-14.05	0.70636	-2.74
SP2	<0.8	-154.96	-19.63	18.95	-14.27	0.70636	
SP3	<0.8	-152.84	-19.84			0.70587	-3.45
SP4	3.2	-155.74	-19.12	42.15	-13.03	0.70689	-8.61
SP5	<0.8	-147.78	-18.10	31.55	-12.51	0.70679	-9.07
SP6	<0.8	-159.22	-20.04			0.70717	-9.52
SP7	2.7	-156.23	-19.39	50.09	-11.21	0.70689	-8.06
SP8	<0.8	-149.25	-19.40	51.20	-12.28	0.70626	
SP9	2.4	-150.60	-18.71	42.40	-13.59	0.70635	-1.94
SP10	<0.8	-153.88	-19.74	18.14	-14.69	0.70626	-5.88
SP11	<0.8	-152.20	-18.96	14.17	-14.84	0.70623	-6.03

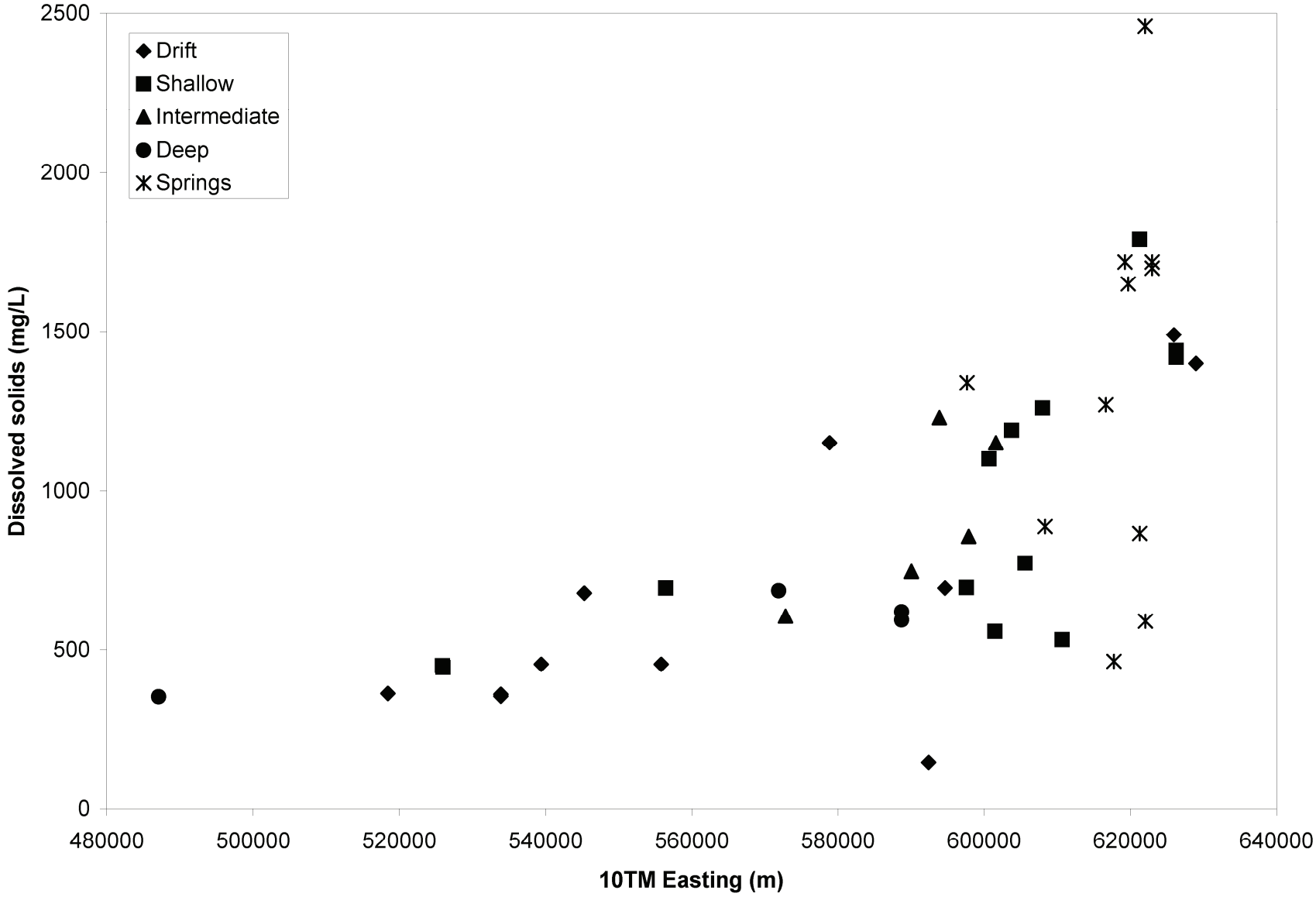

Figure 4. Easting versus concentrations of dissolved solids in groundwater and springwater samples, south-central Alberta. Abbreviation: 10TM, 10-Degree Transverse Mercator.

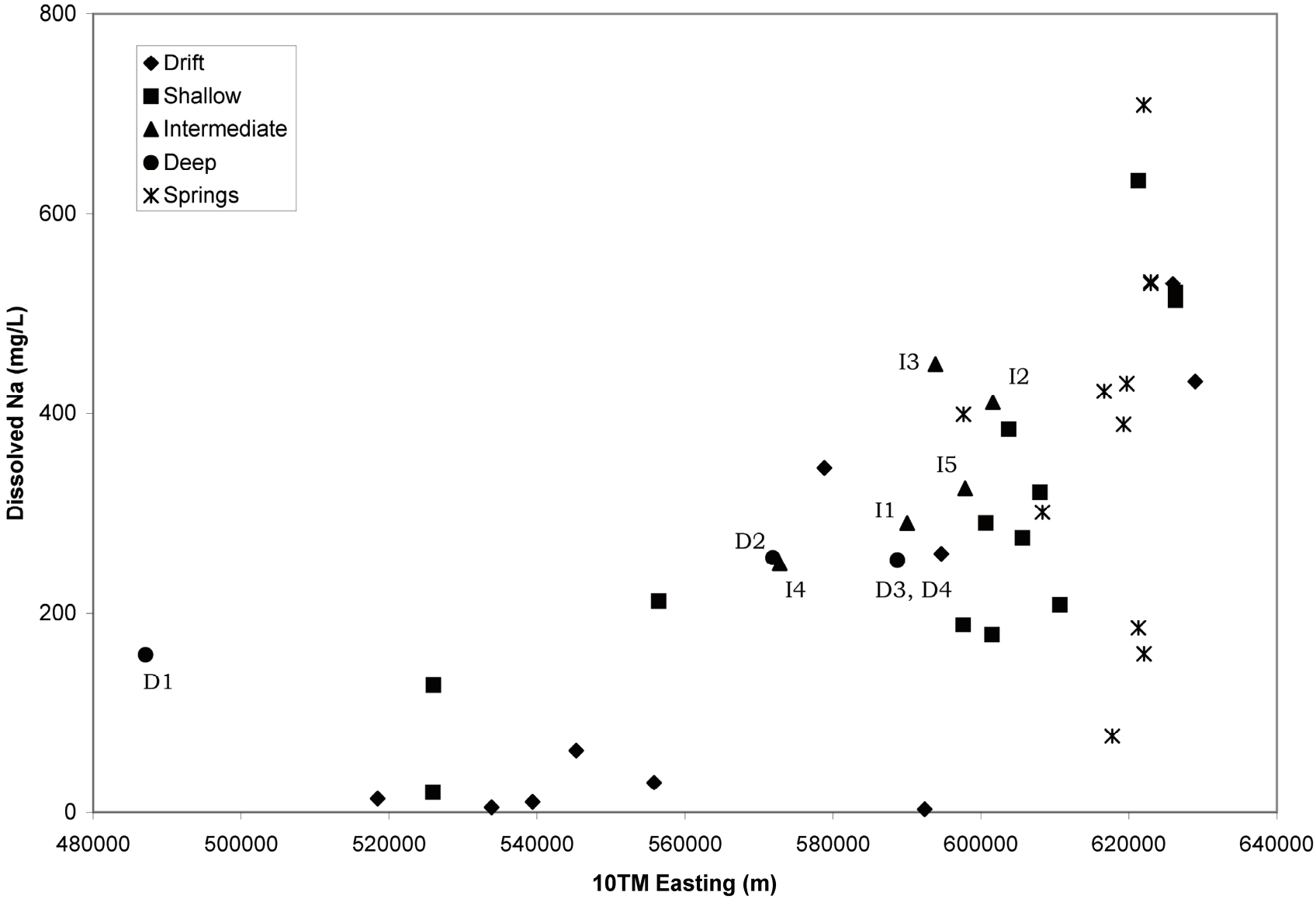

Figure 5. Easting versus concentrations of dissolved Na in groundwater and springwater samples, south-central Alberta.. Abbreviation: 10TM, 10-Degree Transverse Mercator.

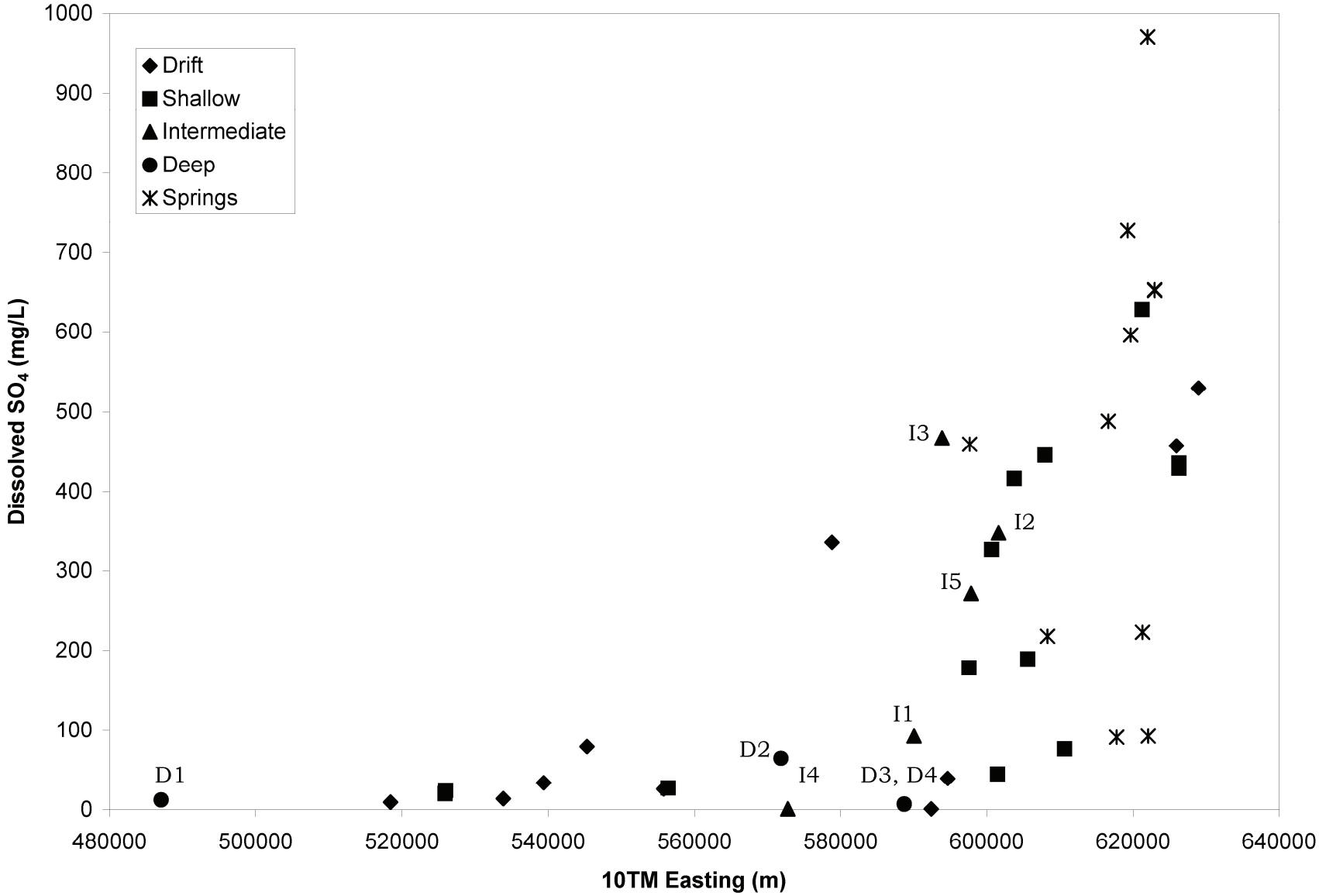

Figure 6. Easting versus concentrations of dissolved SO_4 in groundwater and springwater samples, south-central Alberta. Abbreviation: 10TM, 10-Degree Transverse Mercator.

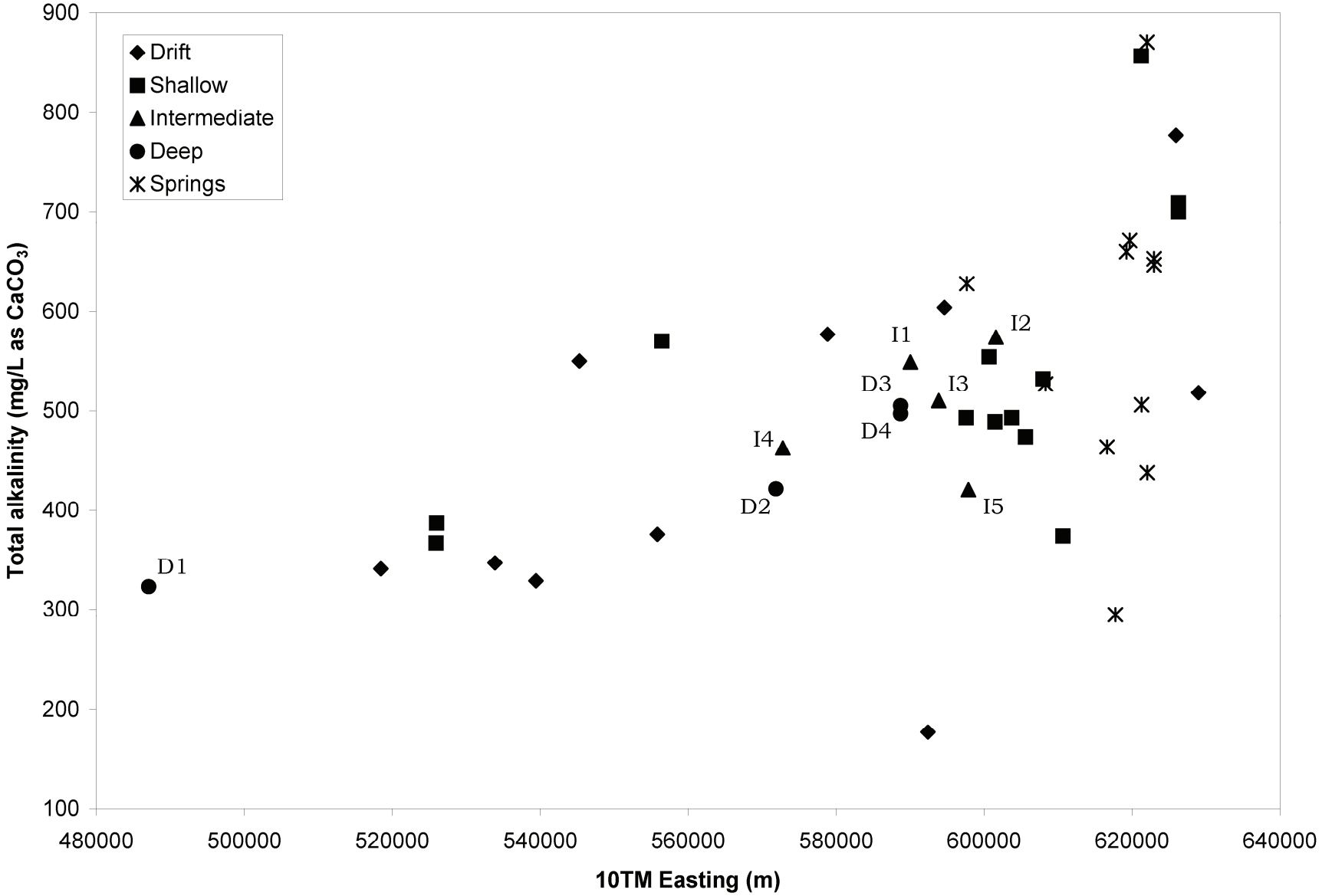

Figure 7. Easting versus alkalinity in groundwater and springwater samples, south-central Alberta. Abbreviation: 10TM, 10-Degree Transverse Mercator.

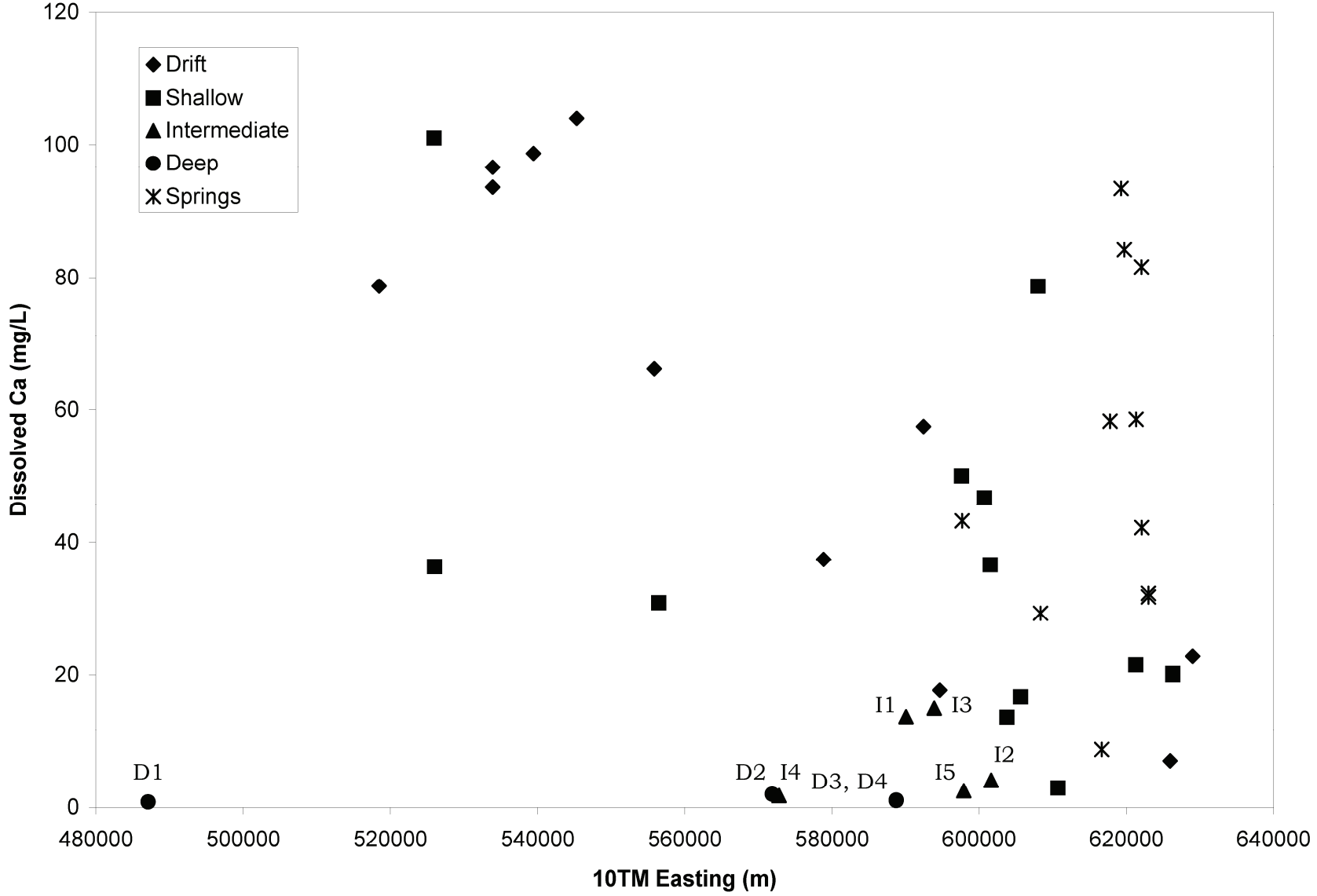

Figure 8. Easting versus concentrations of dissolved Ca in groundwater and springwater samples, south-central Alberta. Abbreviation: 10TM, 10-Degree Transverse Mercator.

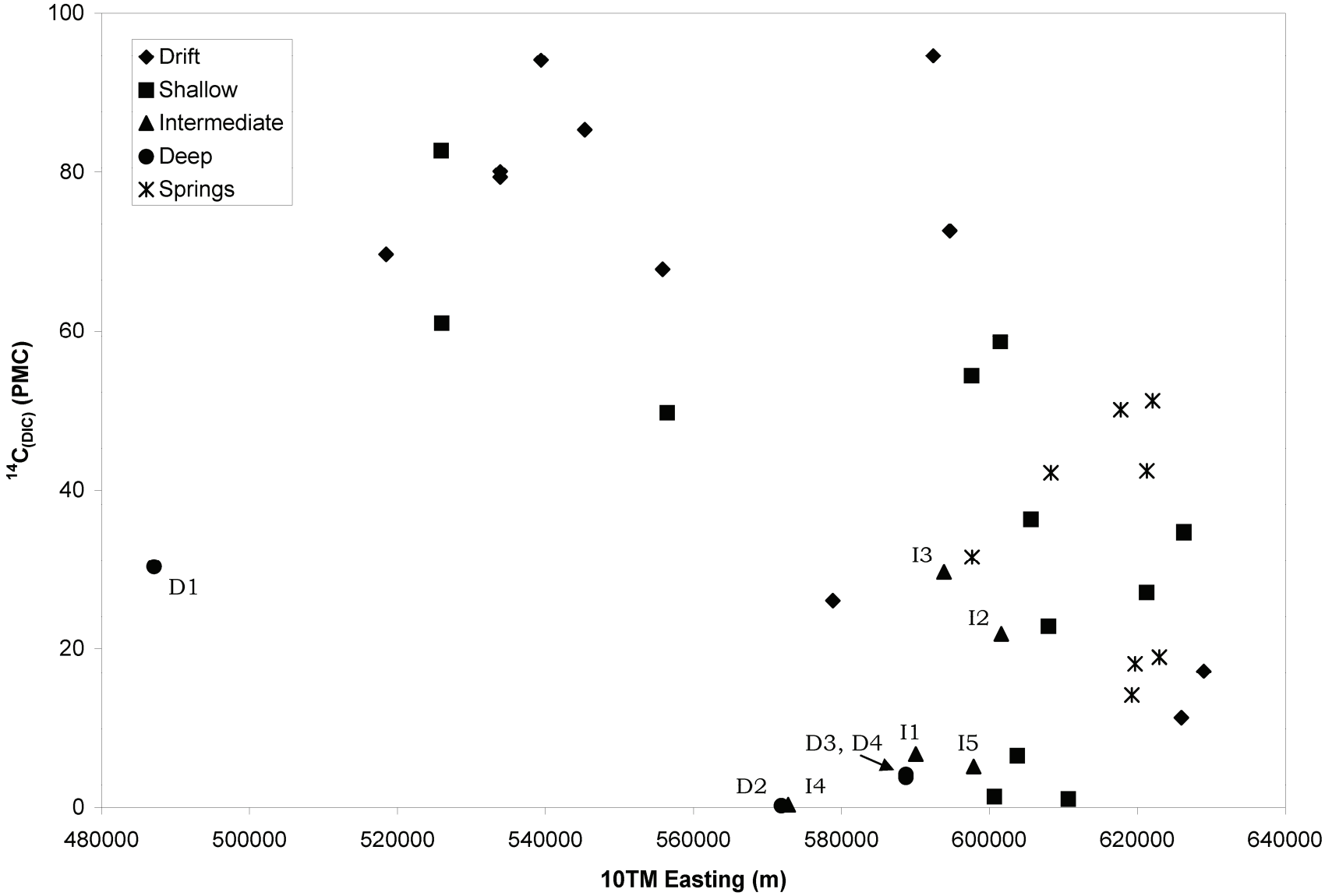

Figure 9. Easting versus values of $^{14}C_{(DIC)}$ in groundwater and springwater samples, south-central Alberta. Abbreviations: 10TM, 10-Degree Transverse Mercator; PMC, per cent modern carbon.

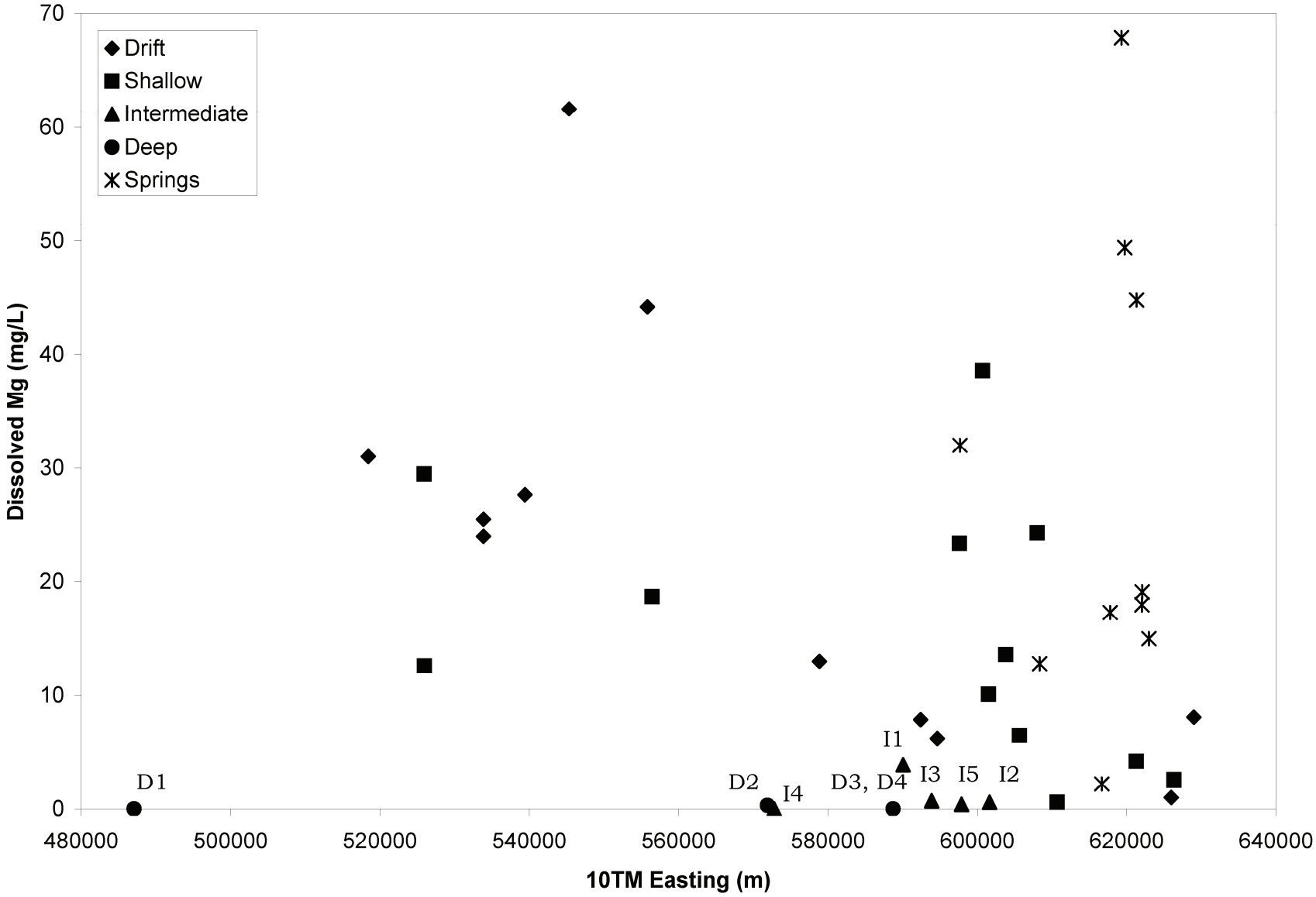

Figure 10. Easting versus concentrations of dissolved Mg in groundwater and springwater samples, south-central Alberta. Abbreviation: 10TM, 10-Degree Transverse Mercator.

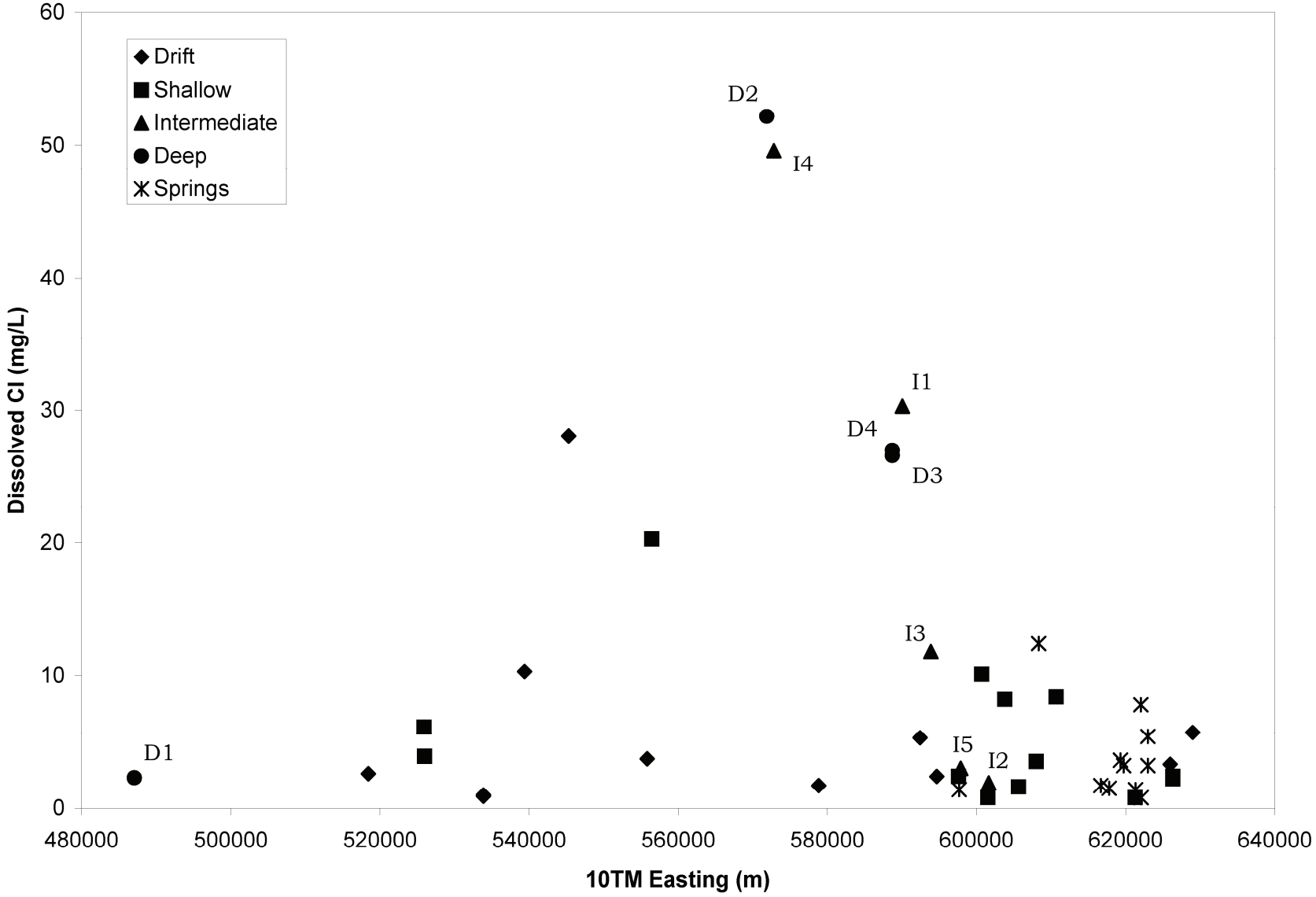

Figure 11. Easting versus concentrations of dissolved Cl in groundwater and springwater samples, south-central Alberta. Abbreviation: 10TM, 10-Degree Transverse Mercator.

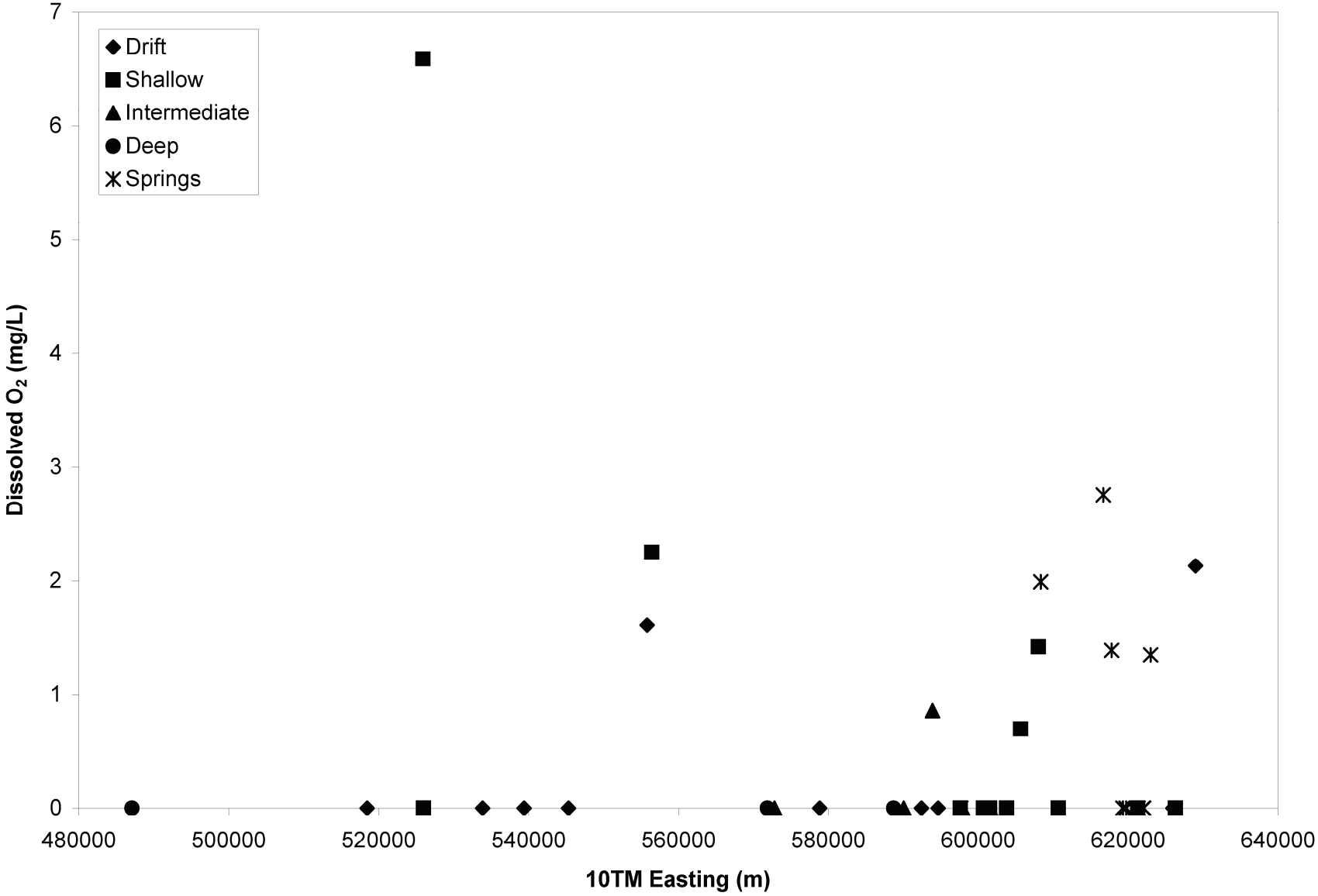

Figure 12. Easting versus concentrations of dissolved O_2 in groundwater and springwater samples, south-central Alberta. Abbreviation: 10TM, 10-Degree Transverse Mercator.

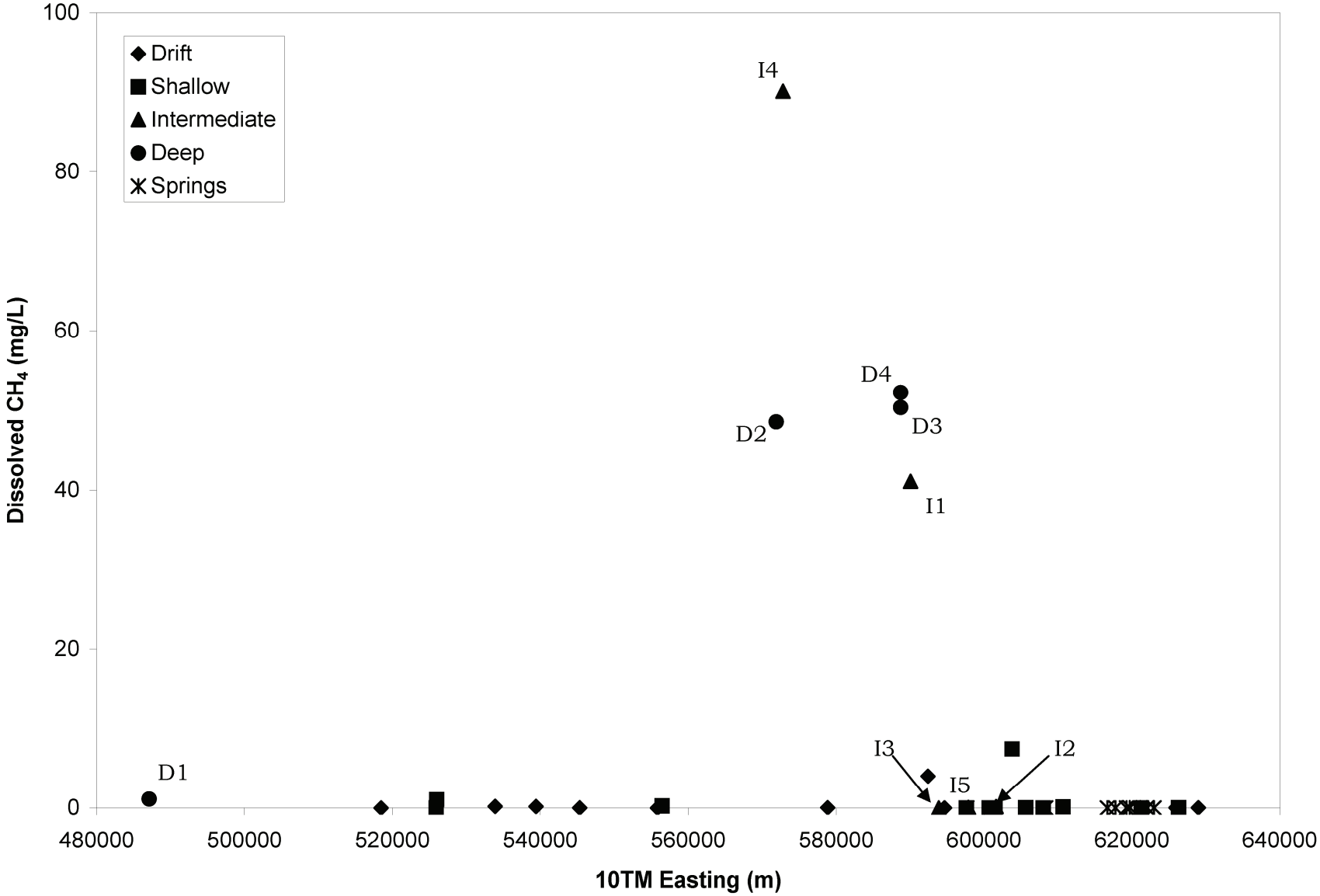

Figure 13. Easting versus concentrations of dissolved CH_4 in groundwater and springwater samples, south-central Alberta. Abbreviation: 10TM, 10-Degree Transverse Mercator.

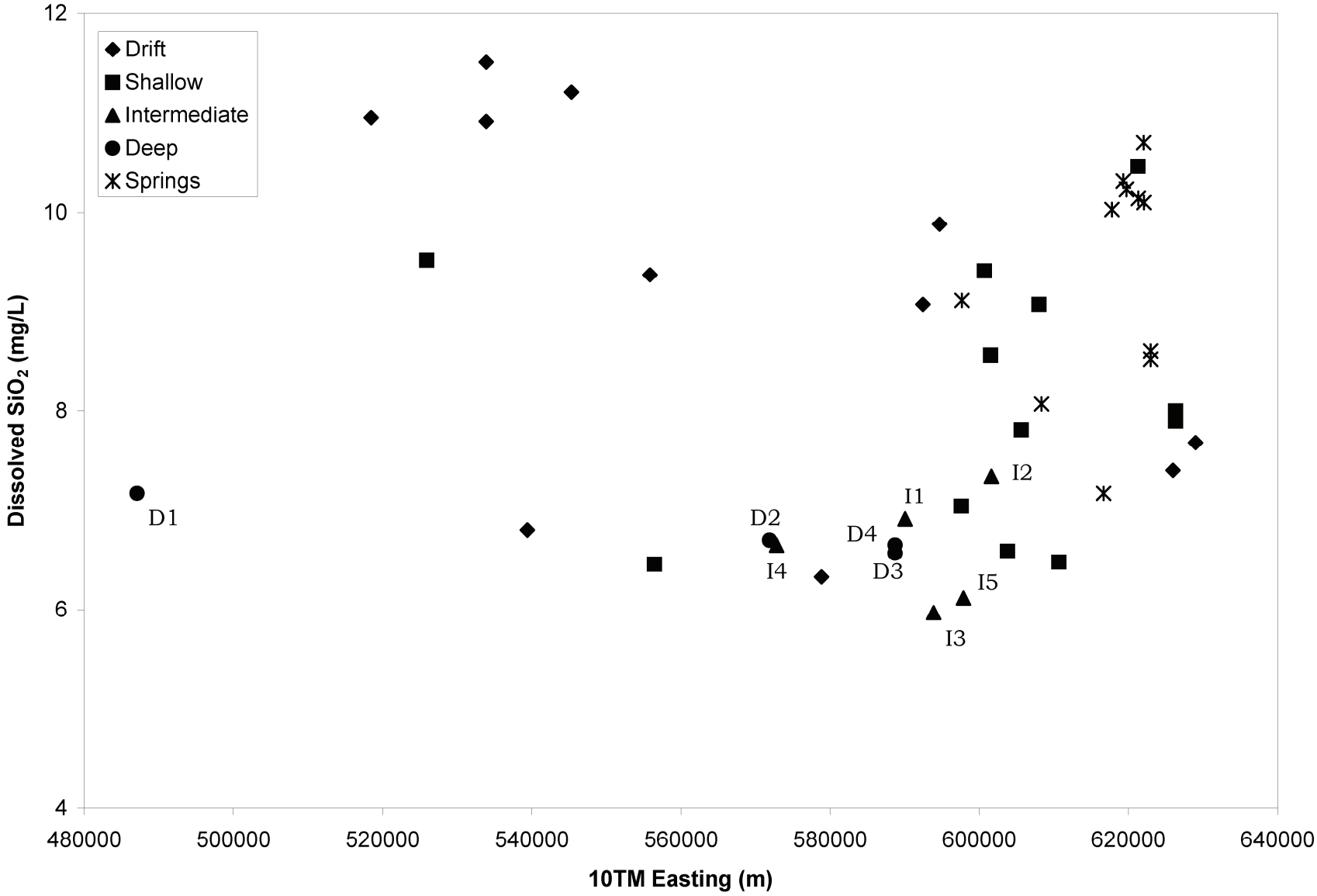

Figure 14. Easting versus concentrations of dissolved SiO_2 in groundwater and springwater samples, south-central Alberta. Abbreviation: 10TM, 10-Degree Transverse Mercator.

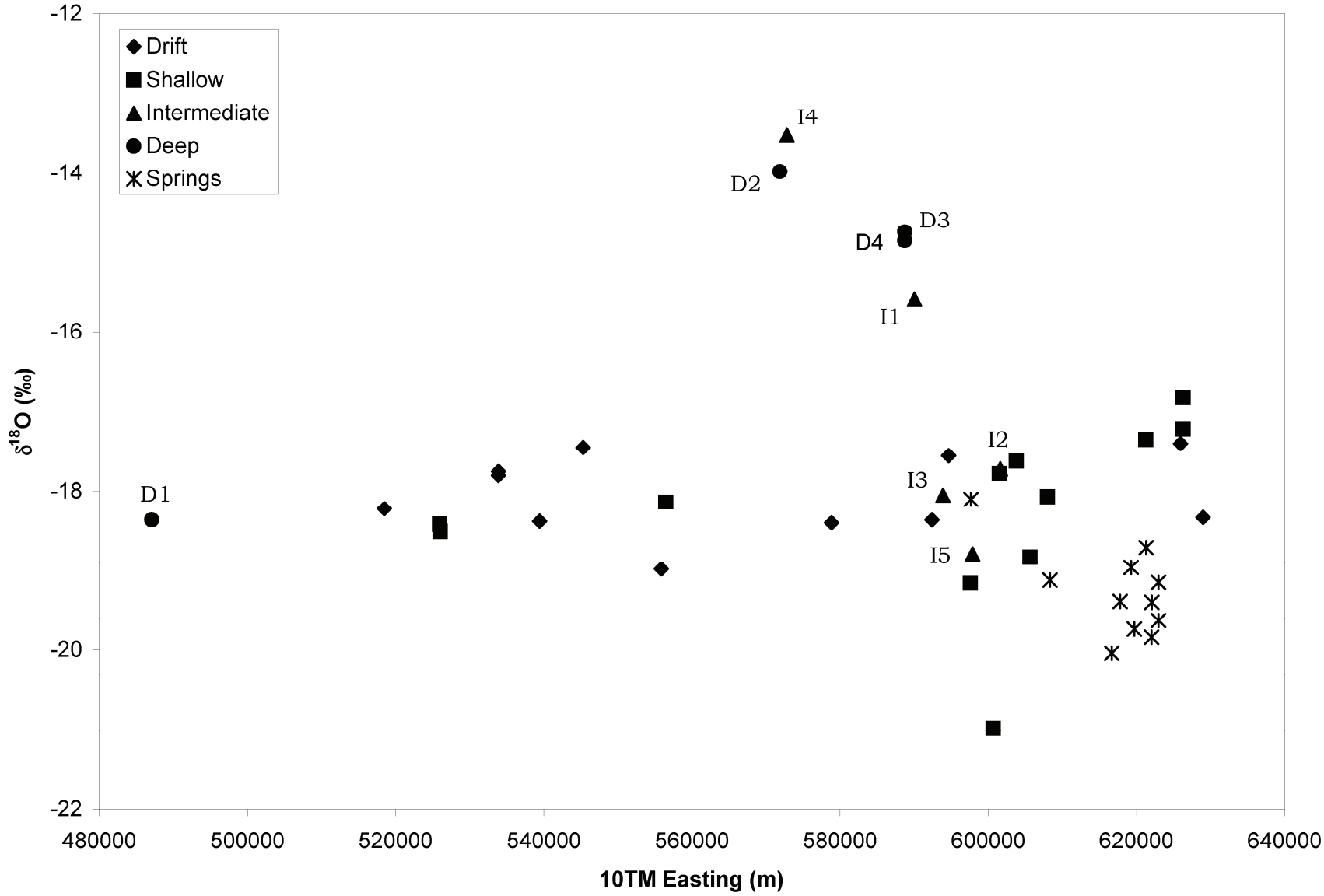

Figure 15. Easting versus values of $\delta^{18}O$ in groundwater and springwater samples, south-central Alberta. Abbreviation: 10TM, 10-Degree Transverse Mercator.

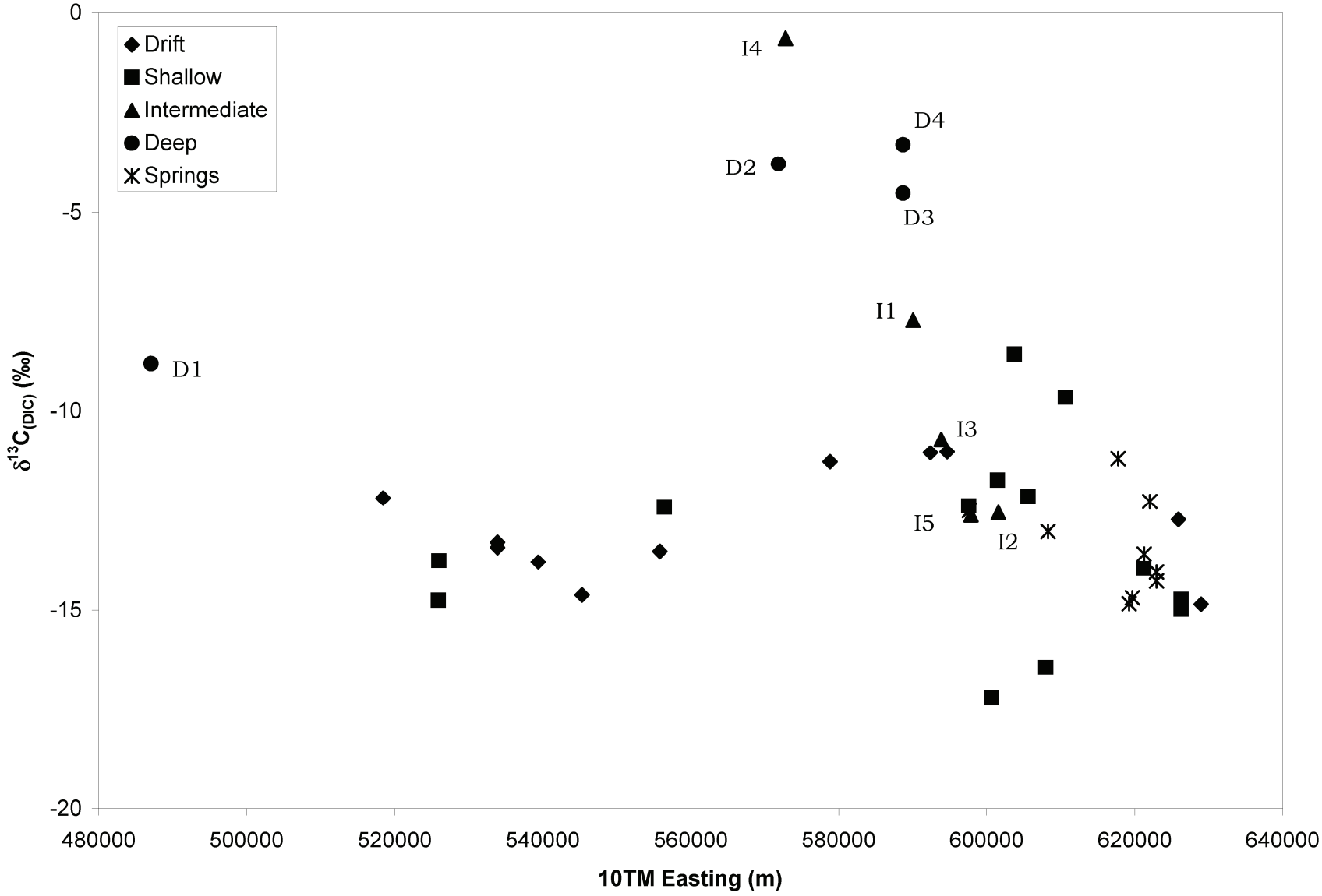

Figure 16. Easting versus values of $\delta^{13}C_{(DIC)}$ in groundwater and springwater samples, south-central Alberta. Abbreviation: 10TM, 10-Degree Transverse Mercator.

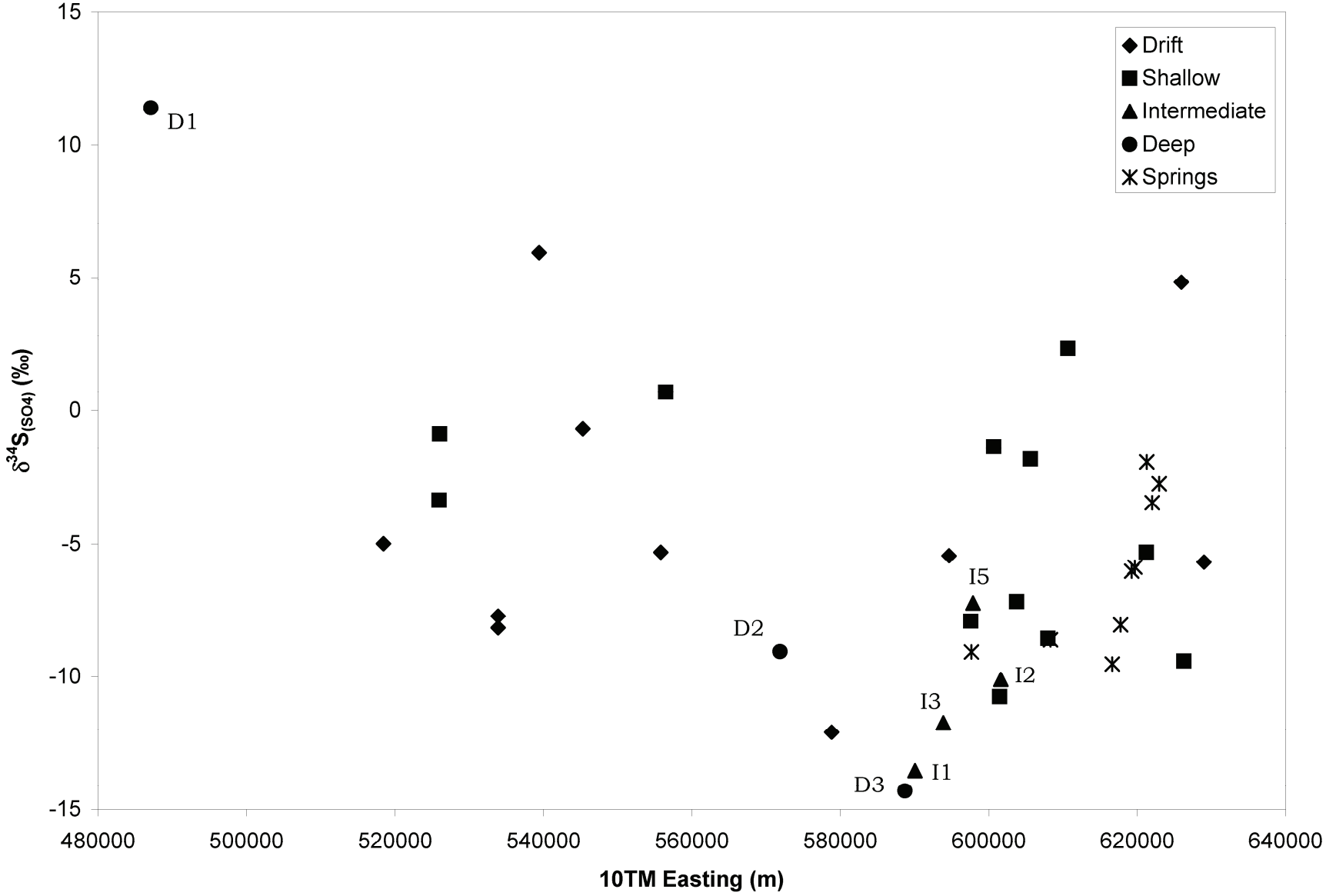

Figure 17. Easting versus values of $\delta^{34}S_{(SO4)}$ in groundwater and springwater samples, south-central Alberta. Abbreviation: 10TM, 10-Degree Transverse Mercator.

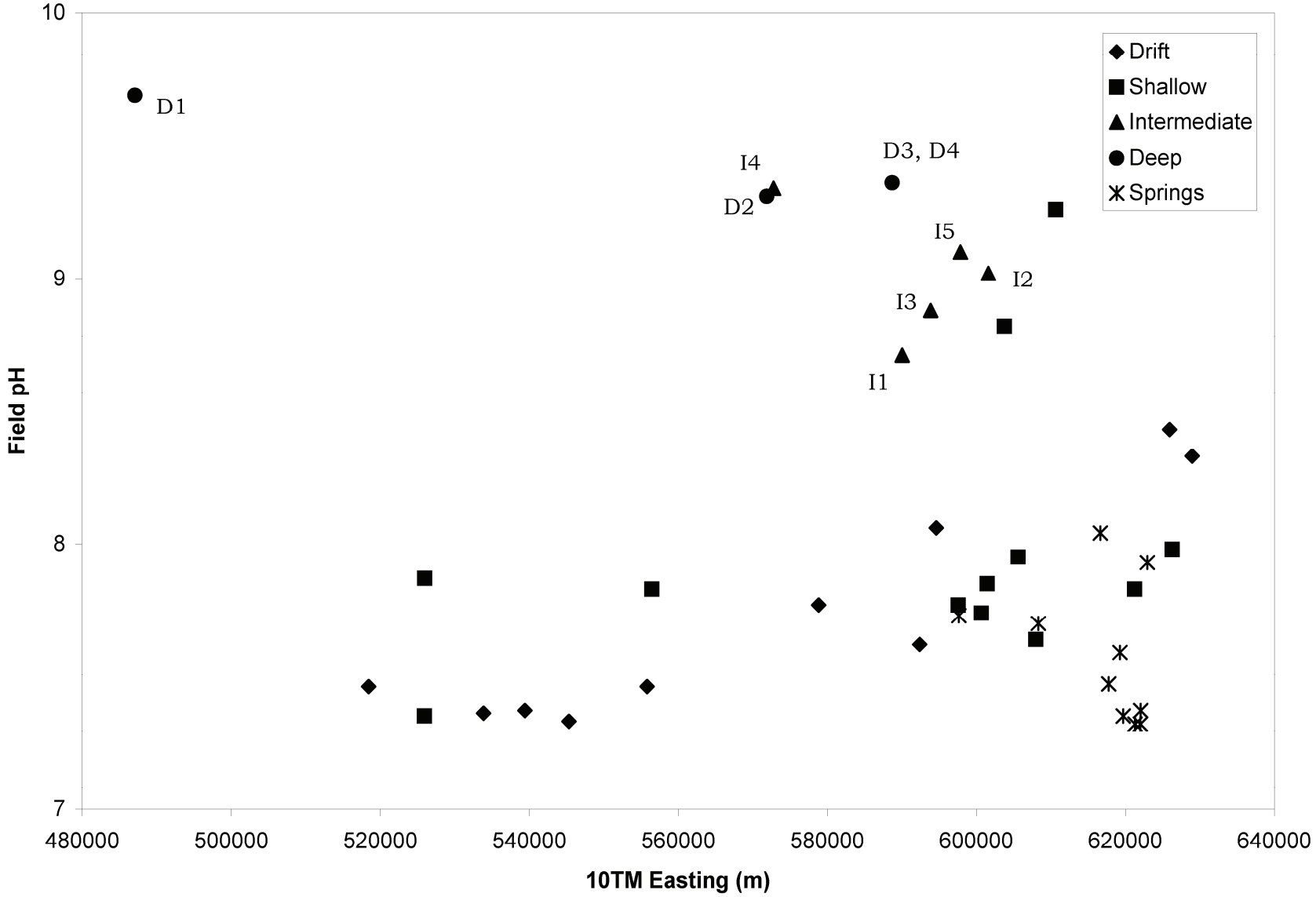

Figure 18. Easting versus values of field pH in groundwater and springwater samples, south-central Alberta. Abbreviation: 10TM, 10-Degree Transverse Mercator.

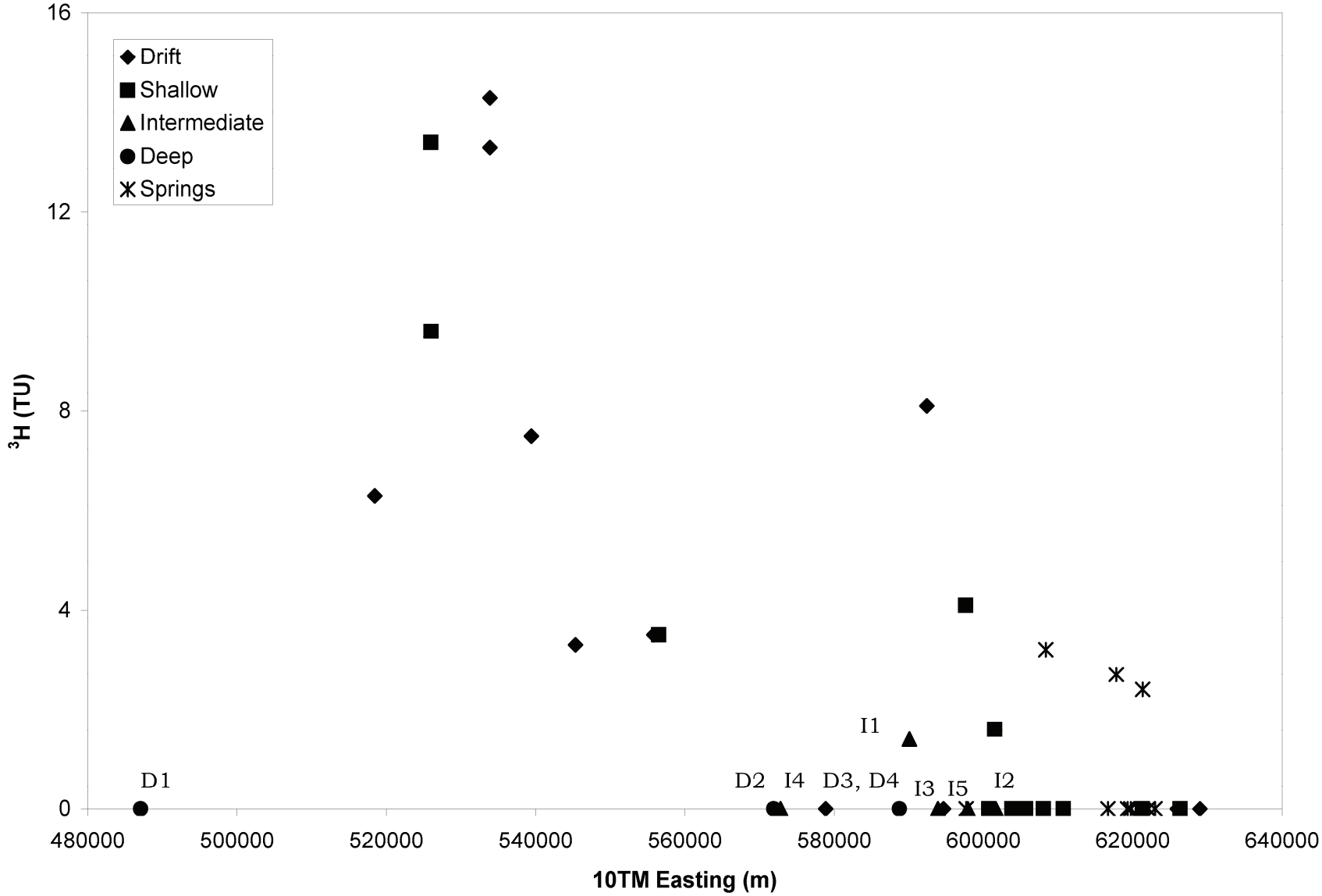

Figure 19. Easting versus concentrations of ^{3}H in groundwater and springwater samples, south-central Alberta. Abbreviations: 10TM, 10-Degree Transverse Mercator; TU, tritium units.

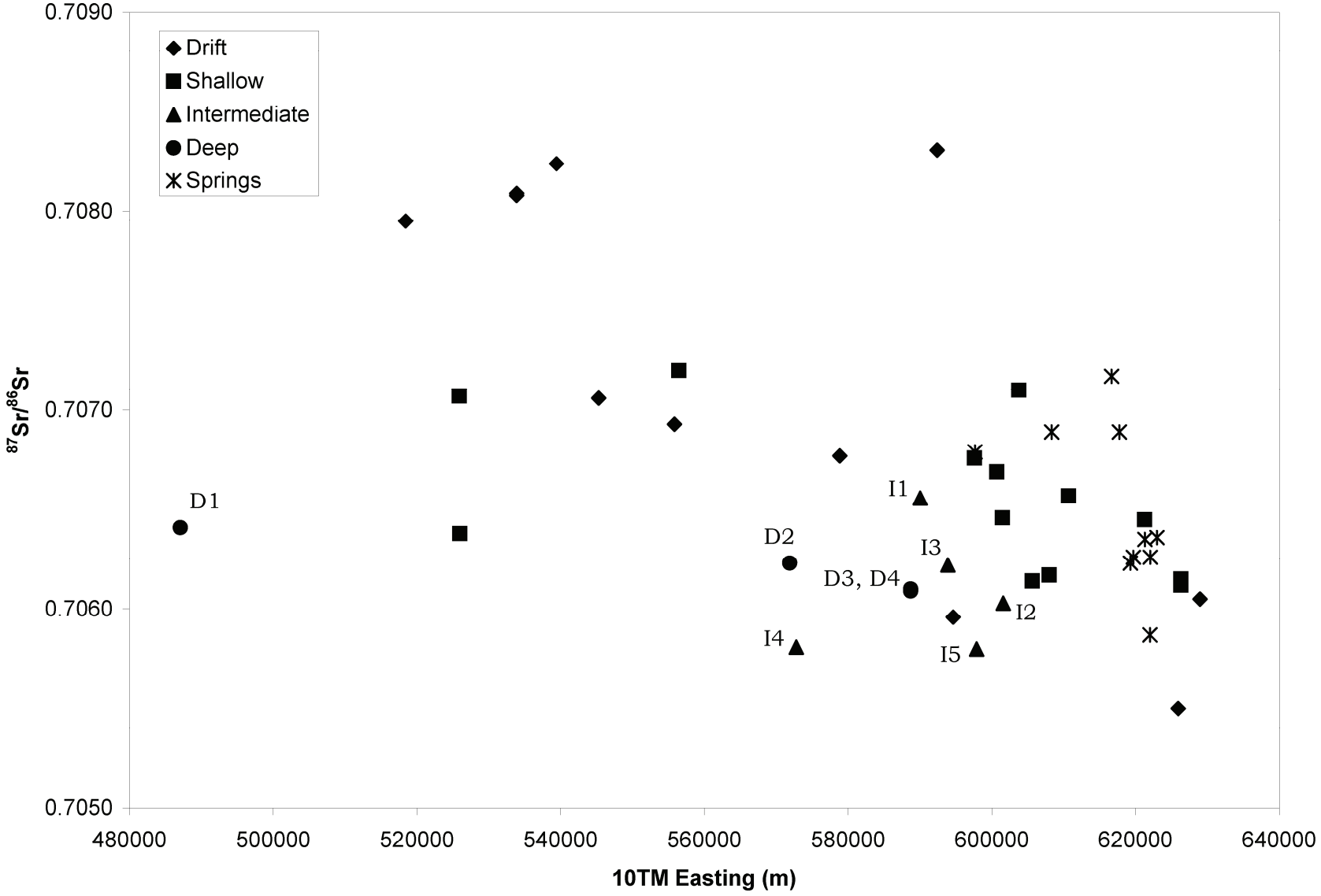

Figure 20. Easting versus values of $^{87}Sr/^{86}Sr$ in groundwater and springwater samples, south-central Alberta. Abbreviation: 10TM, 10-Degree Transverse Mercator.

Vertical changes in groundwater geochemistry within the Paskapoo Formation are, in some instances, more subtle than the lateral changes described above. Concentrations of dissolved Ca (Figure 8) and dissolved Mg (Figure 10) in intermediate and deep samples are less than those in shallower samples collected at similar eastings. Concentrations of dissolved Cl (Figure 11) and dissolved CH_4 (Figure 13) and values of $\delta^{18}O$ (Figure 15) and $\delta^{13}C_{(DIC)}$ (Figure 16) are elevated in samples I1, I4, D2, D3 and D4 relative to shallower samples collected at similar eastings. Values of field pH are elevated in all intermediate and deep samples relative to shallower samples collected at similar eastings (Figure 18).

A plot of $\delta^{18}O$ versus $\delta^{2}H$ (Figure 21) shows that points representing samples I1, I4, D2, D3 and D4 lie in a distinct group and are less depleted in ^{18}O and ^{2}H relative to other groundwater and springwater samples. Samples I1, I4, D2, D3 and D4 show increasing values of $\delta^{13}C_{(DIC)}$ with increasing values of $\delta^{18}O$ (Figure 22) and show increasing concentrations of dissolved CH_4 with increasing values of $\delta^{13}C_{(DIC)}$ (Figure 23). Concentrations of $^{14}C_{(DIC)}$ systematically decrease with increasing alkalinity in drift and shallow Paskapoo Formation samples. Samples I1, I4, D2, D3 and D4 show depletion in $^{14}C_{(DIC)}$ relative to samples of similar alkalinities (Figure 24). Plots of $\delta^{34}S_{(SO4)}$ versus concentrations of dissolved SO_4 (Figure 25) and of $^{34}S/^{32}S$ versus reciprocal dissolved SO_4 concentrations (Figure 26) show no systematic trends or variations.

3.2 Chemical Weathering of Glacial Drift

The study area is generally covered by approximately 5 to 50 m of glacial drift (Pawlowicz and Fenton, 1995; Slattery and Barker, 2010). Maximum glacial drift thicknesses within the study area occur in the eastern (Laurentide) part of the study area. Chemical weathering of Cordilleran-derived glacial drift in the western part of the study area produces a Ca-HCO_3–type water through dissolution of carbonate minerals (Grasby et al., 2008). In the eastern part of the study area, Na-SO_4–type waters occur in association with Laurentide-derived glacial drift. Various authors disagree on the chemical weathering reactions needed to produce Na-SO_4–type waters. Sources of dissolved SO_4 in the groundwater associated with sulphide-mineral–bearing glacial drift are thought to include oxidation of pyrite, oxidation of organic S or a combination of the two (Wallick, 1981; Hendry et al., 1986; Mermut and Arshad, 1987; Keller et al., 1991; Van Stempvoort et al., 1994; Grasby et al., 2010). Suggested sources of dissolved Na in these Na-SO_4–type waters include aluminosilicate-mineral weathering (Wallick, 1981; Mermut and Arshad, 1987; Keller et al., 1991), carbonate dissolution and cation exchange (Hendry et al., 1986), and aluminosilicate-mineral weathering and cation exchange (Grasby et al., 2010). The relative importance of possible geochemical reactions in generating Na-SO_4–type waters from chemical weathering of Laurentide-derived glacial drift has not been studied in the context of a well-constrained mass-balance geochemical model. This study used NETPATH (Plummer et al., 1994), in conjunction with geochemical, mineralogical, thermodynamic and isotopic constraints, in a mass-balance modelling approach to study the generation of Na-SO_4($\pm HCO_3$)–type groundwater in the eastern half of the study area.

3.2.1 Modelling Approach, Model Constraints, Reactive Phases and Data Sources

NETPATH calculates the mass transfer of solid and gas phases into or out of solution to account for chemical changes observed between an initial and final water composition. NETPATH also calculates changes in selected isotopic compositions of water that interact with solid and gas phases. We undertook mass-balance modelling of the chemical weathering of Laurentide-derived glacial drift in the eastern part of the study area using tandem approaches. In the first approach, we reacted selected solid and gas phases with an initial dilute water, acting as a proxy for precipitation, to produce a final water composition matching that of groundwater and springwater samples from the Laurentide-derived glacial drift and groundwater samples from the underlying shallow Paskapoo Formation. In the second approach, we ranked groundwater and springwater samples by alkalinity.

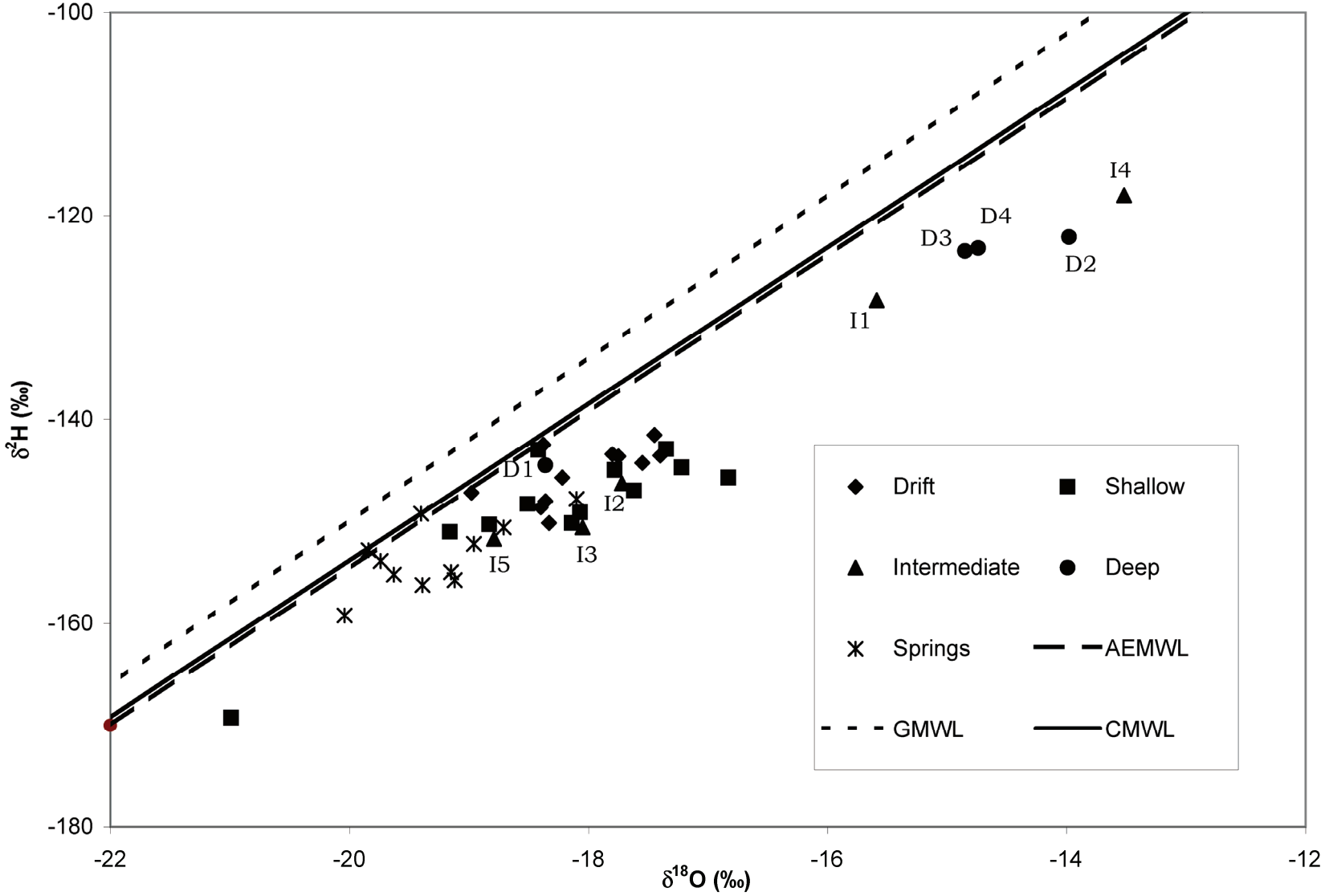

Figure 21. Values of $\delta^{18}O$ versus values of $\delta^{2}H$ in groundwater and springwater samples, south-central Alberta. Also shows the Calgary meteoric waterline (CMWL; Peng et al., 2004), the approximate Edmonton meteoric waterline (AEMWL; International Atomic Energy Agency/World Meteorological Organization, 2001) and the global meteoric waterline (GMWL; Craig, 1961).

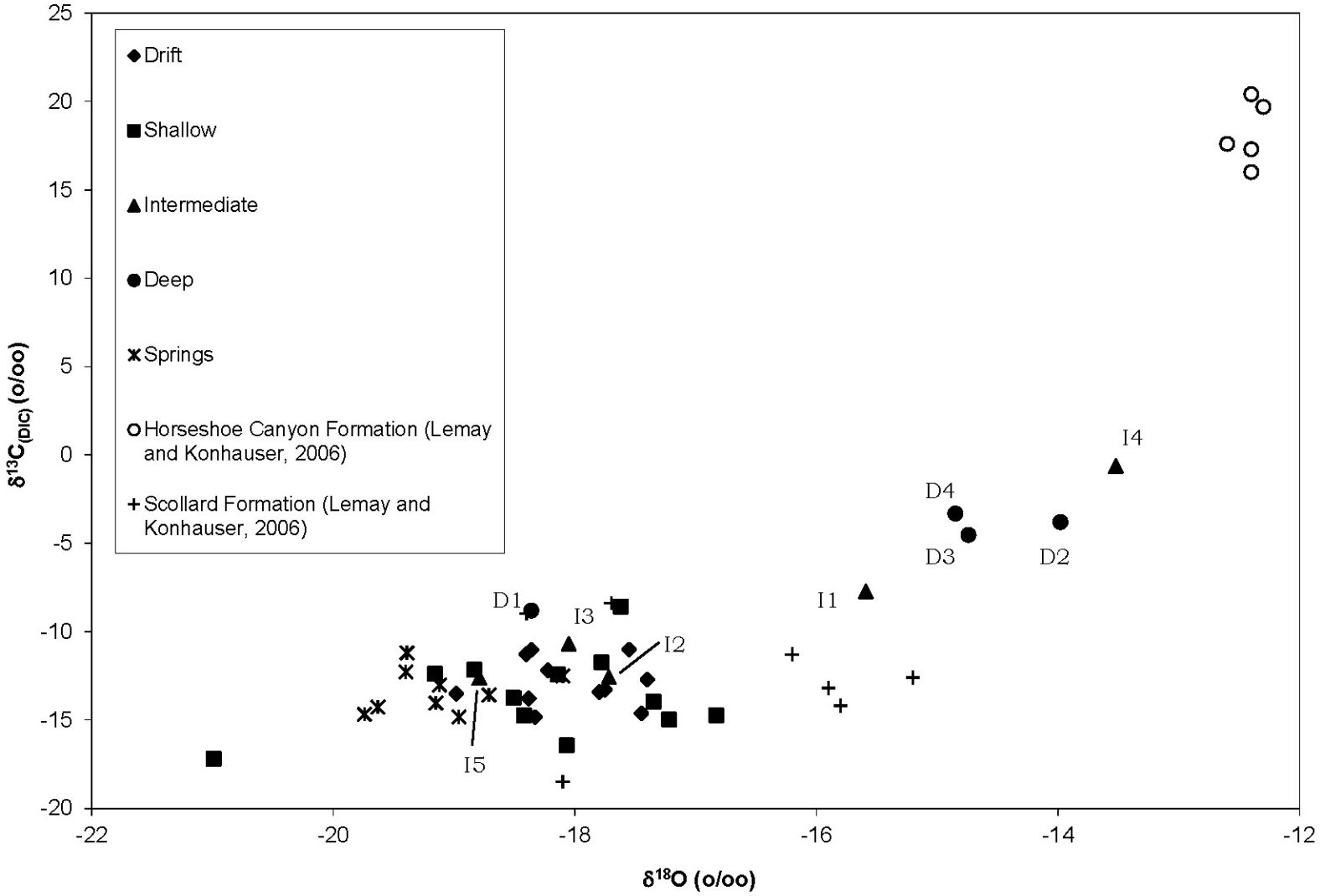

Figure 22. Values of $\delta^{18}O$ versus values of $\delta^{13}C_{(DIC)}$ in groundwater and springwater samples, south-central Alberta.

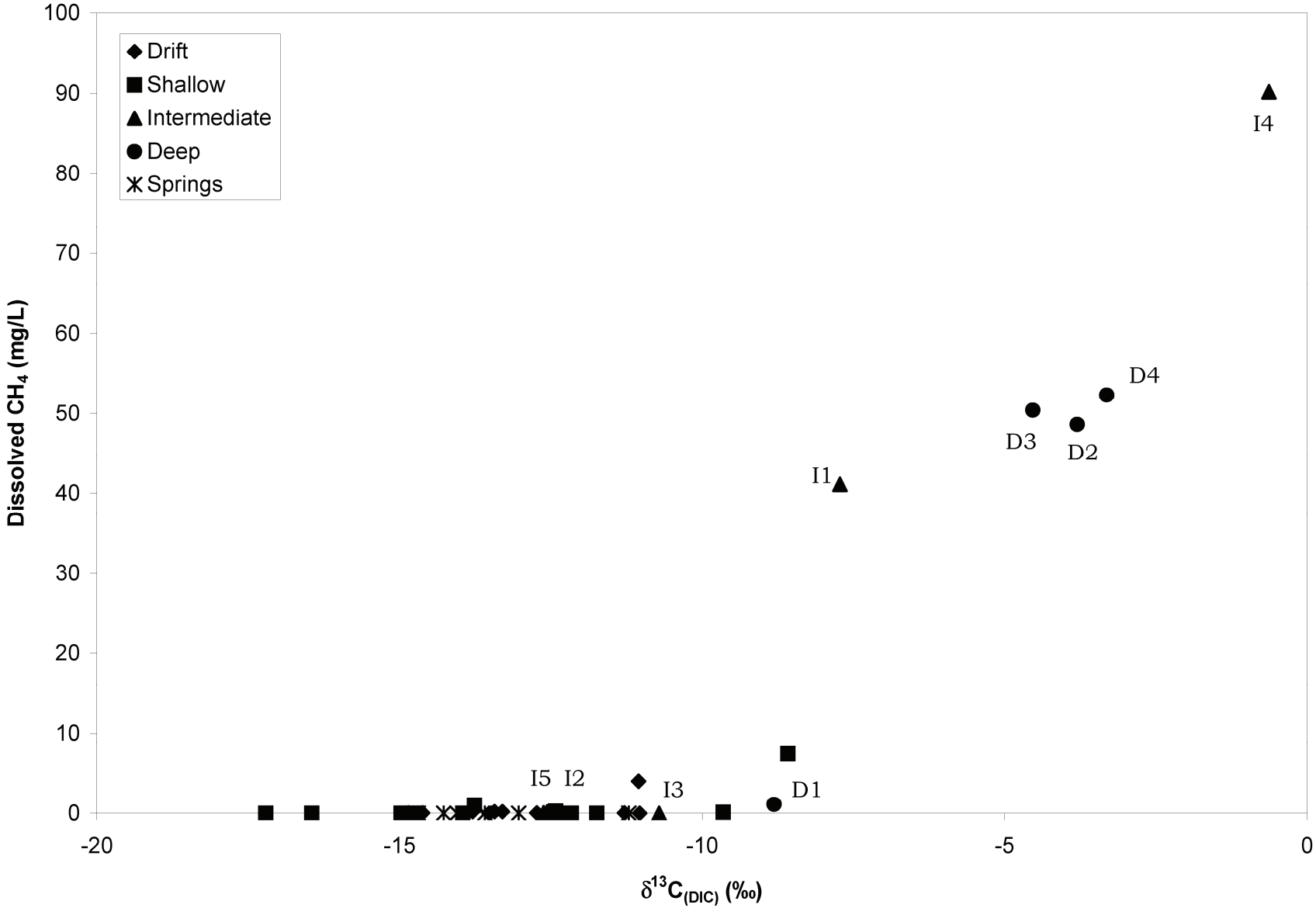

Figure 23. Values of $\delta^{13}C_{(DIC)}$ versus concentrations of dissolved CH_4 in groundwater and springwater samples, south-central Alberta.

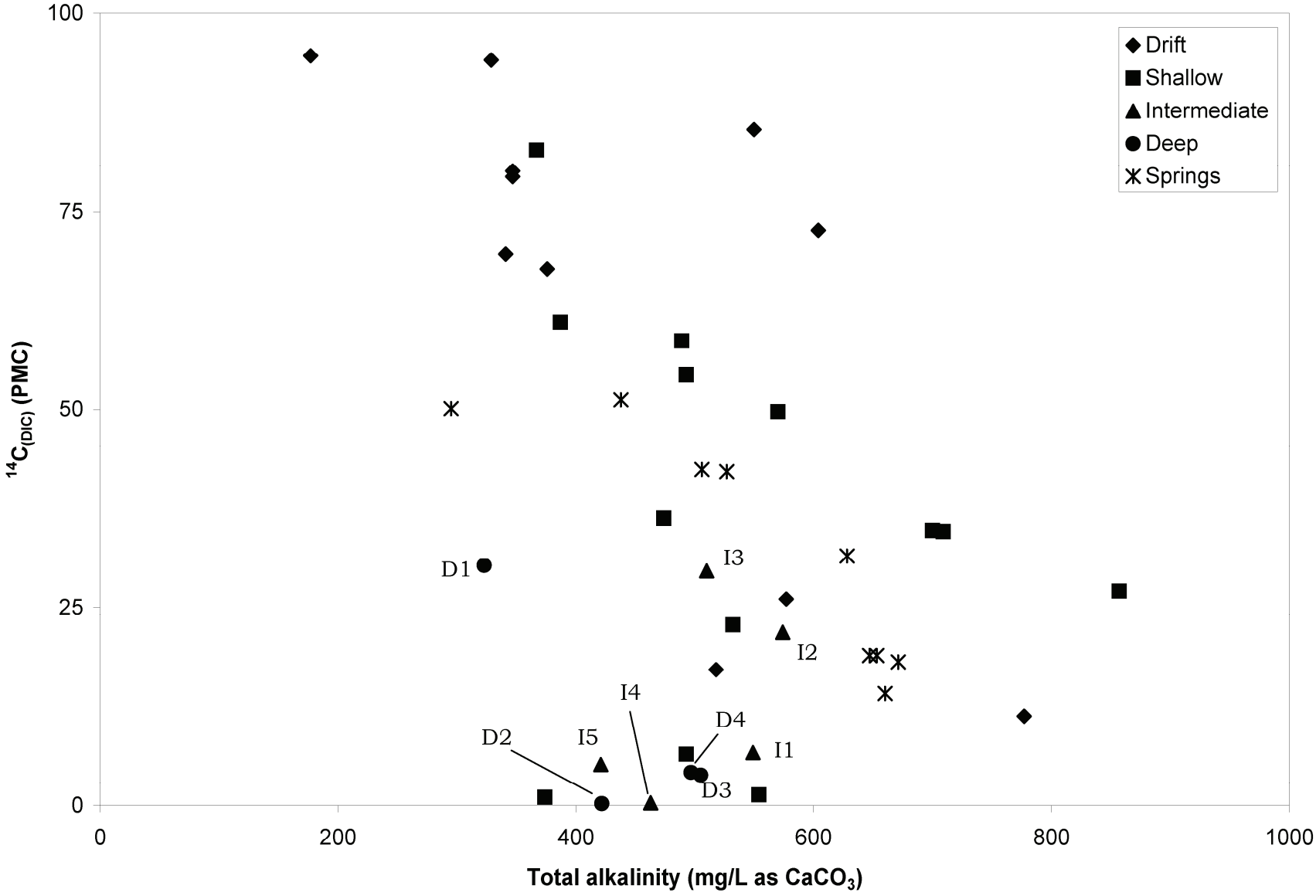

Figure 24. Alkalinity versus concentrations of $^{14}C_{(DIC)}$ in groundwater and springwater samples, south-central Alberta. Abbreviation: PMC, per cent modern carbon.

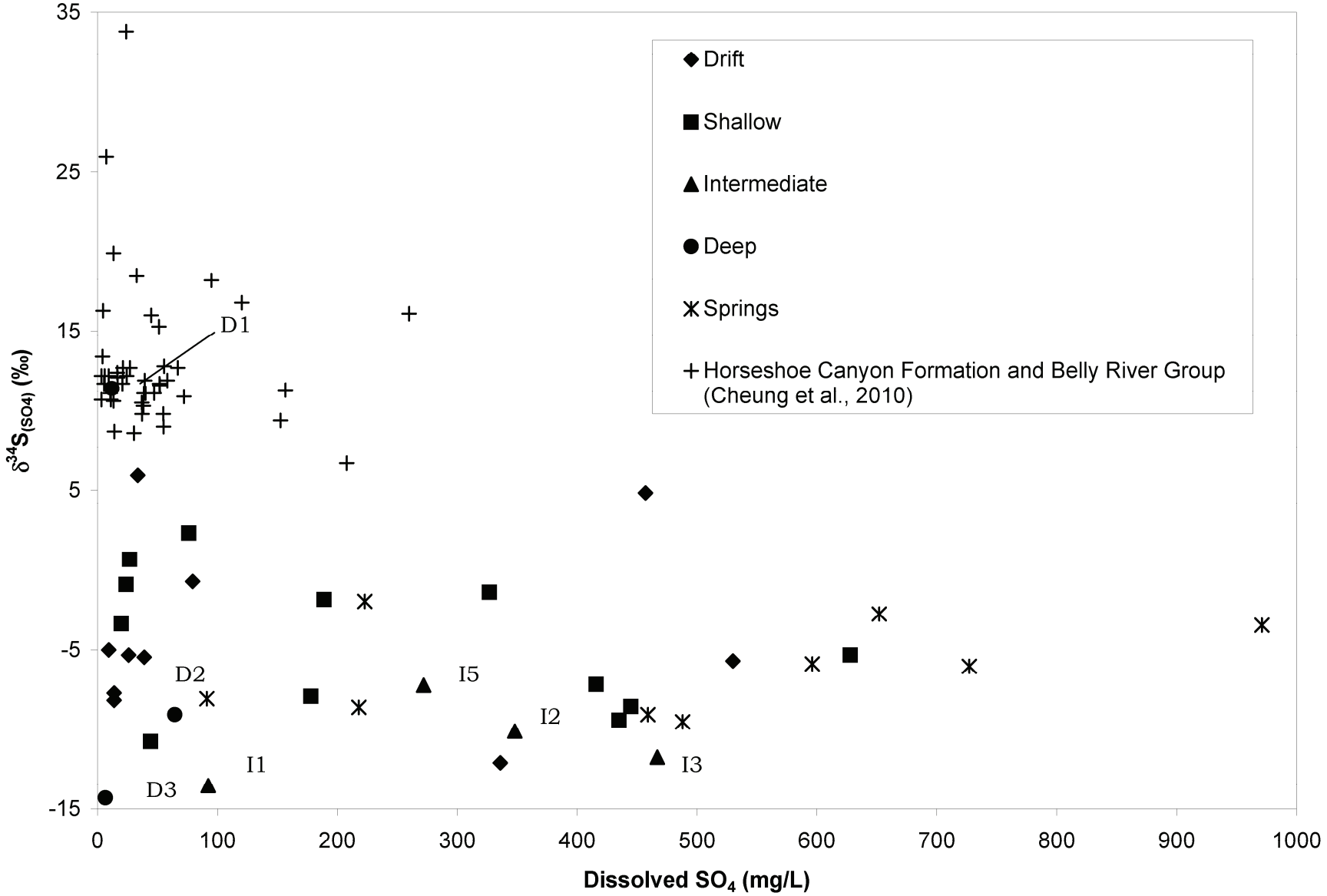

Figure 25. Concentrations of dissolved SO_4 versus values of $\delta^{34}S_{(SO4)}$ in groundwater and springwater samples, south-central Alberta.

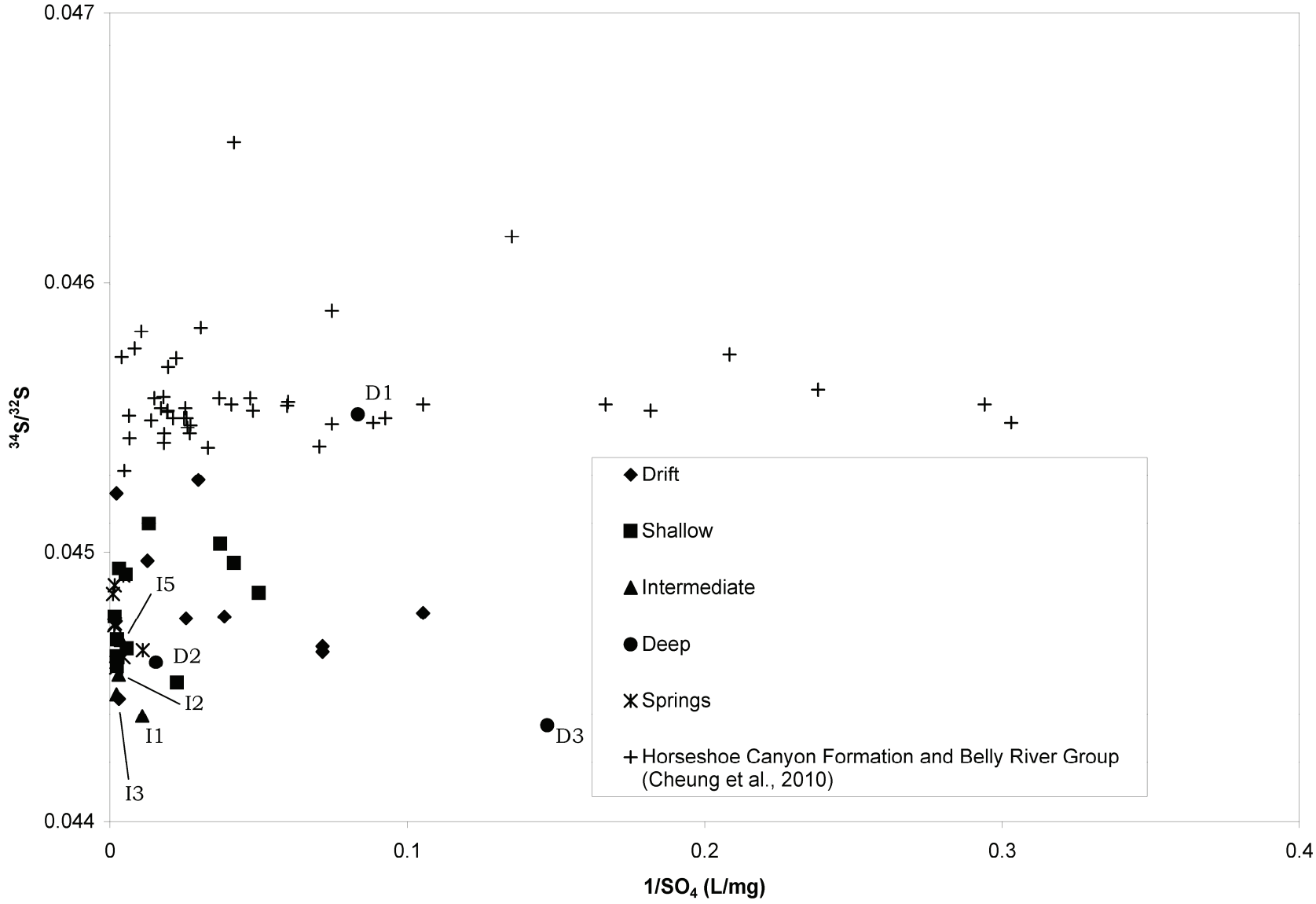

Figure 26. Values of $1/SO_4$ versus values of $^{34}S/^{32}S$ in groundwater and springwater samples, south-central Alberta, and in coalbed methane (CBM) coproduced water from the Horseshoe Canyon Formation and Belly River Group as reported by Cheung et al. (2010), central Alberta.

The sample with the smallest alkalinity was treated as the initial water in NETPATH. This initial water was reacted with selected solid and gas phases to produce a final water composition matching that of groundwater and springwater samples from the Laurentide-derived glacial drift and groundwater samples from the underlying shallow Paskapoo Formation.

NETPATH models that successfully replicated observed changes in concentrations of dissolved Ca, Mg, Na, K, Fe, SO_4, HCO_3 and SiO_2 between initial and final waters were further constrained by requiring agreement between observed and calculated $\delta^{13}C_{(DIC)}$ values in the final water. Concentrations of Al were set to zero in initial and final waters to force conservation of Al during simulated aluminosilicate-mineral weathering. Microbially mediated dolomite precipitation has been suggested to occur in SO_4-reducing (Vasconcelos and McKenzie, 1997) and methanogenic (Roberts et al., 2004) freshwater environments. Neither patterns in the relationship between dissolved SO_4 versus $\delta^{34}S_{(SO4)}$ (Figure 25) nor concentrations of dissolved CH_4 (Table 1) indicate the presence of a SO_4-reducing or methanogenic environment within either the glacial drift or underlying shallow Paskapoo Formation groundwater within the study area. Therefore, NETPATH models requiring the precipitation of dolomite were rejected.

Potentially reactive solid phases included in NETPATH simulations were selected based on published mineralogical descriptions of Laurentide-derived glacial drift and on thermodynamic considerations. Potentially reactive solid phases initially included in NETPATH simulations based on mineralogical descriptions of Laurentide-derived glacial drift included calcite, dolomite, pyrite, siderite, illite and gypsum. Albite (Wallick, 1981) and CO_2 gas (Keller, 1991) were included as potentially reactive phases based on their potential roles in chemical weathering of Laurentide-derived glacial drift. Likewise, Ca/Na and Mg/Na cation exchange were initially included as potentially reactive phases based on the conclusions of Hendry et al. (1986) and Grasby et al. (2010). The apparent approach to thermodynamic equilibrium between quartz/chalcedony and Laurentide-drift groundwater reported by Grasby et al. (2010) justified initial inclusion of SiO_2 as a potentially reactive phase. Samples of Laurentide-drift groundwater and springwater and underlying shallow Paskapoo Formation groundwater collected in our study area cluster near the kaolinite–Na-smectite phase boundary (Figure 27) suggesting an approach to thermodynamic equilibrium between these two phases. Points in Figure 27 that lie off the kaolinite–Na-smectite phase boundary represent groundwater from the Cordilleran-derived glacial drift in the western part of the study area. Therefore, kaolinite and Na-smectite were included as potentially reactive phases.

A well-defined increase in dissolved SO_4 concentrations in glacial drift and shallow Paskapoo Formation groundwater at about 10TM 580000E (Figure 6) infers the approximate contact between Cordilleran-derived glacial drift to the west and Laurentide-derived glacial drift to the east. Water samples from glacial drift, the shallow Paskapoo Formation and springs were screened for inclusion in NETPATH simulations based on two criteria. Criterion 1 required dissolved SO_4 concentrations to be ≥250 mg/L based on information shown in Figure 6. Criterion 2 required dissolved Cl concentrations to be ≤10 mg/L to avoid the potential effects of de-icing salts. Chemical compositions of glacial drift and Paskapoo Formation groundwater samples collected within and adjacent to our study area by Grasby et al. (2010) were screened for inclusion in our NETPATH simulations in an effort to extend our dataset. Screening of the Grasby et al. (2010) dataset used criteria 1 and 2 above plus the requirement that the charge balance of a reported analysis fall within ±5%. The Grasby et al. (2010) dataset contains no analytical data for dissolved SiO_2. However, Grasby et al. (2010) report that more than 80% of their samples show saturation indices for quartz that fall between –0.2 and 0.2 and conclude that groundwater approaches thermodynamic equilibrium with either quartz or chalcedony. We will examine this conclusion in a later section of our report and demonstrate that the saturation indices for quartz calculated by Grasby et al. (2010) are misleading but fortuitous. However, these fortuitous saturation indices can be used to assign approximate dissolved SiO_2 concentrations to the analyses reported by Grasby et al. (2010), which passed our screening criteria, for subsequent use in our NETPATH simulations. PHREEQC (Parkhurst and Appelo, 1999) allows modelling of the composition of aqueous solutions based on the assumption of

thermodynamic equilibrium between aqueous and solid phases. PHREEQC was used to assign approximate dissolved SiO_2 concentrations to the analyses reported by Grasby et al. (2010) and passing our screening criteria by equilibrating the reported solution composition with chalcedony at the reported sampling temperature.

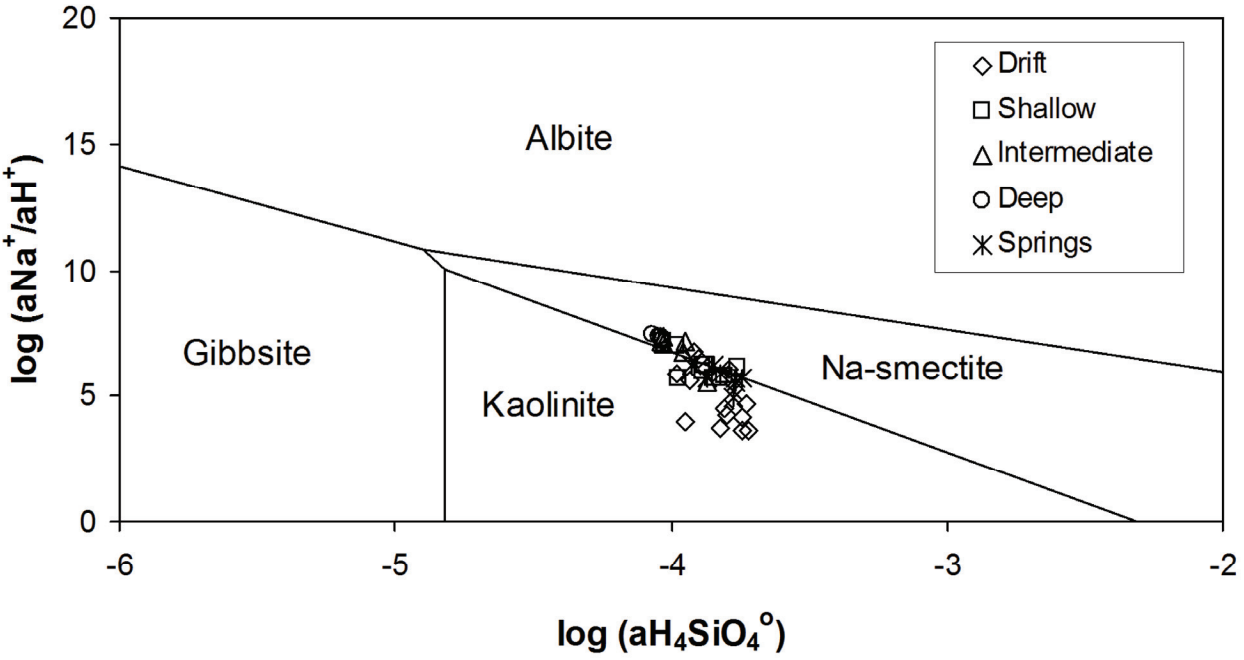

Figure 27. Chemical activities of H_4SiO_4 and Na^+/H^+ on the thermodynamic stability fields of gibbsite, kaolinite, Na-smectite and albite at 1 bar and 25˚C in groundwater and springwater samples, south-central Alberta.

3.2.2 Elimination of Potentially Reactive Phases on Geochemical, Thermodynamic and Isotopic Grounds

Oxidation of pyrite and/or organic S during chemical weathering of sulphide-mineral–bearing glacial drift has commonly been cited as the most likely source of dissolved SO_4 in the associated Na-SO_4–type groundwater (Wallick, 1981; Hendry et al., 1986; Mermut and Arshad, 1987; Keller et al., 1991; Van Stempvoort et al., 1994; Grasby et al., 2010). However, the presence of authigenic gypsum in association with oxidation fronts in sulphide-mineral–bearing glacial till was reported by Van Stempvoort et al. (1994). It is possible that Laurentide-derived glacial drift within our study area contains authigenic or detrital gypsum though none has been reported in available mineralogical descriptions. Dissolution of gypsum would produce equimolar amounts of dissolved Ca and SO_4. The lack of a strong positive correlation between dissolved Ca and dissolved SO_4 (Figure 28), in the absence of evidence for active SO_4 reduction, suggests the need for a Ca sink if dissolved SO_4 is produced through gypsum dissolution. Common Ca sinks include precipitation of calciteand dolomite and cation exchange. As previously discussed, precipitation of dolomite in our study area is unlikely. Cation exchange alone or precipitation of calcite through dedolomitization driven by gypsum dissolution would not cause a net change of alkalinity in solution. Precipitation of calcite in the absence of dissolution of other carbonate minerals would deplete alkalinity from solution. Consumption of dissolved Na, produced through Ca/Na cation exchange, by alteration of kaolinite to Na-smectite would also deplete alkalinity from solution.

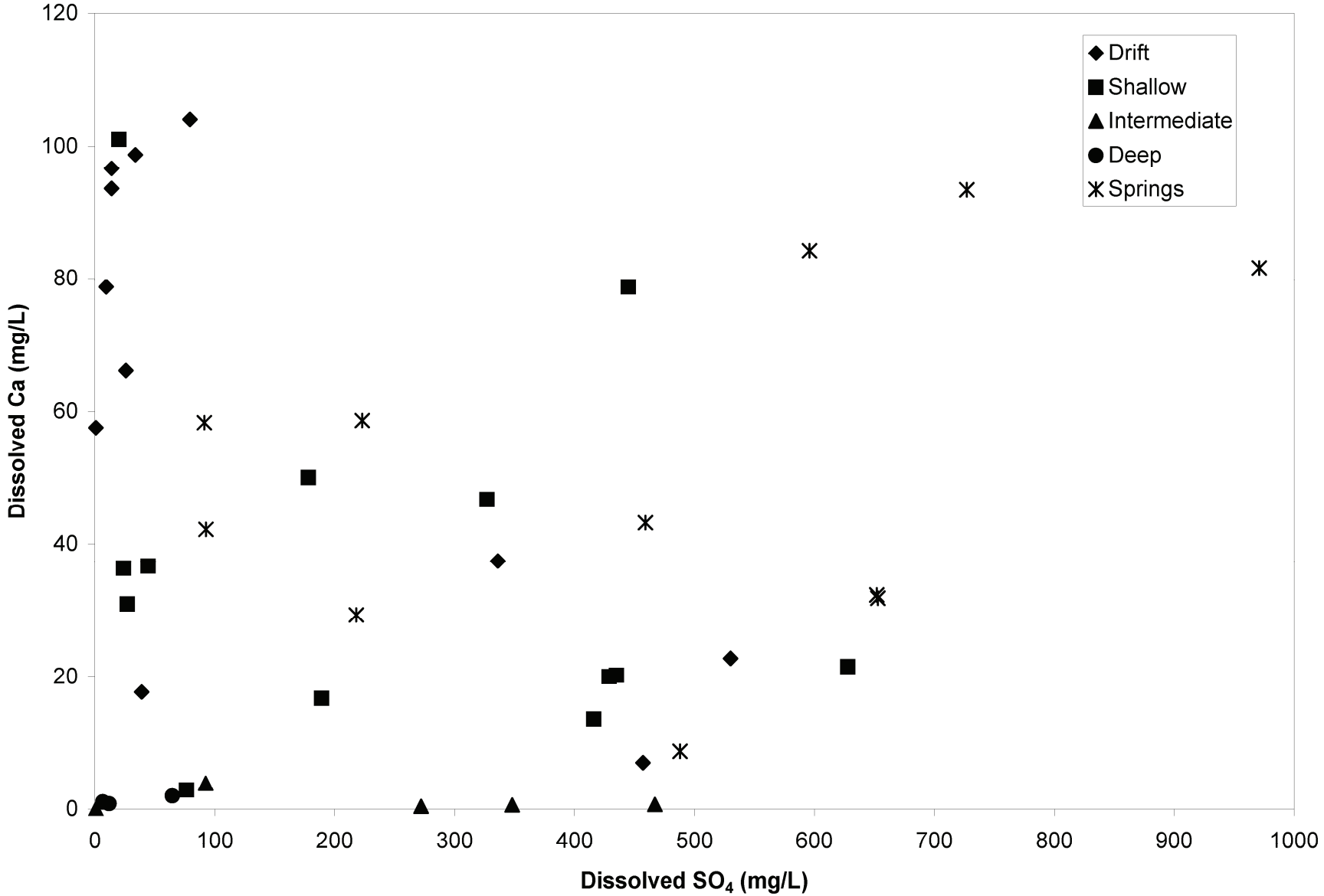

Figure 28. Concentrations of dissolved SO_4 versus concentrations of dissolved Ca in groundwater and springwater samples, south-central Alberta.

Concentrations of dissolved SO_4 and alkalinity in Laurentide-derived glacial-drift and shallow Paskapoo Formation groundwater ($SO_4 \geq 250$ mg/L) show a generally positive correlation (Figure 29), making gypsum dissolution an unlikely source of dissolved SO_4 in groundwater within the eastern part of our study area. The observed correlation between dissolved SO_4 and alkalinity is consistent with consumption of H^+, produced during pyrite oxidation, by aluminosilicate-alteration reactions and/or carbonate-mineral dissolution. Van Stempvoort et al. (1994) reported a $\delta^{34}S$ value of −11.4‰ for pyrite from sulphide-mineral–bearing glacial drift in southeastern Alberta. Groundwater with dissolved SO_4 concentrations ≥250 mg/L show $\delta^{34}S$ values between approximately −5‰ and −10‰, further suggesting pyrite oxidation as the source of dissolved SO_4 in glacial-drift and shallow Paskapoo Formation groundwater within the eastern part of the study area. Strong undersaturation with respect to gypsum (Table 3) makes gypsum precipitation unlikely. The unlikelihood of either gypsum dissolution or precipitation supports removal of gypsum as a potentially reactive phase in NETPATH simulations.

Grasby et al. (2010) reported saturation indices ranging mainly between 0.2 and –0.2 for quartz and suggested that either quartz or chalcedony could act as a sink for SiO_2 generated during chemical weathering of Laurentide-derived glacial drift. In our study, saturation indices calculated for chalcedony in glacial drift and shallow Paskapoo Formation groundwater and springwater samples having dissolved SO_4 concentrations ≥250 mg/L show values of –0.242 to 0.019 (Table 3). Saturation indices of chalcedony calculated in our study and saturation indices reported by Grasby et al. (2010) suggest an apparent approach to thermodynamic equilibrium with a pure SiO_2 solid phase. The solubility of pure SiO_2 phases is known to be largely unaffected by pH at values of approximately 9 or less (Drever, 1982). Laurentide-derived glacial-drift and shallow Paskapoo Formation groundwater show a strong correlation between dissolved SiO_2 concentrations and field pH at field pH values of approximately 8.5 or less (Figure 30). Additionally, saturation indices for quartz and chalcedony calculated for all water samples collected in our study area show a correlation with pH for values of pH approximately 8.5 or less (Figure 31). These correlations would not be expected if dissolved SiO_2 concentrations were buffered by a pure SiO_2 solid phase. Whereas SiO_2 precipitation appears unlikely, negative saturation indices calculated for amorphous silica ($SiO_{2(a)}$; Table 3) and stabilization of dissolved SiO_2 concentrations at pH values of approximately 9 and greater (Figure 30) leave open the possibility of SiO_2 dissolution as a potentially active process in NETPATH simulations.

In our study, >75% of glacial drift groundwater, shallow Paskapoo Formation groundwater and springwater samples with dissolved SO_4 concentrations ≥250 mg/L show calculated saturation indices for calcite that range from -0.2 to 0.4 (Table 3), suggesting an overall approach to thermodynamic equilibrium with respect to calcite. Evidence for an approach to thermodynamic equilibrium between kaolinite and Na-smectite has been previously described. An apparent approach to thermodynamic equilibrium either with solution or between solid phases was, with the exception of SiO_2, used as a criterion for mandatory inclusion of phases in NETPATH simulations. Additional mandatory phases included in each NETPATH simulation included pyrite, siderite and illite, as these phases control the budgets for SO_4, Fe and K, respectively. Representing the K budget in terms of a reaction involving illite was, ultimately, an arbitrary choice. Dissolved K concentrations observed in water samples collected from our study area range from <0.4 to 4.4 mg/L (Table 1). Reactions involving illite that would contribute this relatively small amount of K to solution would have minimal impact on the overall mass-balance budget. Formation of siderite as a product of pyrite oxidation is favoured over formation of Fe-oxide/oxyhydroxides in our simulations due to the prevalent low levels of dissolved O_2 measured in groundwater and the reported presence of siderite in Laurentide-derived glacial drift in northern Alberta (Plouffe et al., 2006). Optional potentially reactive phases (not mandatory in each NETPATH simulation) included dolomite (dissolution only), $SiO_{2(a)}$ (dissolution only), Na/Ca cation exchange, Na/Mg cation exchange and $CO_{2(g)}$. Plausible chemical reactions involving mandatory and optional phases are summarized in Table 4.

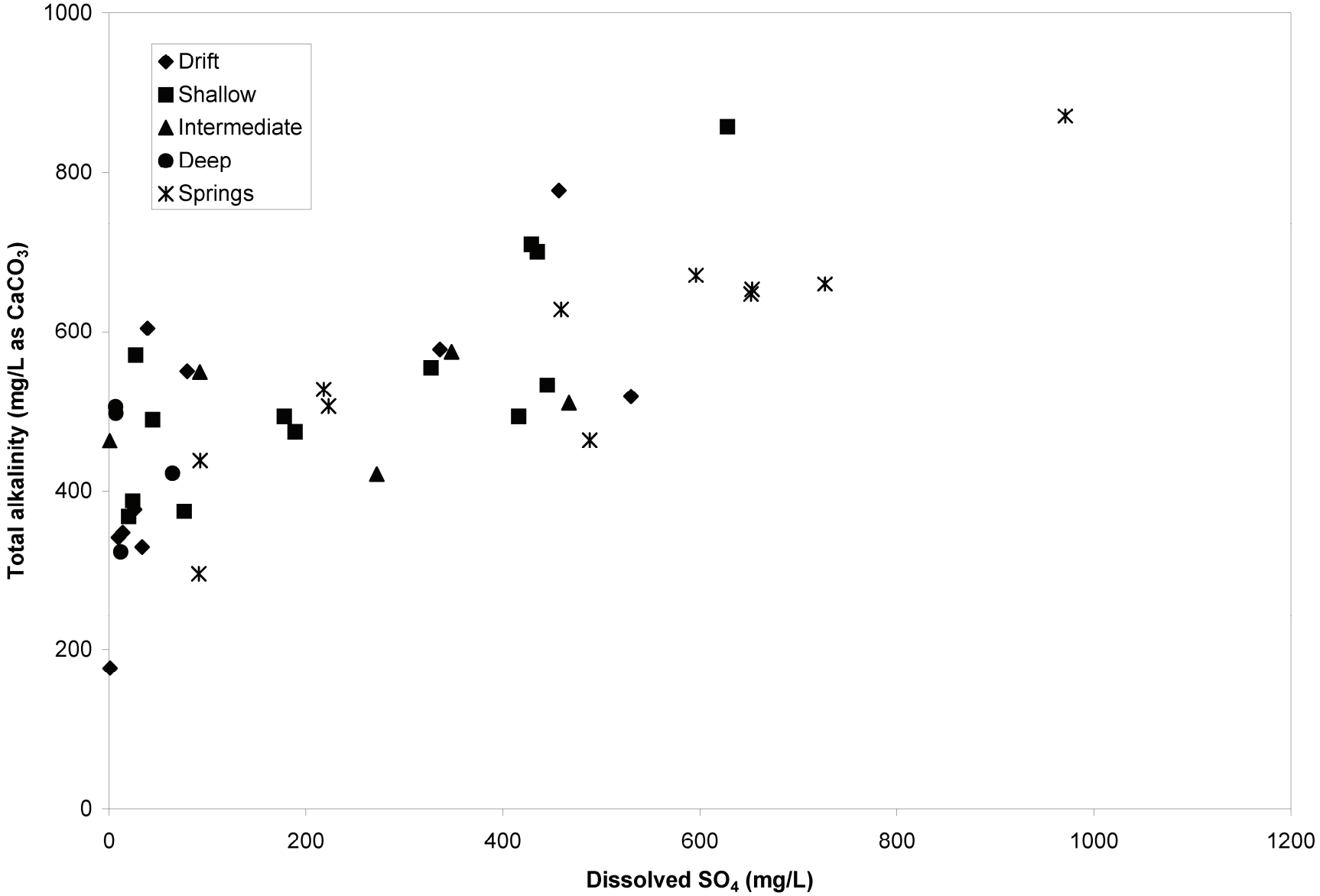

Figure 29. Concentrations of dissolved SO_4 versus alkalinity in groundwater and springwater samples, south-central Alberta.

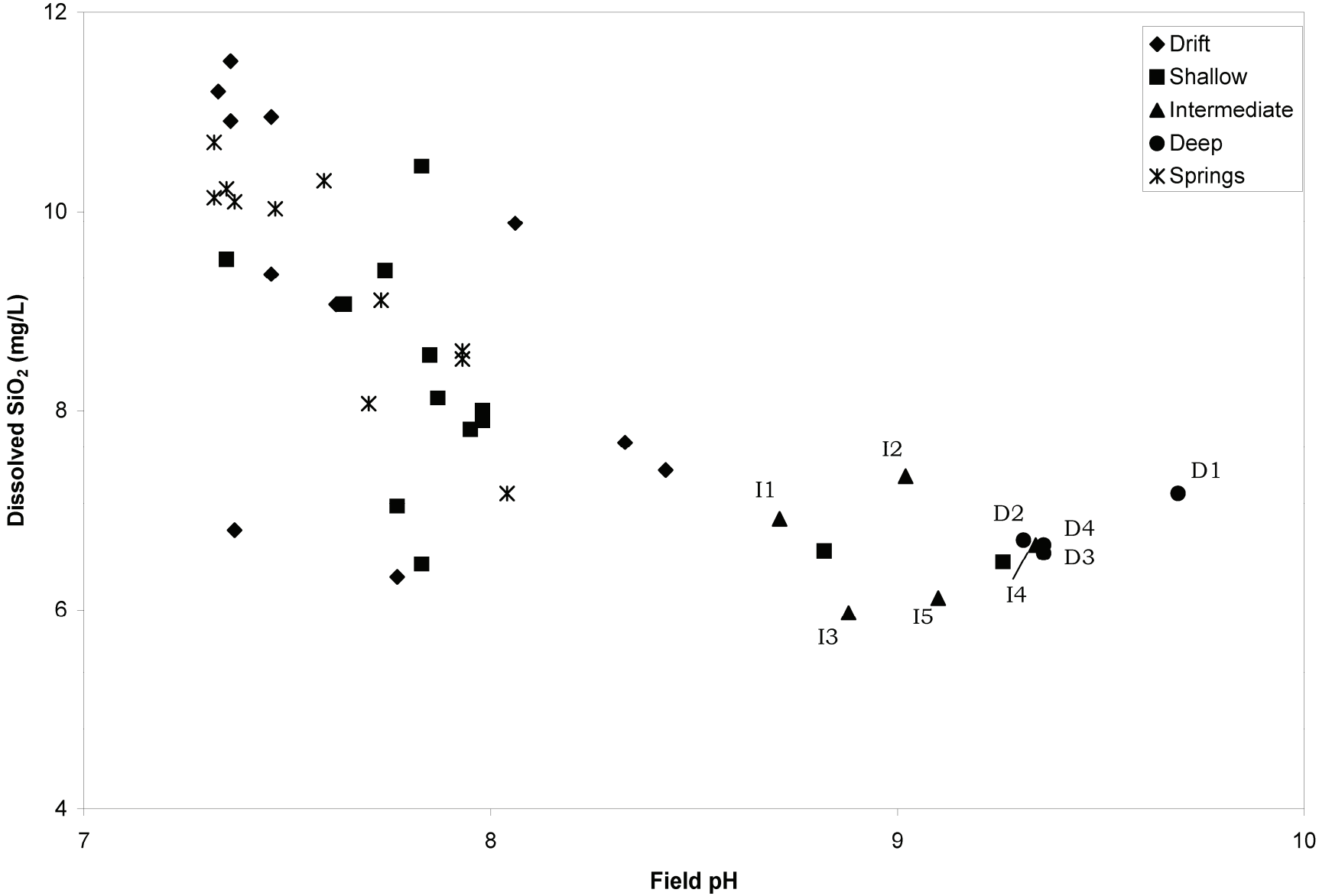

Figure 30. Values of field pH versus concentrations of dissolved SiO_2 in groundwater and springwater samples, south-central Alberta.

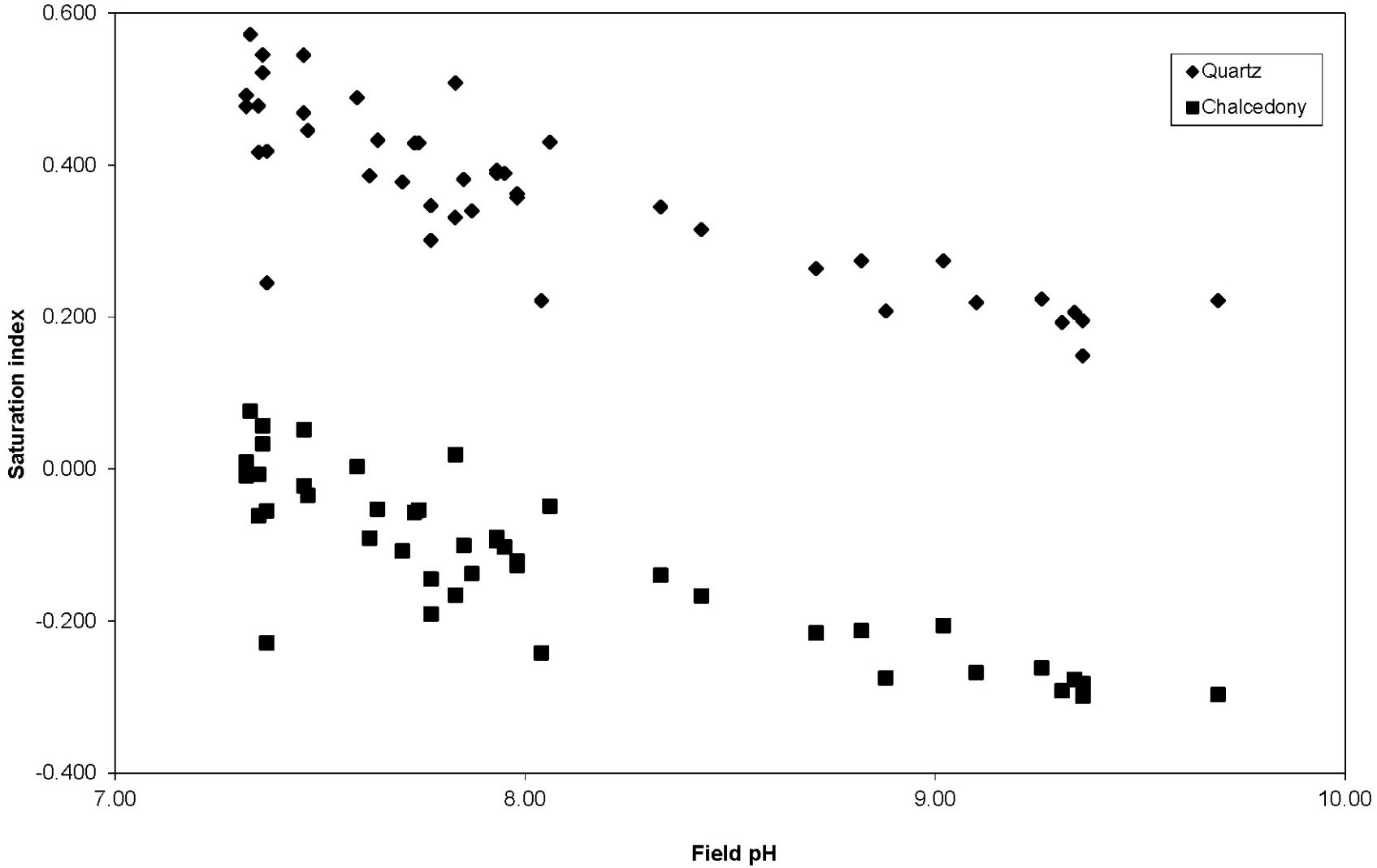

Figure 31. Values of field pH versus calculated saturation indices of quartz and chalcedony in groundwater and springwater samples, south-central Alberta.

Table 3. Saturation indices of selected solid phases, calculated using NETPATH, for groundwater and springwater samples, south-central Alberta.

Sample number	$CaCO_3$	$CaMg(CO_3)_2$	$FeCO_3$	$SrCO_3$	$CaSO_4 \cdot 2H_2O$	$SrSO_4$	SiO_2 (a)	SiO_2 (quartz)	$FeO \cdot OH$	$Fe(OH)_3$ (a)	Chalcedony
DR1	0.287	-0.153	-0.329	-0.783	-2.178	-2.091	-1.064	0.315	8.122	1.623	-0.167
DR2	0.069	-0.599	-0.418	-2.124	-3.573	-4.601	-0.983	0.386	5.913	-0.529	-0.091
DR3	0.263	0.121	-1.235	-1.571	-1.957	-2.621	-1.117	0.245	7.615	1.217	-0.229
DR4	0.266	0.125	0.426	-0.872	-1.494	-1.488	-1.098	0.301	7.423	0.813	-0.191
DR5	0.153	0.175	0.132	-1.185	-2.223	-2.417	-0.930	0.469	8.322	1.717	-0.022
DR6	0.196	-0.137	0.459	-1.755	-2.326	-3.130	-0.871	0.522	7.996	1.423	0.033
DR7	0.208	-0.102	0.460	-1.745	-2.318	-3.123	-0.848	0.545	7.998	1.425	0.057
DR8	0.196	0.021	-1.868	-1.507	-2.558	-3.119	-0.857	0.545	8.715	2.089	0.052
DR9	0.300	0.389	-0.595	-1.028	-1.640	-1.829	-0.837	0.572	8.206	1.544	0.076
DR10	0.531	0.715	1.153	-0.589	-1.582	-1.548	-1.040	0.345	7.401	0.876	-0.140
DR11	0.402	0.468		-0.815	-2.628	-2.684	-0.943	0.430			-0.049
S1	0.750	1.599	-0.002	-0.297	-1.891	-1.788	-1.116	0.274	7.036	0.483	-0.213
S2	0.323	0.442		-0.803	-2.534	-2.522	-1.079	0.331			-0.166
S3	0.420	0.415	0.652	-0.565	-1.109	-0.944	-0.955	0.433	7.575	1.026	-0.053
S4	0.072	-0.214	-1.149	-1.082	-1.999	-2.009	-1.010	0.389	6.209	-0.397	-0.103
S5	0.281	-0.226		-0.902	-1.714	-1.742	-1.020	0.362			-0.121
S6	0.283	-0.234		-0.909	-1.722	-1.760	-1.025	0.357			-0.127
S7	0.356	0.734		-0.767	-1.437	-1.404	-0.951	0.429			-0.054
S8	0.453	0.341		-0.649	-3.147	-3.099	-1.164	0.224			-0.262
S9	0.172	-0.291	0.281	-1.130	-1.595	-1.749	-0.886	0.508	6.450	-0.127	0.019
S10	0.427	0.400	0.384	-0.769	-2.237	-2.276	-0.997	0.381	7.645	1.156	-0.101
S11	0.385	0.488	-0.022	-0.867	-1.573	-1.682	-1.053	0.347	8.048	1.438	-0.145
S12	0.273	0.128		-1.270	-2.176	-2.558	-0.956	0.417			-0.062
S13	0.387	0.441	0.209	-0.756	-2.475	-2.455	-1.030	0.340	6.677	0.232	-0.138
I1	0.820	1.225	0.197	0.293	-2.417	-2.370	-1.111	0.264	5.379	-1.095	-0.216
I2	0.486	0.282	-0.031	-0.400	-2.506	-2.233	-1.102	0.274	7.244	0.763	-0.206
I3	0.857	0.505		-0.556	-1.827	-2.085	-1.174	0.208			-0.275
I4	0.386		0.575	-0.375			-1.175	0.206	8.141	1.632	-0.277
I5	0.235	-0.214	-1.638	-0.609	-2.753	-2.447	-1.170	0.219	9.158	2.609	-0.268
D3	0.212			-0.532	-4.687	-4.273	-1.192	0.222			-0.297
D4	0.167			-0.537	-4.706	-4.252	-1.187	0.193			-0.292
D1	0.130			-0.670	-4.532	-4.183	-1.202	0.149			-0.299
D2	0.373	0.082	0.862	-0.430	-3.433	-3.077	-1.177	0.195	7.458	0.980	-0.282
SP1	0.360	0.494		-0.818	-1.398	-1.420	-0.988	0.393			-0.090
SP2	0.357	0.495		-0.820	-1.404	-1.425	-0.992	0.389			-0.094
SP3	0.219	-0.111		-1.027	-0.931	-1.021	-0.889	0.492			0.009
SP4	0.118	-0.039		-1.180	-1.739	-1.886	-1.009	0.378			-0.108
SP5	0.313	0.589		-0.989	-1.370	-1.520	-0.957	0.429			-0.057
SP6	-0.114	-0.625		-2.645	-2.021	-2.012	-1.120	0.222			-0.242
SP7	0.051	-0.315		-1.242	-1.719	-1.852	-0.930	0.446			-0.035
SP8	-0.015	-0.229	-1.100	-1.300	-1.889	-2.005	-0.944	0.418	3.571	-2.832	-0.055
SP9	0.024	0.016	-1.385	-1.071	-1.458	-1.402	-0.910	0.477	3.245	-3.292	-0.009
SP10	0.222	0.310		-1.023	-1.034	-1.126	-0.907	0.478			-0.007
SP11	0.468	0.886	-0.317	-0.753	-0.935	-1.005	-0.899	0.489	8.011	1.466	0.003

Table 4. Plausible chemical reactions involving mandatory and optional phases used in NETPATH modelling.

Reaction Number	Plausible Chemical Reactions
1	$1.2kaolinite + 0.33Na^+ + 0.33HCO_3^- + 1.4H_4SiO_4 = Na\text{-}smectite + 4.2H_2O + 0.33CO_2$
2	$2albite + 11H_2O + 2CO_2 = kaolinite + 2Na^+ + 2HCO_3^- + 4H_4SiO_4$
3	$illite + 1.1CO_2 + 4.2H_2O = 1.2kaolinite + 1.2H_4SiO_4 + 0.60K^+ + 0.25Mg^{2+} + 1.1HCO_3^-$
4	$calcite + CO_2 + H_2O = Ca^{2+} + 2HCO_3^-$
5	$dolomite + 2CO_2 + 2H_2O = Ca^{2+} + Mg^{2+} + 4HCO_3^-$
6	$pyrite + CO_2 + 3.5O_2 + 2H_2O = siderite + 2SO_4^{2-} + 4H^+$
7	$Ca\text{-}(Na\text{-}smectite) + 2Na^+ = Na\text{-}(Na\text{-}smectite) + Ca^{2+}$
8	$Mg\text{-}(Na\text{-}smectite) + 2Na^+ = Na\text{-}(Na\text{-}smectite) + Mg^{2+}$
9	$SiO_{2(a)} + 2H_2O = H_4SiO_4$
10	$CO_2 + H_2O = H^+ + HCO_3^-$

3.2.3 Development of Initial Conditions and Results of Phase I Mass-Balance Modelling

The initial condition (initial water) in Phase I modelling consisted of an aqueous solution containing 0.01 millimole per kilogram (mmol/kg) of Ca and 0.02 mmol/kg of HCO_3 in which $\delta^{13}C_{(DIC)}$ was set to −7‰. This initial condition was intended to be a reasonable proxy for the composition of precipitation entering the groundwater system at land surface. Calcite and dolomite were assumed to have $\delta^{13}C$ values of 0‰. Sensitivity analyses performed on completed Phase I simulations showed that varying the initial condition $\delta^{13}C_{(DIC)}$ value between −7‰ and −25‰ resulted in changes of the calculated values of $\delta^{13}C_{(DIC)}$ in final waters ($\delta^{13}C_{(DIC)calc}$) by ≤0.02‰.

Mass-balance models containing SiO_2 dissolution uniformly resulted in $\delta^{13}C_{(DIC)calc} >> \delta^{13}C_{(DIC)obs}$. Therefore, SiO_2 was ruled out as a potentially reactive phase. Mass-balance models can be found that do not contain alteration of albite to kaolinite but do describe the geochemical evolution of Laurentide-derived glacial-drift and shallow Paskapoo Formation groundwater in terms of carbonate dissolution, alteration of Na-smectite to kaolinite and cation exchange. However, agreement between $\delta^{13}C_{(DIC)calc}$ and $\delta^{13}C_{(DIC)obs}$ in mass-balance models that do not contain alteration of albite to kaolinite require $\delta^{13}C$ values of CO_2 gas ($\delta^{13}C_{CO2(g)}$) ≤ −40‰ in 77% of simulations. These unrealistically negative $\delta^{13}C_{CO2(g)}$ values argue for the presence of albite as a required phase. Two unique mass-balance models were found during Phase I, neither of which can be excluded on geochemical, thermodynamic, or isotopic grounds. Both mass-balance models incorporate alteration of albite to kaolinite, alteration of kaolinite to Na-smectite, alteration of illite to kaolinite, dissolution/precipitation of calcite, oxidation of pyrite to siderite, and dissolution of $CO_{2(g)}$. Model 1 (Table 5) derives Mg from dissolution of dolomite, whereas model 2 (Table 6) derives Mg from Na/Mg cation exchange. Keller et al. (1991) reported values of $\delta^{13}C_{CO2(g)}$ from three soil gas samples and $\delta^{13}C_{(DIC)}$ from 13 groundwater samples, all associated with sulphide-mineral–bearing glacial till in southern Saskatchewan. Values reported by Keller et al. (1991) ranged from −20.8‰ to −21.9‰ for $\delta^{13}C_{CO2(g)}$ and −11.9‰ to −14.9‰ for $\delta^{13}C_{(DIC)}$.Values of $\delta^{13}C_{(DIC)obs}$ used in models 1 and 2 range from −7.6‰ to −17.2‰ with the exception of sample P3-13 (Grasby et al., 2010), which has a $\delta^{13}C_{(DIC)obs}$ value of −0.5‰. Values of $\delta^{13}C_{CO2(g)}$ required in Phase I modelling, with the exception of sample P3-13, range between −7.9‰ and −22.4‰ in model 1 and −7.8‰ to −19.1‰ in model 2. A $\delta^{13}C_{CO2(g)}$ value of −0.4‰ was required to match the $\delta^{13}C_{(DIC)obs}$ value for sample P3-13 in both models 1 and 2. Values of $\delta^{13}C_{CO2(g)}$ required in models 1 and 2 range from those near present-day atmospheric CO_2 to those slightly more depleted in ^{13}C than reported by Keller et al. (1991).

3.2.4 Results of Phase II Mass-Balance Modelling

Phase II modelling assessed the ability of models 1 and 2 developed in Phase I to accurately describe intersample geochemical changes in groundwater and springwater samples. Reactive phases identified in Phase I were used in Phase II modelling. The approach taken in Phase II began with ranking samples in terms of increasing alkalinity. Alkalinity was chosen as a proxy for the degree of geochemical alteration experienced by a given sample as it is modified during all reactions involving aluminosilicate or carbonate minerals in Phase I models (Table 4). Ranking by alkalinity was followed by NETPATH simulation of the geochemical evolution of the sample with the lowest alkalinity (P05-63) to each of the remaining Laurentide-drift groundwater samples.

Model 2 proved to be the more robust under Phase II conditions, successfully producing simulations of geochemical evolution of sample P05-63 to all remaining Laurentide-drift groundwater samples (Table 7). Values of $\delta^{13}C_{CO2(g)}$ required to match $\delta^{13}C_{(DIC)obs}$ values range from –4.3‰ to –24.2‰, with the exception of sample P3-13, which required a $\delta^{13}C_{CO2(g)}$ value of +4.1. With the exception of sample P3-13, 83% of $\delta^{13}C_{CO2(g)}$ values fall within a reasonable range between values that approach present-day atmospheric CO_2 and values slightly more ^{13}C-depleted than those reported by Keller et al. (1991).

3.2.5 Discussion of Mass-Balance Modelling Results

Rigorous application of mass-balance modelling to the geochemical evolution of water requires geochemical systems to be at steady state (Wigley et al., 1978). Though fundamentally important, this requirement is typically not tested in modelled natural systems. Further, net changes in the geochemical composition of waters between arbitrary initial and final sampling points must be explained by the action of a unique chemical reaction or set of reactions. Geochemical changes attributable to a unique chemical reaction or set of reactions is most likely when water can be assumed to flow along a well-defined flow path containing a uniform set of reactant phases. Typically, many differing chemical reactions or sets of reactions can be identified that satisfy changes observed between initial and final sampling points. Ideally, all but one unique chemical reaction or set of reactions can be eliminated on geochemical, thermodynamic, mineralogical, or isotopic grounds. Simulations using NETPATH assume all reactive phases have uniform and consistent isotopic compositions that lie within the expected ranges of natural materials. Successful development of mass-balance models using NETPATH depends, in part, on how well the modelled system conforms to the above requirements and assumptions.

Phase I mass-balance models are assumed to meet the requirements discussed above and the assumption that all reactive phases have uniform and consistent isotopic compositions. No physical flow path is defined for any of the Phase I simulations. However, the conceptual model that all groundwater and springwater in our study area originated from uniform precipitation that was geochemically modified by subsequent interaction with reactive solid and gas phases is easily understood. Following application of appropriate geochemical, mineralogical, thermodynamic and isotopic constraints, two sets of plausible chemical reactions responsible for geochemical evolution of water samples remain. The two remaining sets of chemical reactions differ only in their sources of dissolved Mg. The values of $\delta^{13}C_{CO2(g)}$ used in NETPATH are not constant between simulations. However, the values of $\delta^{13}C_{CO2(g)}$ used fall within a reasonable range between those reported by Keller et al. (1991) for sulphide-mineral–bearing glacial drift and present-day atmospheric CO_2.

Phase II models fail in respect to a critical assumption in that no discernible flow path can be identified, and likely does not exist, between initial and final waters. Therefore, Phase II modelling results must be interpreted with caution. Phase II modelling confirms that initial and final waters used in simulations can

Table 5. Results of Phase I, model 1 NETPATH simulations, groundwater and springwater samples, south-central Alberta. Amount (in millimoles per kilogram) transferred into or from (-) solution.

Sample number	Source	Kaolinite	Na-smectite	Pyrite	Siderite	CO_2 gas	Albite	Calcite	Dolomite	Illite	$\delta^{13}C_{(DIC)}$ (‰) observed in sample	$\delta^{13}C$ (‰) of CO_2 gas used in NETPATH simulation
DR1	ERCB/AGS	56.23	-67.83	2.38	-2.38	17.61	45.48	0.13	0.03	0.04	-12.7	-12.9
DR4	ERCB/AGS	36.60	-44.25	1.75	-1.74	12.31	29.63	0.42	0.51	0.12	-11.3	-12.6
DR10	ERCB/AGS	45.81	-55.32	2.76	-2.74	12.18	37.08	0.25	0.31	0.09	-14.9	-15.9
S1	ERCB/AGS	40.71	-49.15	2.17	-2.17	11.26	32.95	-0.21	0.54	0.06	-8.6	-10.7
S3	ERCB/AGS	34.02	-41.19	2.32	-2.32	10.60	27.58	1.00	0.96	0.16	-16.5	-21.0
S5	ERCB/AGS	55.29	-66.76	2.27	-2.27	15.95	44.74	0.41	0.08	0.10	-15.0	-15.5
S6	ERCB/AGS	54.44	-65.72	2.24	-2.24	16.11	44.04	0.41	0.08	0.09	-14.7	-15.2
S7	ERCB/AGS	30.70	-37.20	1.70	-1.70	10.50	24.91	-0.39	1.55	0.16	-17.2	-22.4
S9	ERCB/AGS	67.18	-81.10	3.28	-3.28	20.31	54.36	0.38	0.15	0.10	-14.0	-14.4
SP1	ERCB/AGS	56.45	-68.15	3.40	-3.40	15.22	45.68	0.20	0.59	0.09	-14.1	-15.3
SP2	ERCB/AGS	56.24	-67.89	3.41	-3.41	15.36	45.51	0.19	0.60	0.09	-14.3	-15.5
SP3	ERCB/AGS	75.31	-90.91	5.07	-5.07	21.73	60.93	1.32	0.71	0.12	NA	NA
SP4	ERCB/AGS	31.86	-38.51	1.14	-1.14	10.93	25.82	0.22	0.51	0.09	-13.0	-14.5
SP5	ERCB/AGS	42.28	-51.10	2.39	-2.39	13.10	34.25	-0.22	1.29	0.11	-12.5	-14.9
SP6	ERCB/AGS	44.75	-54.04	2.54	-2.54	11.63	36.22	0.14	0.07	0.09	NA	NA
SP9	ERCB/AGS	19.50	-23.67	1.16	-1.16	9.22	15.87	-0.36	1.81	0.13	-13.6	-18.8
SP10	ERCB/AGS	45.62	-55.20	3.11	-3.11	13.89	36.96	0.11	1.99	0.19	-14.7	-18.8
SP11	ERCB/AGS	41.25	-49.92	3.79	-3.79	12.68	33.43	-0.43	2.76	0.17	-14.8	-21.2
P03-03	Grasby et al., 2010	9.85	-12.18	2.61	-2.61	18.01	8.11	1.05	3.44	0.24	-8.4	-11.2
P03-13	Grasby et al., 2010	61.51	-74.25	3.52	-3.52	17.14	49.79	0.18	0.11	0.09	-0.5	-0.4
P03-16	Grasby et al., 2010	71.05	-85.68	5.05	-5.05	11.65	57.48	0.03	0.02	0.03	-12.5	-12.3
P05-04	Grasby et al., 2010	24.32	-29.54	1.94	-1.94	7.41	19.76	0.63	1.11	0.18	-11.5	-15.7
P05-06	Grasby et al., 2010	40.21	-48.58	2.22	-2.22	11.24	32.58	0.16	0.10	0.09	-7.6	-7.9
P05-07	Grasby et al., 2010	45.56	-55.09	3.15	-3.15	10.10	36.91	0.33	0.25	0.14	-11.7	-12.6
P05-09	Grasby et al., 2010	50.89	-61.50	3.65	-3.65	11.34	41.21	0.33	0.46	0.13	-8.5	-9.3
P05-15	Grasby et al., 2010	38.05	-45.95	1.88	-1.88	11.34	30.84	0.04	0.03	0.05	-8.8	-8.9
P05-27	Grasby et al., 2010	17.92	-21.82	1.80	-1.80	6.12	14.60	0.30	1.69	0.17	-11.4	-18.0
P05-29	Grasby et al., 2010	54.04	-65.21	2.65	-2.65	13.06	43.74	0.05	0.03	0.06	-11.2	-11.3
P05-30	Grasby et al., 2010	65.80	-79.45	4.10	-4.10	15.80	53.25	0.27	0.22	0.12	-12.3	-12.7
P05-40	Grasby et al., 2010	39.17	-47.35	2.20	-2.20	11.31	31.74	0.40	0.47	0.10	-15.0	-16.7
P05-41A	Grasby et al., 2010	58.31	-70.39	3.67	-3.67	13.39	47.20	0.30	0.39	0.08	-12.8	-13.9
P05-59	Grasby et al., 2010	45.53	-55.00	3.68	-3.68	10.17	36.88	0.06	0.14	0.09	-10.5	-10.7
P05-63	Grasby et al., 2010	22.15	-26.87	1.81	-1.81	5.53	18.01	0.49	0.63	0.13	-11.1	-14.5

Table 6. Results of Phase I, model 2 NETPATH simulations, groundwater and springwater samples, south-central Alberta. Amount (in millimoles per kilogram) transferred into or from (-) solution.

Sample number	Source	Kaolinite	Na-smectite	Pyrite	Siderite	CO_2 gas	Albite	Calcite	Mg/Na exchange	Illite	$\delta^{13}C_{(DIC)}$ (‰) observed in sample	$\delta^{13}C$ (‰) of CO_2 gas used in NETPATH simulation
DR1	ERCB/AGS	56.38	-68.01	2.38	-2.38	17.64	45.60	0.16	-0.03	0.04	-12.7	-12.8
DR4	ERCB/AGS	39.08	-47.23	1.75	-1.74	12.81	31.63	0.92	-0.51	0.12	-11.3	-12.0
DR10	ERCB/AGS	47.34	-57.16	2.76	-2.74	12.49	38.31	0.56	-0.31	0.09	-14.9	-15.5
S1	ERCB/AGS	43.37	-52.35	2.17	-2.17	11.81	35.09	0.33	-0.54	0.06	-8.6	-10.0
S3	ERCB/AGS	39.70	-46.84	2.32	-2.32	11.56	31.36	1.96	-0.96	0.16	-16.5	-19.1
S5	ERCB/AGS	55.69	-67.24	2.27	-2.27	16.04	45.06	0.49	-0.08	0.10	-15.0	-15.4
S6	ERCB/AGS	54.83	-66.19	2.24	-2.24	16.19	44.36	0.49	-0.08	0.09	-14.7	-15.1
S7	ERCB/AGS	38.27	-46.32	1.70	-1.70	12.05	31.02	1.16	-1.55	0.16	-17.2	-18.8
S9	ERCB/AGS	67.90	-81.96	3.28	-3.28	20.45	54.94	0.53	-0.15	0.10	-14.0	-14.3
SP1	ERCB/AGS	59.35	-71.65	3.40	-3.40	15.82	48.02	0.80	-0.59	0.09	-14.1	-14.7
SP2	ERCB/AGS	59.14	-71.40	3.41	-3.41	15.96	47.85	0.79	-0.60	0.09	-14.3	-14.9
SP3	ERCB/AGS	78.79	-95.10	5.07	-5.07	22.45	63.74	2.03	-0.71	0.12	NA	NA
SP4	ERCB/AGS	34.33	-41.48	1.14	-1.14	11.44	27.81	0.72	-0.51	0.09	-13.0	-13.8
SP5	ERCB/AGS	48.59	-58.70	2.39	-2.39	14.40	39.34	1.07	-1.29	0.11	-12.5	-13.4
SP6	ERCB/AGS	45.09	-54.45	2.54	-2.54	11.70	36.49	0.21	-0.07	0.09	NA	NA
SP9	ERCB/AGS	28.35	-34.34	1.16	-1.16	11.04	23.01	1.45	-1.81	0.13	-13.6	-15.2
SP10	ERCB/AGS	55.33	-66.90	3.11	-3.11	15.88	44.80	2.10	-1.99	0.19	-14.7	-18.7
SP11	ERCB/AGS	54.70	-66.13	3.79	-3.79	15.44	44.29	2.33	-2.76	0.17	-14.8	-16.9
P03-03	Grasby et al., 2010	26.65	-32.41	2.61	-2.61	21.45	21.67	4.49	-3.44	0.24	-8.4	-9.4
P03-13	Grasby et al., 2010	62.02	-74.87	3.52	-3.52	17.24	50.20	0.29	-0.11	0.09	-0.5	-0.4
P03-16	Grasby et al., 2010	71.16	-85.82	5.05	-5.05	11.68	57.57	0.05	-0.02	0.03	-12.5	-12.3
P05-04	Grasby et al., 2010	29.73	-36.06	1.94	-1.94	8.53	24.13	1.74	-1.11	0.18	-11.5	-13.6
P05-06	Grasby et al., 2010	40.71	-49.18	2.22	-2.22	11.34	32.99	0.26	-0.10	0.09	-7.6	-7.8
P05-07	Grasby et al., 2010	46.81	-56.58	3.15	-3.15	10.35	37.91	0.59	-0.25	0.14	-11.7	-12.2
P05-09	Grasby et al., 2010	53.15	-64.22	3.65	-3.65	11.80	43.03	0.79	-0.46	0.13	-8.5	-8.9
P05-15	Grasby et al., 2010	38.19	-46.12	1.88	-1.88	11.37	30.96	0.07	-0.03	0.05	-8.8	-8.8
P05-27	Grasby et al., 2010	26.16	-31.74	1.80	-1.80	7.81	21.25	1.99	-1.73	0.17	-11.4	-14.0
P05-29	Grasby et al., 2010	54.17	-65.37	2.65	-2.65	13.09	43.85	0.07	-0.03	0.06	-11.2	-11.2
P05-30	Grasby et al., 2010	66.87	-80.74	4.10	-4.10	16.02	54.11	0.49	-0.22	0.12	-12.3	-12.5
P05-40	Grasby et al., 2010	41.46	-50.10	2.20	-2.20	11.78	33.59	0.86	-0.47	0.10	-15.0	-16.1
P05-41A	Grasby et al., 2010	60.22	-72.69	3.67	-3.67	13.78	48.74	0.69	-0.39	0.08	-12.8	-13.5
P05-59	Grasby et al., 2010	46.23	-55.84	3.68	-3.68	10.31	37.45	0.21	-0.14	0.09	-10.5	-10.5
P05-63	Grasby et al., 2010	25.21	-30.56	1.81	-1.81	6.15	20.48	1.11	-0.63	0.13	-11.1	-13.0

Table 7. Results of Phase II, model 2 NETPATH simulations, groundwater and springwater samples, south-central Alberta. Amount (in millimoles per kilogram) transferred into or from (-) solution.

	Amount (mmol/kg) transferred into or from (-) solution									$\delta^{13}C_{(DIC)}$ (‰)	$\delta^{13}C$ (‰) of CO_2 gas
Reaction path	Kaolinite	Na-smectite	Pyrite	Siderite	CO_2 gas	Albite	Calcite	Mg/Na exchange	Illite	observed in terminal sample	used in NETPATH simulation
P05-63 --> P03-16	45.95	-55.26	3.24	-3.24	5.52	37.09	-1.06	0.60	-0.10	-12.5	-13.0
P05-63 --> P05-59	21.02	-25.28	1.86	-1.86	4.16	16.97	-0.91	0.48	-0.04	-10.5	-9.5
P05-63 --> P05-27	0.95	-1.18	-0.01	0.01	1.66	0.77	0.87	-1.06	0.04	-11.4	NA
P05-63 --> P05-04	4.52	-5.50	0.13	-0.13	2.37	3.65	0.62	-0.48	0.05	-11.5	-11.8
P05-63 --> P05-07	21.60	-26.02	1.33	-1.33	4.20	17.43	-0.52	0.37	0.01	-11.7	-12.2
P05-63 --> SP6	19.87	-23.89	0.73	-0.73	5.55	16.01	-0.90	0.57	-0.04	NA	NA
P05-63 --> S1	18.16	-21.79	0.36	-0.36	5.65	14.61	-0.78	0.10	-0.06	-8.6	-8.8
P05-63 --> SP9	3.13	-3.78	-0.65	0.65	4.89	2.53	0.34	-1.19	0.00	-13.6	NA
P05-63 --> DR10	22.12	-26.60	0.95	-0.93	6.34	17.83	-0.55	0.33	-0.04	-14.9	-17.8
P05-63 --> P05-09	27.94	-33.66	1.84	-1.84	5.65	22.55	-0.32	0.16	0.00	-8.5	-6.2
P05-63 --> S3	13.49	-16.28	0.51	-0.51	5.41	10.88	0.84	-0.34	0.03	-16.5	-24.2
P05-63 --> P03-03	1.44	-1.86	0.79	-0.79	15.29	1.19	3.37	-2.84	0.12	-8.4	-9.0
P05-63 --> P05-06	15.49	-18.63	0.40	-0.40	5.19	12.51	-0.85	0.54	-0.04	-7.6	-4.3
P05-63 --> DR4	13.86	-16.67	-0.06	0.06	6.66	11.14	-0.19	0.12	-0.01	-11.3	NA
P05-63 --> P05-15	12.98	-15.56	0.06	-0.06	5.21	10.47	-1.04	0.62	-0.08	-8.8	-6.5
P05-63 --> P05-40	16.24	-19.54	0.38	-0.38	5.63	13.11	-0.25	0.16	-0.03	-15.0	-18.6
P05-63 --> SP5	23.38	-28.14	0.58	-0.58	8.24	18.86	-0.04	-0.66	-0.02	-12.5	-13.4
P05-63 --> P05-29	28.96	-34.81	0.84	-0.84	6.94	23.37	-1.04	0.62	-0.07	-11.2	-11.2
P05-63 --> SP1	34.14	-41.09	1.59	-1.59	9.66	27.54	-0.32	0.04	-0.03	-14.1	-15.5
P05-63 --> SP11	29.55	-35.57	1.98	-1.98	9.28	23.81	1.21	-2.14	0.04	-14.8	-18.6
P05-63 --> SP10	30.11	-36.34	1.30	-1.30	9.73	24.32	0.98	-1.38	0.06	-14.7	-17.9
P05-63 --> P05-41A	35.01	-42.13	1.86	-1.86	7.63	28.26	-0.42	0.25	-0.05	-12.8	-13.9
P05-63 --> S5	30.48	-36.68	0.46	-0.46	9.88	24.57	-0.62	0.55	-0.03	-15.0	-17.0
P05-63 --> P05-30	41.66	-50.18	2.29	-2.29	9.87	33.63	-0.62	0.41	-0.01	-12.3	-12.7
P05-63 --> DR1	31.17	-37.45	0.57	-0.57	11.49	25.12	-0.95	0.62	-0.09	-12.7	-13.4
P05-63 --> P03-13	36.81	-44.32	1.71	-1.71	11.09	29.72	-0.82	0.53	-0.04	-0.5	4.1
P05-63 --> S9	42.69	-51.41	1.46	-1.46	14.30	34.46	-0.59	0.49	-0.03	-14.0	-14.9
P05-63 --> SP3	53.58	-64.55	3.26	-3.26	16.30	43.26	0.92	-0.08	-0.01	NA	NA

be linked through a unique set of chemical reactions identified in Phase I. However, the final waters almost certainly did not evolve from the initial water used in these simulations. Phase I modelling indicates a large degree of heterogeneity in $\delta^{13}C_{CO2(g)}$ values within the shallow Paskapoo Formation and overlying glacial drift in the eastern part of our study area. Therefore, $\delta^{13}C_{CO2(g)}$ values used in Phase II modelling represent, at least in part, quantities needed to 'correct' for simulated evolution of final water in $\delta^{13}C_{CO2(g)}$ environments that differ from the initial water environments. Although it may be comforting that $\delta^{13}C_{CO2(g)}$ values required in Phase II modelling fall within a reasonable range, this should not be taken as a confirmation of simulation validity.

All models simulate oxidation of pyrite as the source of dissolved SO_4 in Laurentide-derived glacial-drift and shallow Paskapoo groundwater and identify alteration of albite to kaolinite as the primary source of dissolved Na and dissolved SiO_2 (Tables 8 and 9). Mass-balance budgets of Na and SiO_2 are balanced principally by alteration of kaolinite to Na-smectite. All simulations that successfully reproduce $\delta^{13}C_{(DIC)obs}$ values consume CO_2 gas.

Phase I and II NETPATH simulations show alteration of albite to kaolinite as the primary source of alkalinity in solution. It is reasonable to assume that H^+ generated by oxidation of pyrite plays a role in alteration of albite to kaolinite. Although there is a general trend in the relationship between dissolved SO_4 concentrations and alkalinity, there is also considerable scatter in the relationship (Figure 29). Values of pH in glacial-drift and shallow Paskapoo Formation groundwater do not systematically vary across our study area (Figure 18) suggesting that H^+ produced during pyrite oxidation is largely consumed by mineral alteration or dissolution reactions. If SO_4 is assumed to behave conservatively (no reduction of SO_4 to sulphide or SO_4-bearing mineral precipitation), and all H^+ produced during pyrite oxidation is consumed by mineral alteration or dissolution reactions, one would expect a very strong relationship between alkalinity and dissolved SO_4. Oxidation of varying amounts of organic S during glacial drift weathering, as suggested by Van Stempvoort et al. (1994), provides an alternative source of dissolved SO_4 that would not produce a corresponding increase in alkalinity, potentially accounting for a degree of the observed scatter in Figure 29. The potential contribution of organic S oxidation to dissolved SO_4 concentrations suggests that our NETPATH simulations may be in error in attributing all dissolved SO_4 to oxidation of pyrite.

3.3 Geochemical Evolution of Groundwater at Intermediate and Deep Intervals in the Paskapoo Formation

Groundwater geochemistry shows little to no systematic change between drift and shallow Paskapoo Formation samples collected at similar eastings across the study area. This lack of systematic change with depth carries two implications: (1) groundwater geochemistry of the shallow Paskapoo Formation is controlled largely by the results of chemical weathering of overlying glacial drift, and (2) there exists a downward component of groundwater flow in the shallow interval of the Paskapoo Formation. Implication 1 is consistent with the observations of Gabert (1975) and Grasby et al. (2008, 2010). Implication 2 is consistent with the observations of Meyboom (1961), Le Breton (1971) and Grasby et al. (2008, 2010).

Changes in groundwater geochemistry between shallow and deeper intervals within the Paskapoo Formation in the eastern part of the study area generally show that as depth increases values of field pH increase (Figure 18) and concentrations of dissolved Ca (Figure 8), dissolved Mg (Figure 10) and dissolved SiO_2 (Figure 14) all decrease. Concentrations of dissolved Cl (Figure 11) and dissolved CH_4 (Figure 13) and values of $\delta^{18}O$ (Figure 15) and $\delta^{13}C_{(DIC)}$ (Figure 16) are elevated in samples I1, I4, D2, D3 and D4 relative to shallower samples collected at similar eastings. Concentrations of dissolved Na (Figure 5), dissolved SO_4 (Figure 6) and alkalinity (Figure 7) show little change between shallow and deeper intervals. Saturation-state calculations made using NETPATH show that Paskapoo Formation

Table 8. Geochemical budget for dissolved Na and SiO_2 in Phase I modelling, groundwater and springwater samples, south-central Alberta. Abbreviation: mmol/kg, millimole per kilogram.

Sample number	Source	Phase I, model 1		Phase I, model 2		
		Net SiO_2 transferred to solution through aluminosilicate reactions (mmol/kg)	Net Na transferred to solution through aluminosilicate reactions (mmol/kg)	Net SiO_2 transferred to solution through aluminosilicate reactions (mmol/kg)	Na transferred to solution through aluminosilicate reactions (mmol/kg)	Na tranferred into or from (-) solution through cation exchange reactions (mmol/kg)
DR1	ERCB/AGS	0.10	22.87	0.10	22.93	-0.06
DR4	ERCB/AGS	0.11	14.88	0.14	15.89	-1.02
DR10	ERCB/AGS	0.15	18.64	0.15	19.26	-0.62
S1	ERCB/AGS	0.10	16.57	0.10	17.64	-1.08
S3	ERCB/AGS	0.17	13.85	2.14	15.75	-1.92
S5	ERCB/AGS	0.14	22.49	0.14	22.65	-0.16
S6	ERCB/AGS	0.12	22.13	0.14	22.30	-0.16
S7	ERCB/AGS	0.17	12.51	0.17	15.58	-3.10
S9	ERCB/AGS	0.15	27.33	0.18	27.62	-0.30
SP1	ERCB/AGS	0.14	22.96	0.12	24.14	-1.18
SP2	ERCB/AGS	0.17	22.88	0.11	24.05	-1.20
SP3	ERCB/AGS	0.19	30.63	0.20	32.04	-1.42
SP4	ERCB/AGS	0.16	12.98	0.17	13.98	-1.02
SP5	ERCB/AGS	0.16	17.22	0.16	19.77	-2.58
SP6	ERCB/AGS	0.15	18.21	0.13	18.34	-0.14
SP9	ERCB/AGS	0.20	7.98	0.16	11.56	-3.62
SP10	ERCB/AGS	0.20	18.56	0.20	22.50	-3.98
SP11	ERCB/AGS	0.18	16.79	0.17	22.25	-5.52
P03-03	Grasby et al., 2010	0.17	4.05	0.21	10.87	-6.88
P03-13	Grasby et al., 2010	0.21	25.04	0.18	25.24	-0.22
P03-16	Grasby et al., 2010	0.20	28.92	0.18	28.96	-0.04
P05-04	Grasby et al., 2010	0.14	9.91	0.14	12.11	-2.22
P05-06	Grasby et al., 2010	0.19	16.39	0.21	16.60	-0.20
P05-07	Grasby et al., 2010	0.16	18.55	0.19	19.05	-0.50
P05-09	Grasby et al., 2010	0.16	20.71	0.16	21.62	-0.92
P05-15	Grasby et al., 2010	0.16	15.52	0.17	15.59	-0.06
P05-27	Grasby et al., 2010	0.16	7.33	0.18	10.67	-3.46
P05-29	Grasby et al., 2010	0.19	22.00	0.19	22.06	-0.06
P05-30	Grasby et al., 2010	0.19	26.77	0.17	27.20	-0.44
P05-40	Grasby et al., 2010	0.14	15.96	0.17	16.89	-0.94
P05-41A	Grasby et al., 2010	0.17	23.74	0.17	24.51	-0.78
P05-59	Grasby et al., 2010	0.17	18.55	0.19	18.84	-0.28
P05-63	Grasby et al., 2010	0.17	9.05	0.16	10.29	-1.26

Table 9. Geochemical budget for dissolved Na and SiO_2 in Phase II modelling, groundwater and springwater samples, south-central Alberta. Abbreviation: mmol/kg, millimole per kilogram.

	Phase II, model 2		
Reaction path	Net SiO_2 transferred to or from (-) solution through aluminosilicate reactions (mmol/kg)	Na transferred to or from (-) solution through aluminosilicate reactions (mmol/kg)	Na transferred to or from (-) solution through cation exchange reactions (mmol/kg)
P05-63 --> P03-16	0.02	18.67	1.26
P05-63 --> P05-59	0.03	8.54	0.98
P05-63 --> P05-27	0.02	0.38	-2.14
P05-63 --> P05-04	-0.02	1.82	-0.98
P05-63 --> P05-07	0.03	8.76	0.74
P05-63 --> SP6	-0.05	8.05	1.14
P05-63 --> S1	-0.03	7.35	0.20
P05-63 --> SP9	-0.02	1.27	-2.38
P05-63 --> DR10	-0.03	8.96	0.66
P05-63 --> P05-09	0.00	11.33	0.32
P05-63 --> S3	-0.02	5.45	-0.68
P05-63 --> P03-03	0.04	0.57	-5.68
P05-63 --> P05-06	0.00	6.30	1.08
P05-63 --> DR4	-0.07	5.58	0.24
P05-63 --> P05-15	-0.02	5.28	1.24
P05-63 --> P05-40	-0.01	6.60	0.32
P05-63 --> SP5	0.00	9.48	-1.32
P05-63 --> P05-29	0.03	11.77	1.24
P05-63 --> SP1	-0.01	13.84	0.08
P05-63 --> SP11	0.13	11.95	-4.28
P05-63 --> SP10	0.02	12.21	-2.76
P05-63 --> P05-41A	0.01	14.22	0.50
P05-63 --> S5	-0.05	12.34	1.10
P05-63 --> P05-30	0.01	16.90	0.82
P05-63 --> DR1	-0.06	12.64	1.24
P05-63 --> P03-13	-0.02	14.95	1.06
P05-63 --> S9	-0.02	17.32	0.98
P05-63 --> SP3	0.01	21.74	-0.16

groundwater is near equilibrium or slightly oversaturated with respect to calcite and undersaturated with respect to gypsum and $SiO_{2(a)}$ (Table 3). A plot of chemical activities of H_4SiO_4 versus Na^+/H^+ (Figure 27) indicates an approach to thermodynamic equilibrium between kaolinite and Na-smectite and that albite is thermodynamically unstable when in contact with Laurentide-derived glacial-drift and Paskapoo Formation groundwater.

Changes in the geochemistry of Paskapoo Formation groundwater between shallow and deeper intervals, with the exceptions of samples I1, I4, D2, D3 and D4, can be explained by alteration of albite to kaolinite, equilibrium between kaolinite and Na-smectite, precipitation of carbonate minerals and possible dissolution of SiO_2. Alteration of albite to kaolinite consumes CO_2 from and releases Na^+, HCO_3^- and H_4SiO_4 to solution. Assuming the Paskapoo Formation is closed to atmospheric CO_2 at intermediate and

deep intervals, consumption of CO_2 would act to increase the pH of groundwater. Increasing pH and increasing HCO_3^- produced by albite alteration could drive precipitation of authigenic calcite, thereby reducing concentrations of dissolved Ca. Incorporation of Mg into authigenic calcite or precipitation of Mg in an additional Mg-bearing authigenic carbonate mineral could explain the observed decrease in the concentration of dissolved Mg. Production of Na^+, HCO_3^- and H_4SiO_4 on alteration of albite to kaolinite would favour alteration of kaolinite to Na-smectite. The relative consistency of dissolved Na concentrations and alkalinity suggest buffering by alteration of kaolinite to Na-smectite. Available Ca likely limits the ability of calcite precipitation to buffer pH in intermediate and deep intervals of the Paskapoo Formation. Concentrations of dissolved SiO_2 at pH values of approximately 8.5 or less show a strong inverse correlation with values of field pH (Figure 30). The solubility of SiO_2 is known to increase markedly as values of pH approach 9 (Drever, 1982,). Concentrations of dissolved SiO_2 appear to stabilize at field-pH values of approximately 8.5 (Figure 30). Dissolution of an increasingly soluble SiO_2 phase may add H_4SiO_4 to solution, allowing alteration of kaolinite to Na-smectite to proceed without apparent consumption of dissolved SiO_2.

The presence of authigenic pyrite (Grasby et al., 2007), decreasing SO_4 concentrations along groundwater flow paths (Meyboom, 1961), and decreasing values of SO_4/Cl with increasing depth (Gabert, 1975) suggest that SO_4 reduction may play a role in the geochemical evolution of Paskapoo Formation groundwater. However, our data show no systematic shifts in $\delta^{34}S_{(SO4)}$ values indicative of SO_4 reduction either with easting (Figure 17) or with concentrations of dissolved SO_4 (Figure 25). Thus, our data do not confirm SO_4 reduction to be currently operating within our study area. However, SO_4 reduction may be an active process outside the study area and/or may have occurred in groundwater within the study area at some time in the past.

3.4 Processes Affecting the Compositions of Samples I1, I4, D2, D3 and D4

Samples I1, I4, D2, D3 and D4 show enrichment in δ^2H and $\delta^{18}O$ relative to other groundwater and surface water collected in our study (Figure 21). Observed increases in $\delta^{13}C_{(DIC)}$ values with increasing concentrations of dissolved CH_4 (Figure 23) suggest that samples I1, I4, D2, D3 and D4 have been exposed to, or mixed with groundwater exposed to, a methanogenic environment. Samples I1, I4, D2, D3 and D4 show correlation between values of $\delta^{18}O$ and $\delta^{13}C_{(DIC)}$ (Figure 22) and are slightly elevated in concentrations of dissolved Cl (Figure 11). Additionally, samples I1, I4, D2, D3 and D4 show lower $^{14}C_{(DIC)}$ concentrations than samples collected at similar eastings (Figure 9) and similar alkalinities (Figure 24).

Observed patterns in $\delta^{18}O$, δ^2H, $\delta^{13}C_{(DIC)}$, dissolved Cl, dissolved CH_4 and ^{14}C in samples I1, I4, D2, D3 and D4 could be explained by mixing of Paskapoo Formation groundwater with groundwater from depth. The correlation of increasing dissolved CH_4 concentrations with increasing $\delta^{13}C_{(DIC)}$ values indicates that dissolved CH_4 did not enter samples I1, I4, D2, D3 and D4 as a free gas phase. Rather, dissolved CH_4 is present in association with a methanogenically CH_4-charged groundwater of external origin. Groundwater from depth would need to meet criteria including enrichment in ^2H, ^{18}O, ^{13}C, dissolved Cl and dissolved CH_4 and depletion in ^{14}C with respect to Paskapoo Formation groundwater. High-salinity subsurface water meeting these criteria exists within Lower Cretaceous to Devonian geological units in the Western Canada Sedimentary Basin (Connolly et al., 1990a, b). A plot of reciprocal dissolved Sr concentrations versus $^{87}Sr/^{86}Sr$ values (Figure 32) indicates that the compositions of samples I1, I4, D2, D3 and D4 cannot be explained by simple mixing of Paskapoo Formation groundwater with groundwater from Lower Cretaceous to Devonian geological units in central Alberta. Further, available Br and Cl data (Figure 33) specifically eliminates the Mannville Group as a potential source of water modifying the composition of samples I1, I4, D2, D3 and D4.

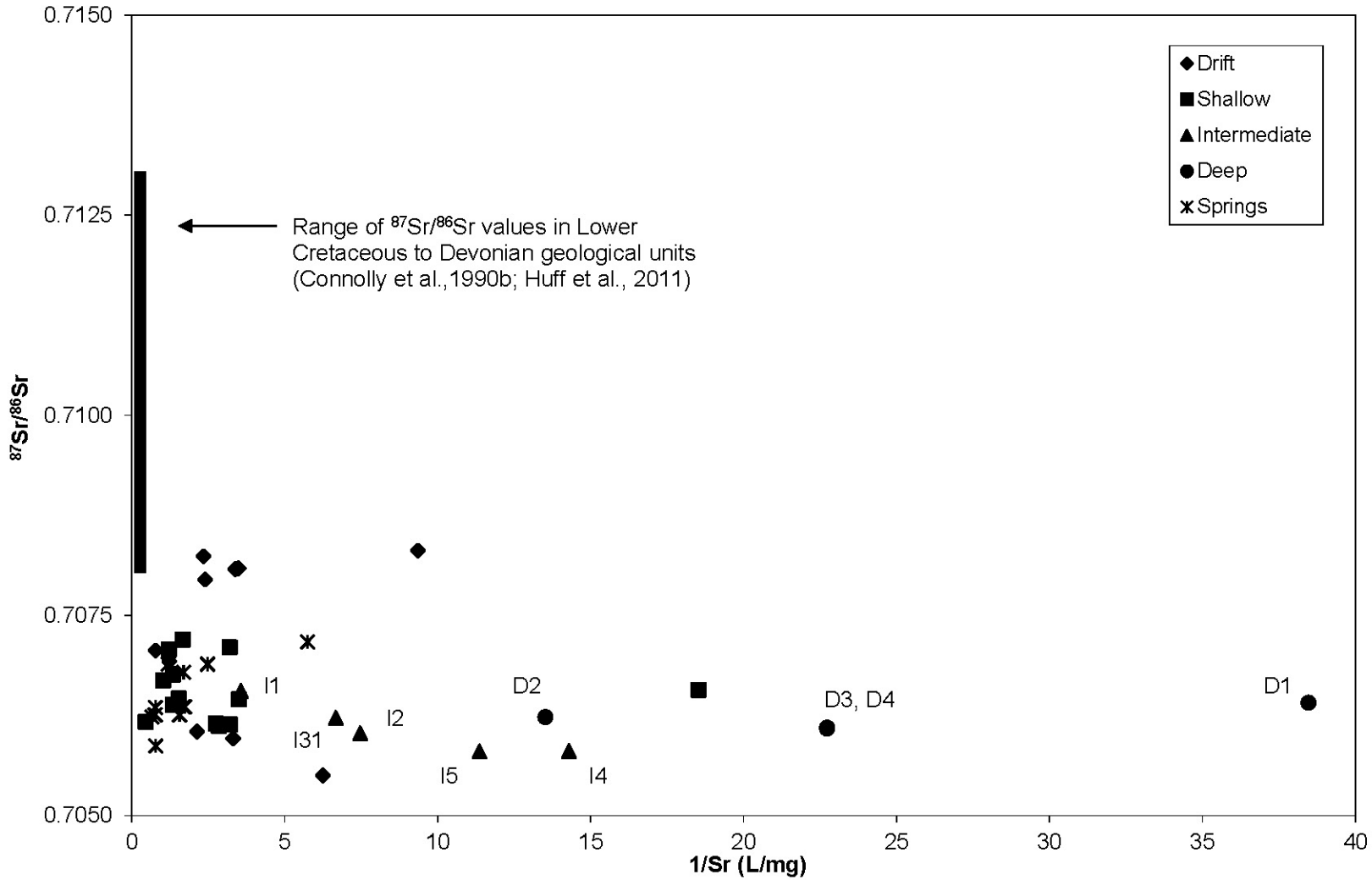

Figure 32. Values of 1/Sr versus values of $^{87}Sr/^{86}Sr$ in groundwater and springwater samples and in saline water in Lower Cretaceous to Devonian geological units in central Alberta as reported by Connolly et al. (1990b) and Huff et al. (2011).

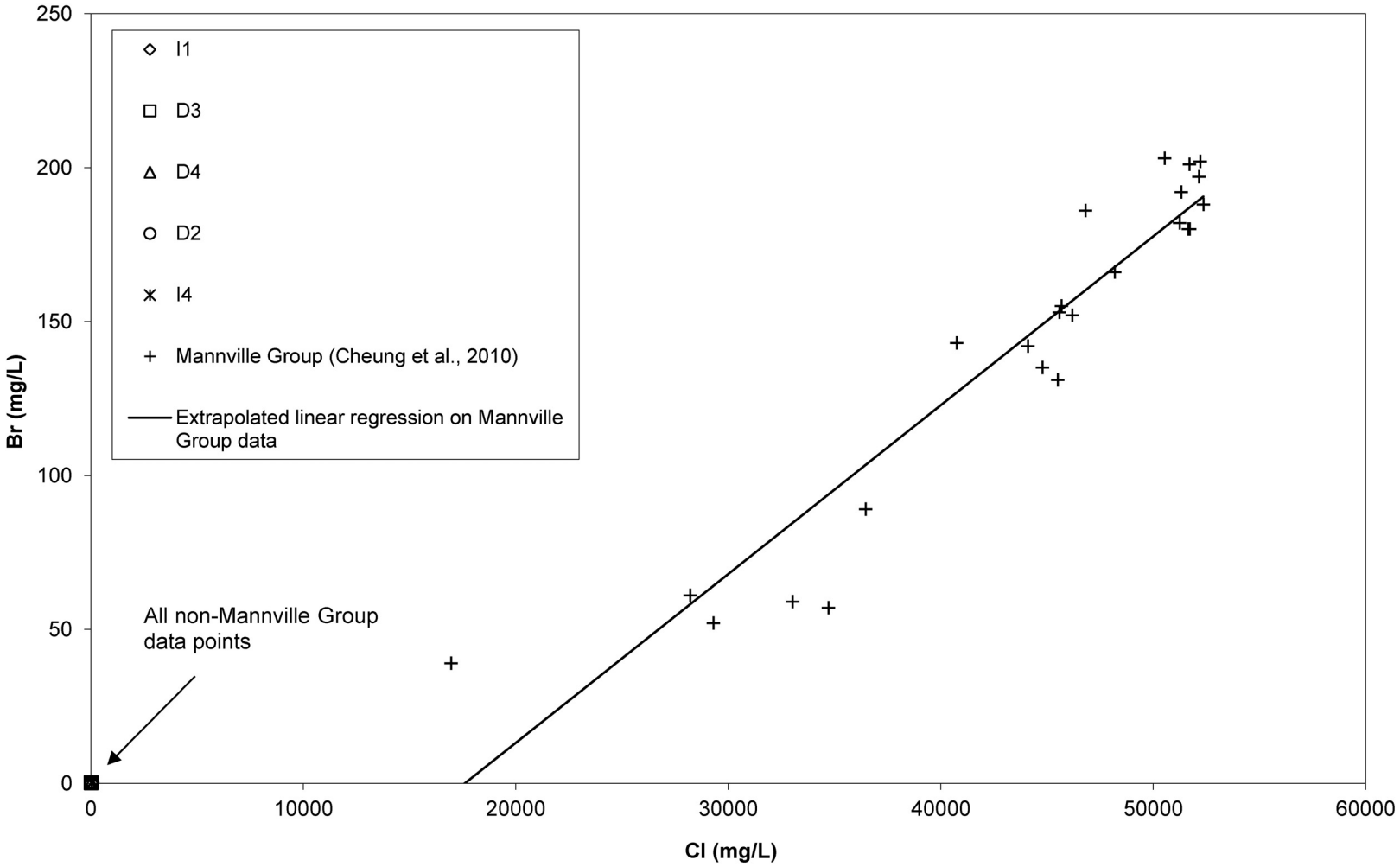

Figure 33. Concentrations of dissolved Br and Cl in samples I1, I4, D2, D3 and D4 and in Mannville Group water as reported by Cheung et al. (2010), south-central Alberta.

Similarly, relationships between dissolved SO_4 concentrations and $\delta^{34}S_{(SO4)}$ values (Figure 25) and between reciprocal dissolved SO_4 concentrations and $^{34}S/^{32}S$ ratios (Figure 26) indicate that the compositions of samples I1, I4, D2, D3 and D4 cannot be explained by simple mixing of Paskapoo Formation groundwater with groundwater from the Horseshoe Canyon Formation or Belly River Group. Potentially methanogenic environments exist within the modern-day Paskapoo and Scollard formations. However, no modern-day processes are known to exist in either the Paskapoo or Scollard Formation that could account for the apparently covariant δ^2H and $\delta^{18}O$ enrichment observed in samples I1, I4, D2, D3 and D4 (Figure 21). A satisfactory explanation for the compositions of samples I1, I4, D2, D3 and D4 cannot be formed from currently available information.

4 Implications of the Distribution of ^3H and ^{14}C in Groundwater and Springwater

Tritium (^3H) is a radioactive isotope of hydrogen with a half-life of approximately 12.3 years (Lucas and Underweger, 2000). Multiple factors affect the concentration of ^3H in groundwater and springwater, including the initial concentration of ^3H on infiltration, possible atmospheric contamination during sample collection or analysis, the degree of any mixing between 'younger' and 'older' waters, and the elapsed time since equilibration with atmospheric ^3H. We will assume that initial atmospheric concentrations of ^3H across our study area have been uniform for any given time.

Carbon-14 (^{14}C) is a radioactive isotope of carbon with a half-life of approximately 5730 years (Godwin, 1962). Factors affecting the concentration of ^3H also affect the concentration of $^{14}C_{(DIC)}$. Additionally, $^{14}C_{(DIC)}$ concentrations can be affected by water/rock geochemical interaction and microbial activity.

4.1 ^3H

All intermediate and deep groundwater samples, with the exception of sample I1, show ^3H concentrations <0.8 TU (Figure 19). We interpret ^3H concentrations <0.8 TU to represent waters having residence times in subsurface environments closed to atmospheric input for periods greater than the duration of detectable concentrations of ^3H. Sample I1 (1.4 TU) may have accumulated a small amount of ^3H from any of the potential sources described above but likely does not retain detectable amounts of ^3H originally present at atmospheric closure.

The preponderance of water samples from the eastern side of the study area show ^3H concentrations <0.8 TU whereas all water samples from the western side of the study area show detectable concentrations of ^3H (Figure 19). We interpret the observed distribution of ^3H to represent longer residence times of water within the Laurentide-derived, clay-rich, glacial drift overlying the eastern part of our study area. This contrasts with shorter residence times within the Cordilleran-derived, relatively clay-poor, glacial drift overlying the western part of our study area. The differing ^3H-based apparent residence times imply that water flows through the western glacial drift more rapidly than the eastern glacial drift, similar to the conclusion of Meyboom (1961). Shorter western residence times, coupled with a general east to west increase in annual precipitation in central Alberta (Barker et al., 2011), suggests increasing groundwater recharge rates from east to west across the study area.

4.2 $^{14}C_{(DIC)}$

Concentrations of $^{14}C_{(DIC)}$ in glacial-drift groundwater, shallow Paskapoo Formation groundwater, and springwater generally decrease from west to east across our study area (Figure 9), whereas alkalinity is generally greater in all samples within the eastern part of our study area (Figure 7). The strong negative correlation between alkalinity and $^{14}C_{(DIC)}$ in glacial-drift and shallow Paskapoo Formation groundwater and springwater (Figure 24) suggests that the $^{14}C_{(DIC)}$ pool is being diluted through addition of ^{14}C-dead CO_2 during aluminosilicate-alteration reactions. Keller (1991) suggested microbial degradation of in situ organic matter in glacial-drift sediments as a local source of ^{14}C-dead CO_2. Dilution of $^{14}C_{(DIC)}$ is likely more pronounced over the eastern part of our study area. Phase I modelling indicates a wide range of

values for $^{13}C_{(CO2)}$, suggesting an isotopically heterogeneous groundwater environment in which varying amounts of ^{13}C have been locally added to the $^{13}C_{(DIC)}$ pool during aluminosilicate-alteration reactions. It is logical to assume that similarly heterogeneous conditions exist with respect to $^{14}C_{(DIC)}$. Calculations of groundwater residence times based on changes in $^{14}C_{(DIC)}$ along flow paths through radioactive decay of ^{14}C are possible if the compounding effects of changes on $^{14}C_{(DIC)}$ through water/rock/organic matter interaction are accounted for (Wigley et al., 1978; Plummer et al., 1983, 1994). Accurate ^{14}C-based residence time calculations require a quantitative model of water/rock interaction and accurate knowledge of the isotopic composition of all reacting phases. The variability in $^{14}C_{(CO2)}$ inferred from Phase I modelling precludes calculation of accurate ^{14}C-based groundwater residence times within our study area.

5 Conclusions

Groundwater in the Paskapoo Formation and overlying glacial drift show lateral and vertical changes in geochemistry within our study area. Lateral changes from west to east include increasing concentrations of dissolved solids, dissolved Na, dissolved SO_4 and alkalinity and decreasing concentrations of dissolved Ca and $^{14}C_{(DIC)}$. Dissolved O_2 concentrations, with the exception of one shallow groundwater sample, are all <3.0 mg/L and most were <0.01 mg/L. Most ^{3}H concentrations in the eastern part of our study area <0.8 TU; however, ^{3}H concentrations are generally greater in the western shallow and drift samples. Values of $^{87}Sr/^{86}Sr$ are slightly greater in western drift samples, likely due to differing glacial-drift mineralogies. Vertical changes in groundwater geochemistry within the Paskapoo Formation are, in some instances, more subtle than lateral changes. Concentrations of dissolved Ca and dissolved Mg in intermediate and deep samples are less than those of shallower samples collected at similar eastings. Concentrations of dissolved Cl and dissolved CH_4 and values of $\delta^{18}O$ and $\delta^{13}C_{(DIC)}$ are elevated in samples I1, I4, D2, D3 and D4 relative to shallower samples collected at similar eastings. Values of field pH are elevated in all intermediate and deep samples relative to shallower samples collected at similar eastings. Values of $\delta^{18}O$ and $\delta^{2}H$ in most water samples fall parallel to meteoric waterlines. Points representing samples I1, I4, D2, D3 and D4 lie in a distinct group and are enriched in ^{2}H and ^{18}O relative to glacial-drift and shallow Paskapoo Formation groundwater. Samples I1, I4, D2, D3 and D4 show increasing values of $\delta^{18}O$, increasing concentrations of dissolved CH_4 with increasing values of $\delta^{13}C_{(DIC)}$, and decreasing concentrations of $^{14}C_{(DIC)}$ with increasing alkalinity from west to east across the study area.

Mass-balance modelling of chemical weathering of Laurentide-derived glacial drift identified alteration of albite to kaolinite as the source of dissolved Na and alkalinity and the primary source of dissolved SiO_2 in glacial-drift and shallow Paskapoo Formation groundwater and springwater. Mass-balance budgets of Na and SiO_2 are balanced principally by alteration of kaolinite to Na-smectite. Processes including carbonate-mineral dissolution/precipitation and cation exchange play relatively minor roles in the geochemical evolution of glacial-drift and shallow Paskapoo Formation groundwater and springwater. All simulations that successfully reproduce $\delta^{13}C_{(DIC)obs}$ values consume CO_2 gas. Dissolved SO_4 in groundwater and springwater originates primarily from oxidation of pyrite with apparent local contributions from oxidation of organic S. Changes in the geochemistry of Paskapoo Formation groundwater between shallow and deeper intervals, with the exceptions of those evident in samples I1, I4, D2, D3 and D4, appear to be controlled by alteration of albite to kaolinite, alteration of kaolinite to Na-smectite, precipitation of carbonate minerals, and possible dissolution of SiO_2.

Differing apparent residence times, based on ^{3}H concentrations, imply that water flows through the western glacial drift more rapidly than through the eastern glacial drift. Shorter western residence times, coupled with a general west to east decrease in annual precipitation in central Alberta, suggests decreasing groundwater recharge rates from west to east across our study area. Decreasing concentrations of $^{14}C_{(DIC)}$ are strongly correlated with increasing alkalinity in glacial-drift and shallow Paskapoo Formation groundwater suggesting that the $^{14}C_{(DIC)}$ pool is being diluted with ^{14}C-dead CO_2 during aluminosilicate-alteration reactions.

6 References

Bachu, S. and Michael, K. (2003): Possible controls of hydrological and stress regimes on the producibility of coalbed methane in Upper Cretaceous–Tertiary strata of the Alberta Basin, Canada; American Association of Petroleum Geologists, Bulletin, v. 87, p. 1729–1754.

Bachu, S. and Underschultz, J.R. (1995): Large-scale underpressuring in the Mississippian-Cretaceous succession, southwestern Alberta basin; American Association of Petroleum Geologists, Bulletin, v. 79, p. 989–1004.

Barker, A.A., Riddell, J.T.F., Slattery, S.R., Andriashek, L.D., Moktan, H., Wallace, S., Lyster, S., Jean, G., Huff, G.F., Stewart, S.A. and Lemay, T.G., (2011): Edmonton-Calgary Corridor groundwater atlas; Energy Resources Conservation Board, ERCB/AGS Information Series 140, 90 p., URL <http://www.ags.gov.ab.ca/groundwater/ecc-atlas.html> [September 2011].

Bekele, E.B., Rostron, B.J. and Person, M.A. (2003): Fluid pressure implications of erosional unloading, basin hydrodynamics and glaciation in the Alberta Basin, Western Canada; Journal of Geochemical Exploration, v. 78, p. 143–147.

Cheung, K., Klassen, P., Mayer, B., Goodarzi, F. and Aravena, R. (2010): Major ion and isotope geochemistry of fluids and gases from coalbed methane and shallow groundwater wells in Alberta, Canada; Applied Geochemistry, v. 25, p. 1307–1329.

Clissold, R.J. (1967): Mapping of naturally occurring surficial phenomena to determine groundwater conditions in two areas near Red Deer, Alberta; M.Sc. thesis, University of Alberta, 126 p.

Connolly, C.A., Walter, L.M., Baadsgaard, H. and Longstaffe, F.J. (1990a): Origin and evolution of formation waters, Alberta Basin, Western Canada Sedimentary Basin – I. Chemistry; Applied Geochemistry, v. 5, p. 375–395.

Connolly, C.A., Walter, L.M., Baadsgaard, H. and Longstaffe, F.J. (1990b): Origin and evolution of formation waters, Alberta Basin, Western Canada Sedimentary Basin – II. Isotope systematics and water mixing; Applied Geochemistry, v. 5, p. 397–413.

Corbet, T.F. and Bethke, C.M. (1992): Disequilibrium fluid pressures and groundwater flow in the Western Canada Sedimentary Basin; Journal of Geophysical Research, v. 97, p. 7203–7217.

Craig, H. (1961): Isotopic variations in meteoric waters; Science, v. 133, p. 1702–1703.

Demchuk, T.D. and Hills, L.V. (1991): A re-examination of the Paskapoo Formation in the central Alberta Plains: the designation of three new members; Bulletin of Canadian Petroleum Geology, v. 39, p. 270–282.

Drever, J.I. (1982): The geochemistry of natural waters; Prentice-Hall, Inc., Englewood Cliffs, New Jersey, p. 90–91.

Energy Resources Conservation Board (2009): Table of formations, Alberta; Energy Resources Conservation Board, URL <http://www.ercb.ca/docs/products/catalog/TOF.pdf> [September 2011].

Farvolden, R.N. (1961): Groundwater resources, Pembina area, Alberta; Research Council of Alberta, Earth Sciences Report 1961-04, 26 p., URL <http://www.ags.gov.ab.ca/publications/ESR/PDF/ESR_1961_04.pdf> [September 2011].

Fulton, R.J. (1995): Surficial materials of Canada; Geological Survey of Canada, Map 1880A, scale 1:5 000 000.

Gabert, G.M. (1975): Hydrogeology of Red Deer and vicinity, Alberta; Alberta Research Council, Bulletin 31, 100 p., URL <http://www.ags.gov.ab.ca/publications/abstracts/BUL_031.html> [September 2011].

Godwin, H. (1962): Half-life of radiocarbon; Nature, v. 195, p. 984.

Grasby, S., Tan, W., Chen, Z. and Hamblin, A.P. (2007): Paskapoo groundwater study. Part I: hydrogeological properties of the Paskapoo Formation determined from six continuous cores; Geological Survey of Canada, Open File 5392, 6 p.

Grasby, S.E., Chen, Z., Hamblin, A.P., Wozniak, P.R.J. and Sweet, A.R. (2008): Regional characterization of the Paskapoo bedrock aquifer system, southern Alberta; Canadian Journal of Earth Sciences, v. 45, p. 1501–1516.

Grasby, S., Osborn, J., Chen, Z. and Wozniak, P.R.J. (2010): Influence of till provenance on regional groundwater chemistry; Chemical Geology, v. 273, p. 225–237.

Hamblin, A.P. (2007): Paskapoo groundwater study part III: detailed core measured sections of the Paskapoo Formation in central Alberta; Geological Survey of Canada, Open File 5537, 13 p.

Hamilton, W.N., Price, M.C. and Langenberg, C.W. (1999): Geological map of Alberta; Alberta Energy and Utilities Board, Alberta Geological Survey, Map 236, scale 1:1,000,000, URL <http://www.ags.gov.ab.ca/publications/MAP/PDF/MAP_236.pdf> [September 2012].

Hendry, M.J., Cherry, J.A. and Wallick, E.I. (1986): Origin and distribution of sulfate in a fractured till in southern Alberta, Canada; Water Resources Research, v. 22, p. 45–61.

Huff, G.F., Stewart, S.A., Riddell, J.T.F. and Chisholm, S. (2011): Water geochemical data, saline aquifer project; Energy Resources Conservation Board, ERCB/AGS Digital Data Release 2011-0007, URL <http://www.ags.gov.ab.ca/publications/abstracts/DIG_2011_0007.html> [September 2011].

International Atomic Energy Agency/World Meteorological Organization (2001): Global network for isotopes in precipitation; International Atomic Energy Agency, URL <http://isohis.iaea.org> [March 2011].

Jackson, L.E., Jr. (1980): Glacial history and stratigraphy of the Alberta portion of the Kananaskis Lakes map area; Canadian Journal of Earth Sciences, v. 17, p. 459–477.

Jerzykiewicz, T. (1997): Stratigraphic framework of the uppermost Cretaceous to Paleocene strata of the Alberta Foreland Basin; Geological Survey of Canada, Bulletin 510, 121 p.

Johnston, D.I., Henderson, C.M. and Schmidt, M.J. (2010): Upper Devonian to Lower Mississippian conodont biostratigraphy of the uppermost Wabamun Group and Palliser Formation to lowermost Banff and lodgepole Formations, southern Alberta and southeastern British Columbia: Implications for correlations and sequence stratigraphy; Bulletin of Canadian Petroleum Geology, v. 58, p. 295–341.

Keller, C.K. (1991): Hydrogeochemistry of a clayey till – 2. Sources of CO_2; Water Resources Research, v. 27, p. 2555–2564.

Keller, C.K., van der Kamp, G. and Cherry, J.A. (1991): Hydrogeochemistry of a clayey till – 1. Spatial variability; Water Resources Research, v. 27, p. 2543–2554.

Le Breton, G.E. (1971): Hydrogeology of the Red Deer area, Alberta; Research Council of Alberta, Earth Sciences Report 1971-01, 14 p., URL <http://www.ags.gov.ab.ca/publications/abstracts/ESR_1971_01.html> [September 2011].

Lemay, T.G. and Konhauser, K.O. (2006): Water chemistry of coalbed methane reservoirs; Alberta Energy and Utilities Board, EUB/AGS Special Report 081, 372 p., URL <http://www.ags.gov.ab.ca/publications/abstracts/SPE_081.html> [September 2011].

Lucas, L.L. and Underweger, M.P. (2000): Comprehensive review and critical evaluation of the half-life of Tritium; Journal of Research of the National Institute of Standards and Technology, v. 105, p. 541–549.

Lyster, S. and Andriashek, L.D. (2012): Geostatistical rendering of the architecture and hydrostratigraphic units within the Paskapoo Formation, central Alberta; Energy Resources Conservation Board, Alberta Geological Survey Bulletin 66, 103 p., URL <http://www.ags.gov.ab.ca/publications/BUL/PDF/BUL_066.pdf> [August 2012].

Matthews, W.H. (1974): Surface profiles of the Laurentide ice sheet in its marginal areas; Journal of Glaciology, v. 13, p. 37–43.

Macqueen, R.W. and Sandberg, C.A. (1970): Stratigraphy, age and interregional correlation of the Exshaw Formation, Alberta Rocky Mountains; Bulletin of Canadian Petroleum Geology, v. 18, p. 32-66.

Mermut, A.R. and Arshad, M.A. (1987): Significance of sulphide oxidation in soil salinization in southeastern Saskatchewan, Canada; Soil Science Society of America Journal, v. 51, p. 247–251.

Meyboom, P. (1961): Groundwater resources of the City of Calgary and vicinity; Research Council of Alberta, Bulletin 8, 72 p., URL <http://www.ags.gov.ab.ca/publications/abstracts/BUL_008.html> [September 2011].

Michael, K. and Bachu, S. (2002): Origin, chemistry, and flow of formation waters in the Mississippian-Jurassic sedimentary succession in the west-central part of the Alberta Basin, Canada; Marine and Petroleum Geology, v. 19, p. 289–306.

Moran, S.R. (1986): Surficial geology of the Calgary urban area; Alberta Research Council, Bulletin 53, 46 p., URL <http://www.ags.gov.ab.ca/publications/abstracts/BUL_053.html> [September 2011].

Neuzil, C.E. and Pollock, D.W. (1983): Erosional unloading and fluid pressures in hydraulically ‘tight’ rocks; Journal of Geology, v. 91, p. 179–193.

Parkhurst, D.L. and Appelo, C.A.J. (1999): User’s guide to PHREEQC (version 2) – a computer program for speciation, batch-reaction, one-dimensional transport, and inverse geochemical calculations; United States Geological Survey, Water-Resources Investigations Report 99-4259, 312 p.

Parks, K.P. and Tóth, J. (1995): Field evidence for erosion-induced underpressuring in the Upper Cretaceous and Tertiary strata, west central Alberta, Canada; Bulletin of Canadian Petroleum Geology, v. 43, p. 281–292.

Pawlowicz, J.G. and Fenton, M.M. (1995): Drift thickness of Alberta; Alberta Energy and Utilities Board, EUB/AGS Map No. 227, scale 1:2 000 000, URL <http://www.ags.gov.ab.ca/publications/abstracts/MAP_227.html> [September 2011].

Peng, H., Mayer, B., Harris, S. and Krouse, H.R. (2004): A 10-year record of stable isotope ratios of hydrogen and oxygen in precipitation at Calgary, Alberta, Canada; Tellus, v. 56B, p. 147–159.

Plouffe, A., Paulen, R.C. and Smith, J.R. (2006): Indicator mineral content and geochemistry of glacial sediments from northwest Alberta (NTS 84L, M): new opportunities for mineral exploration; Geological Survey of Canada, Open File 5121 and Alberta Energy and Utilities Board, EUB/AGS Special Report 77, 29 p., URL <http://www.ags.gov.ab.ca/publications/abstracts/SPE_077.html> [September 2011].

Plummer, L.N., Parkhurst, D.L. and Thorstenson, D.C. (1983): Development of reaction models for groundwater systems; Geochimica et Cosmochimica Acta, v. 47, p. 665–685.

Plummer, L.N., Prestemon, E.C. and Parkhurst, D.L. (1994): An interactive code (NETPATH) for modeling NET geochemical reactions along a flow PATH, version 2.0; United States Geological Survey, Water-Resources Investigation Report 94-4169, 130 p.

Richards, B.C. and Higgins, A.C. (1988): Devonian-Carboniferous boundary beds of the Palliser and Exshaw Formations at Jura Creek, Rocky Mountains, southwestern Alberta; *in* Devonian of the World; N.J McMillan, A.F. Embry and D.J Glass (eds.), Canadian Society of Petroleum Geology, Memoir 14, v. 2., p. 399–412.

Roberts, J.A., Bennett, P.C., Gonzalez, L.A., Macpherson, G.L. and Milliken, K.L. (2004): Microbial precipitation of dolomite in methanogenic groundwater; Geology, v. 32, p. 277–280.

Slattery, S.R. and Barker, A.A. (2010): Thickness of Quaternary and Neogene sediments in the Edmonton–Calgary Corridor, Alberta (NTS 82O, 82P, 83A, 83B, 83G and 83H); Energy Resources and Conservation Board, ERCB/AGS, Map 548, scale 1:500 000, URL <http://www.ags.gov.ab.ca/publications/abstracts/MAP_548.html> [September 2011].

Storer, J.E. (1976): Mammals of the Hand Hills Formation, southern Alberta; in Athlon: Essays on Paleontology in Honour of Loris Shano Russell, C.S. Churcher (ed.), Royal Ontario Museum, Life Sciences Miscellaneous Contributions, p. 186–209.

Tharin, J.C. (1960): Glacial geology of the Calgary area; Ph.D. thesis, University of Illinois at Urbana, 127 p.

Tóth, J. (1966): Groundwater geology, movement, chemistry, and resources near Olds, Alberta; Research Council of Alberta, Bulletin 17, 126 p., URL <http://www.ags.gov.ab.ca/publications/abstracts/BUL_017.html> [September 2011].

Tóth, J. and Corbet, T. (1986): Post-Paleocene evolution of regional groundwater flow-systems and their relation to petroleum accumulations, Taber area, southern Alberta, Canada; Bulletin of Canadian Petroleum Geology, v. 34, p. 339–363.

U.S. Geological Survey (2006): Collection of water samples (version 2.0); United States Geological Survey, Techniques of Water-Resources Investigations, book 9, chap. A4.

Van Stempvoort, D.R., Hendry, M.J., Schoenau, J.J. and Krouse, H.R. (1994): Sources and dynamics of sulphur in weathered till, western glaciated plains of North America; Chemical Geology, v. 111, p. 35–56.

Vasconcelos, C. and McKenzie, J.A. (1997): Microbial mediation of modern dolomite precipitation and diagenesis under anoxic conditions (Lagoa Vermelha, Rio de Janeiro, Brazil); Journal of Sedimentary Research, v. 67, p. 378–390.

Vonhof, J.A. (1969): Tertiary gravels and sands in the Canadian Great Plains; Ph.D. thesis, University of Saskatchewan, 279 p.

Wallick, E.I. (1981): Chemical evolution of groundwater in a drainage basin of Holocene age, east-central Alberta, Canada; Journal of Hydrology, v. 54, p. 245–283.

Wigley, T.M., Plummer, L.N. and Pearson, F.J., Jr. (1978): Mass transfer and carbon isotope evolution in natural water systems; Geochimica et Cosmochimica Acta, v. 42, p. 1117–1139.

Wilde, F.D. ed. (variously dated): Field measurements; U.S. Geological Survey techniques of water-resources investigations, book 9, chap. A6, URL <http://pubs.water.usgs.gov/twri9A6/> [October 2011].